Supporting Information

A Thermodynamic Based Interpretation of Protein Expression Heterogeneity in Different GBM Tumors Identifies Tumor Specific Unbalanced Processes

Nataly Kravchenko-Balasha[1,2], Hannah Johnson[3,] Forest M. White[4], James R. Heath[1,5] and R. D. Levine [5,6]

[1] NanoSystems Biology Cancer Center, Division of Chemistry, Caltech, Pasadena, CA, United States. [2] Bio-Medical Sciences department, The Faculty of Dental Medicine,The Hebrew University of Jerusalem, Jerusalem, Israel. [3]Signaling Programme, the Babraham Institute, Babraham, Cambridge, United Kingdom. [4]Department of Biological Engineering, MIT, Cambridge, MA, United States. [5]Department of Molecular and Medical Pharmacology, David Geffen School of Medicine and Department of Chemistry and Biochemistry, UCLA, Los Angeles, CA, United States. [6]The Institute of Chemistry, The Hebrew University of Jerusalem, Jerusalem, Israel

Table of content

There is an additional separate excel table, Additional Table *SI*

1. Theory and experimental procedures

a. Surprisal analysis

A detailed discussion of the implementation of surprisal analysis in biology can be found in [1, 2]. Briefly, we assume that a biological system, including a cell in a tumor, is in a state of minimal free energy subject to constraints. In a spontaneous process at a given temperature and pressure the free energy goes down. The constraints preclude the free energy from decreasing and so maintain the state. A change in the state is thereby described as a change in the constraints. The most stable state of a system is a state of minimal free energy without any constraints. Such a state is steady because it cannot change spontaneously. Surprisal analysis uses the measured protein expression levels in GBM tumors to identify the constraints that prevent the tumor cells from spontaneously reaching a state of minimum of free energy. These constraints define the deviations from that most stable steady state. The constraints are recognized and quantified by identifying how the protein expression levels change from their value at the steady state due to the presence of those constraints. Thus the biological constraints that we identify in the main text are the manifestation of unbalanced processes that take place in the cell.

For each measured protein the extent of influence of a given unbalanced process on a protein *i* is defined by our procedure of surprisal analysis [1-4]. Protein levels can be influenced by more than one unbalanced process. Surprisal analysis seeks to represent the expression level of each protein as a sum of terms (sum on the right hand side of equation (1) below) representing the constraints. α is an index of the constraints, $\alpha = 1,2,..$. The analysis is separately done for every tumor and *k* is the index of the tumor, here $k = 1,..,8$ . . SVD is used as a mathematical tool to determine two sets of parameters from (logarithm of the) expression level $X_i(k)$ of protein *i* in the particular tumor *k* (as described in the sub-section "*Calculation of the parameters* λ_α *and* $G_{i\alpha}$ *")*:

1) The tumor-dependent weights of the constraints $\lambda_\alpha(k)$ (For technical reason it is also called the Lagrange multiplier),

2) The extent of influence of an unbalanced process α on a protein *i* , $G_{i\alpha}$. Surprisal analysis identifies weights $G_{i\alpha}$ that have the same numerical value for all tumors.

The two sets of parameters are obtained by fitting equation (1) to the measured protein expression levels

$$\ln X_i(k) \;=\; \ln X_i^o(k) - \sum_{\alpha=1} G_{i\alpha}\lambda_\alpha(k) \quad (1)$$

Here $\ln X_i^o(k)$ is the (logarithm of the) expression level in the steady state. As discussed in figure 1 of the text, we hypothesize and then validate that the steady state is common for all tumors. The deviation terms are labeled as $\alpha = 1,2,..$ in order of their decreasing size. When all the constraints are kept in the sum above it is an exact

representation of the data and not an approximation. But in practice a few terms suffice to represent the data for each protein. For every constraint we find that levels of about 100 proteins deviate significantly in either the upper ($G_{i\alpha} > 0.03$) or lower direction ($G_{i\alpha} < -0.03$) from the steady state as shown in Fig. S1 (Lists of those proteins and their corresponding $G_{i\alpha}$ values are included in Additional excel Table SI). There are some proteins that are influenced by several constraints and some that are influenced by only one of the $\alpha = 1,2\ldots7$. For many proteins the extent of influence, $G_{i\alpha}$, is about zero for $\alpha = 1,2\ldots7$, meaning that they are mostly players in the steady state. Only those proteins with the values $G_{i\alpha} > 0.03$ or $G_{i\alpha} < -0.03$ were included in the classification of biological processes using David database [5] as reported in Tables S1-S8.

Derivation of the equation (1)

To obtain Equation (1) in the main text or above, we relate protein concentrations $X_i(k)$ in a tumor *k* to the chemical potential (under constant temperature and pressure) using the fundamental physic-chemical relations [6]:

$$\begin{aligned} \underbrace{\mu_i}_{\text{free energy of protein } i} &= \underbrace{\mu_i^{ss}}_{\text{standard free energy}} + kT \ln X_i(k) \\ \underbrace{\mu_i^{O}}_{\substack{\text{free energy of protein } i \\ \text{at the steady state}}} &= \underbrace{\mu_i^{ss}}_{\text{standard free energy}} + kT \ln X_i^{O}(k) \end{aligned} \qquad (2)$$

The equations above relate the experimental expression level of protein *i* to its value in the steady state:

$$\ln X_i(k) = \ln X_i^{O}(k) + (\mu_i - \mu_i^{O}) / kT \qquad (3)$$

Given the experimental data we seek to obtain $X_i^{O}(k)$, which is expected protein expression level at the steady state, as well as $(\mu_i - \mu_i^{O}) / kT$, which is the deviation from the steady state. Equation (3) represents the changes in the chemical potential for each measured protein. From it we can get the change in the *free energy* of the proteomic system as a whole when the constraint(s) are changing and so therefore do the expression levels of the proteins, ($\Delta G = \sum_i X_i(k)(\mu_i - \mu_i^{O}) \neq 0$). To calculate the steady state expression levels, $X_i^{O}(k)$, and deviations thereof, $(\mu_i - \mu_i^{O}) / kT$, we use a procedure described in [2].

In the numerical procedure it is convenient to represent the steady state level as $X_i^o(k) = \exp\left(-G_{i0}\lambda_0(k)\right)$ [2]. $\lambda_{0\,(k)}$ represents the weight of the steady state term in every measured cell. The weight of the proteins when all cellular processes are balanced are described by G_{i0}. The deviations from the steady state are the terms labelled as α=1,2 in the order of their decreasing weight as given by $\lambda_\alpha(k)$. The extent of influence of a given unbalanced process α=1,2... on a protein *i*, is given by $G_{i\alpha}$. Thus a change in the chemical potential of protein *i*, $(\mu_i - \mu_i^o)/kT$, due to the constraints α=1,2... is represented by $\sum_{\alpha=1} G_{i\alpha}\lambda_{\alpha\,(k)}$.

The proteins are correlated due to the constraints. In each constraint all the participating proteins act collectively. This is because each given constraint influences the levels of specific proteins causing a deviation from the steady state limit. That subset of specific proteins that deviate in a similar manner (up or down to the reference limit) are analyzed to give biological meaning to the constraint as described below.

Calculation of the parameters λ_α *and* $G_{i\alpha}$ We want to fit the sum of the terms as shown on the right-hand side of equation (1) to the logarithm of the measured expression level of protein *i* in a tumor *k*. This has to be repeated for every tumor. We use the singular value decomposition [2] (SVD, and more below) as a method for diagonalizing a matrix that includes mean values of (the logarithm of) protein intensities at tumor *k*.

SVD To apply the mathematical procedure of SVD we generate a matrix **Y** utilizing the natural logarithm of the protein intensity levels, as measured [2]. The columns of **Y** are (logarithms of) measurements for a particular tumor. The rows of **Y** are (logarithms of) measurements for a particular protein. Using SVD, we construct two square (and symmetric) matrices. The first one is: $\mathbf{Y}^T\mathbf{Y}$. To determine constraints we diagonalize this matrix: $\mathbf{Y}^T\mathbf{Y}\,\boldsymbol{\lambda}_\alpha = \omega_\alpha^2\,\boldsymbol{\lambda}_\alpha$, $\alpha = 0,1,2,..,$ A-1. $\boldsymbol{\lambda}_\alpha$ is an eigenvector and ω_α^2 is an eigenvalue of the matrix $\mathbf{Y}^T\mathbf{Y}$. The components of the vector $\boldsymbol{\lambda}_\alpha$ provide the weights of the constraint α at each of the distance ranges *r*. The maximal number of non-zero eigenvalues $\boldsymbol{\lambda}_\alpha$ is A, where A is the smaller of the dimensions of the matrix **Y** (here A=8 since we analye 8 GBM tumors). The mathematically exact statement is that A is the rank of the matrix **Y**. The maximal number of possible constraints is equal to A-1 [2].

To determine the $G_{\alpha i}$ we generate a second square matrix: $\mathbf{Y}\mathbf{Y}^T$ [2]. This conjugated matrix has the same value of eigenvalues ω_α^2 : $\mathbf{Y}\mathbf{Y}^T\mathbf{G}_\alpha = \omega_\alpha^2\mathbf{G}_\alpha$, $\alpha = 0,1,2,..,$A-1. $\mathbf{G}_\alpha$ is a column vector of ~1800 components, each component corresponding to a measured protein in the constraint α .

Biological classification Lists of the proteins that are influenced significantly either by the unbalanced processes (Fig.S1 Theoretical approach), or principle components (PCA, Fig.S7) or clusters (k-means clustering, Table S14) were generated. These lists were classified according to biological categories using David database [5]. Biological categories were considered as statistically significant enriched groups if they had EASE score and Benjamini correction [5] values ≤ 0.05.

b. Implementation of Surprisal analysis to data measured by the iTRAQ technology

Surprisal analysis provides a theoretical expression for the concentration [2]. We show how Surprisal analysis can be implemented for iTRAQ proteomic measurements, where protein intensities rather than protein concentrations are generated as an output. As shown below unbalanced biological processes are identified in a similar fashion from either protein copy numbers or protein intensities datasets.

In iTRAQ the expected ion peak is related to the observed ion peak through a set of multiplicative factors. These include the technical biological factors but also such aspects as the relation of a peptide concentration to the associated protein concentration, etc [7]. It is therefore suggestive to recast the observed data in a logarithmic form so that the effects are additive, see for example equation (4) in [7]. When we use a logarithmic form the factors enter in an additive fashion.

Let X_i be the intensity (abundance) of protein *i* as determined from the observed value of the corresponding peptides. That intensity is related to the concentration of protein *i*. Y_i, as a

$$\ln Y_i = \ln X_i - \sum_n \ln F_{in} \qquad (4)$$

where the sum is over all the relevant factors, representing mass spectral experimental uncertainties, as listed e.g., in Table 2 of Hill et al [7]. As in Karpeivitch et al and Hill et al we take it that the terms in equation (4) are uncorrelated. In general and in the case we analyze here there are different samples so that there is a label on the intensities corresponding to the different conditions, here different GBM tumors - *k*.

For $\ln Y_i$ we use equation (1) of the main text:

$$\ln X_i(k) = \ln X_i^o(k) - \sum_{\alpha=1} G_{i\alpha}\lambda_\alpha(k) + \sum_n \ln F_{in} \qquad (5)$$

Since the majority of the factors in Hill et al.[7] are condition independent, the sum $\sum_n \ln F_{in}$ (representing different iTRAQ factors as presented in table 2 in [7]) will be included mostly in the zero eigenvector of the Surprisal analysis. The condition dependent uncertainty in other eigenvectors is estimated as described below and in Gross et al.[8].

We can rewrite the equation (5):

$$\ln X_i(GBM) = (\ln X_i^o(k) + \sum_n \ln F_{in}) - \sum_{\alpha=1} G_{i\alpha}\lambda_\alpha(k)$$

The sum $(\ln X_i^o(k) + \sum_n \ln F_{in})$ will be fitted mostly by the 0'th term of Surprisal analysis (generated from the first eigenvectors of the SVD analysis [2] and denoted as $G_{i0}\lambda_0$). The condition/tumor dependent uncertainty for the terms representing biological constraints can be directly translated [8] to an error in the lambdas. In the theory, see for example [2], the lambdas are Lagrange multipliers. Each multiplier is a measure by how much the ongoing process reduces the entropy. When a multiplier vanishes the process is balanced. When the error $\delta\lambda_\alpha(k)$ in a particular $\lambda_\alpha(k)$ is comparable to it, the process need not be included.

In summary, we represent the fitted intensities as

$$\ln X_i(k) \quad = \quad \ln X_i^o(k) - \sum_{\alpha=1} G_{i\alpha}\lambda_\alpha(k)$$

where the sum is restricted to such $\lambda_\alpha(k)$ whose error is small $\delta\lambda_\alpha(k) < \lambda_\alpha(k)$.

c. Error determination in surprisal analysis.

The experiment was performed in four biological replicates and the standard deviation, *s.d.* was taken for each expression level when given. Surprisal analysis was performed 3 times. Once for the mean values of the proteins, once for the mean values of the protein expression $+s.d.$ for each measured protein, and once for the mean of the protein expression $-s.d.$ Proteins with large $s.d.$, so that their values of $(mean - s.d) < 0$, were excluded from the analysis. Thus three values for the weights $\lambda_\alpha(r)$ were obtained. Results of Suprisal analysis presented in the article are the mean values of the corresponded parameters $\pm s.d.$ [8]

d. Minor unbalanced processes

The higher index constraints usually exhibit smaller influences on protein/transcript expression levels [1, 2]. Constraints 5, 6 and 7 were found to influence significantly GBM 8, 15, 26 and 6. To validate the significance of these last constraints we analyzed a smaller data set that included only those four GBM tumors. Surprisal analysis of the smaller matrix showed that the stable state term remains the same, to within experimental error, as when it is calculated using all 7 tumors (Fig. S5a). When only the dataset for the four tumors is analyzed, 3 constraints are readily resolved. Those constraints correspond roughly to the constraints 5-7 when the data for all tumors is analyzed. This is shown in Fig. S5b,c and in Fig.S6, and validates that we do in fact resolve all 7 constraints when analyzing the whole data set. Fig. S5d illustrates the influence of constraints 5-7 on a couple of different proteins. These results confirm the significance of the minor unbalanced processes in GBM tumors and also provide an illustration of the robustness of surprisal analysis.

The minor constraints provide a higher resolution for differentiation of the 8 GBM tumors (Fig. S5 and Fig. S6). For example, the constraint $\alpha = 5$ distinguishes between GBM6 and GBM15 (Fig. S6). This constraint increases the expression of key proteins participating in Ras/MAPK signaling, as well as in glycolysis through oxidative phosphorylation in GBM6. Proteins that are influenced include multiple ATP synthases, aldolase A, LDHB, IDH2, pMAPK3, pP38 (MAPK14), and pMAPK12 (Table S6).

e. Experimental procedure and processing of the raw proteomic data

Experimental procedure

Detailed description of all experimental procedures related to the iTRAQ proteomic dataset is described in detail in [9]. Here we provide essential information for understanding of the current paper. GBM xenografts were labeled using the iTRAQ 8plex channels as follows: 113-GBM6; 114-GBM8; 115-GBM10; 116-GBM12; 117-GBM15; 118-GBM26; 119-GBM39; and 121-GBM59 throughout all four biological replicates. GBM6 biological replicate 1 and biological replicate 4 were analyzed in the place of biological replicate 2 and 3 respectively.

The way that the iTRAQ intensities were generated as follows; the raw iTRAQ8plex intensities were summed for all peptides (and all instances of each peptide) derived from a particular protein were quantified. This was also done for all instances that a peptide or phosphotyrosine peptide was quantified. For either protein expression quantification or phosphotyrosine quantification this was carried out within each analysis (i.e. for each biological replicate) and then across all 4 biological replicates. The implication of this is that the peptides that have a greater intensity are weighted more towards the total iTRAQ8plex intensity readout for each given protein or phosphotyrosine peptide. This effectively reduces the impact of instrumental noise on the resulting intensities. These raw values were then normalized to the iTRAQ8plex ratios to account for protein loading within each of the iTRAQ8plex channels. These final intensities can then also be expressed as ratios either relative for the mean of all 8 channels or expressed as a ratio relative to a single channel.

Processing of the raw proteomic data

A decoy database search strategy was used to estimate the false discovery rate (FDR), defined as the percentage of decoy proteins identified against the total protein identification. The FDR was calculated by searching the spectra against the NCBI nonredundant Homo sapiens decoy database. Before filtering the protein expression data (explained above), the protein level FDR was calculated at 1%, corresponding to 2357, 2122, 2434, and 2222 proteins in biological replicates 1, 2, 3, and 4 respectively. After application of the above filter criteria, the estimated FDR value was <1% (at the protein level) for each of the biological replicates analyzed, indicating a high reliability in the proteins identified. Peptide summaries were exported from ProteinPilotTM and isotope correction and relative quantification was calculated in Excel. Based on the biological variation, observed proteins with iTRAQ ratios below 0.75 were considered to be reduced in expression and proteins with iTRAQ ratios above 1.25 were considered to be increased in expression.

For the phosphotyrosine data a Mascot score cutoff of 25 was used to initially filter the data (this corresponds to a FDR cutoff of 1%). We further interrogated the data by manually validating the spectra and only included spectra

where we were sure of the peptide sequence and the location of the phosphorylation site on the peptide sequence. All validated mass spectra for the phosphotyrosine peptides are included in the original manuscript.

The overlapping data was discussed in [9]. The overlapping phosphotyrosine peptides and proteins quantified across each biological replicate. As each analysis included all 8 of the GBM xenograft lines there were no instances of missing data. There were only instances of peptides or phosphorylation sites that were not quantified across more than 1 biological replicate [9].

2. Biological classification of the proteins participating in the Unbalanced processes $\alpha = 1,2,...7$

Only statistically significant biological groups (EASE score and Benjamini correction values ≤ 0.05) were included in biological interpretation of the constraints. Similar statistical considerations were applied to all unbalanced processes. A more complete list of proteins that are influenced significantly by the different constraints is provided in the **Additional Table SI**. Tables S1-S8 include both proteins with altered expression and altered phosphorylation. To distinguish between proteins with altered expression and altered phosphorylation in every constraint see **Additional Table SI**.

Table S1. GO classification of the proteins influenced mostly by the Steady state term.

GO Term	Count	EASE score	Proteins	Benjamini correction
GO:0006412~translation	65	4.33E-30	EIF6, EIF5, EIF5B, QARS, RPS3, RPS3A, RPLP0, RPL10, RPL11, RPL12, TPR, RPS27A, CARS, YARS, DARS, EIF2S3, EIF4G1, EIF4G2, TARS, RPS19, RPS17, RARS, EIF2S1, RPS14, EIF4A2, EIF4A1, RPS12, HARS, FARSB, FARSA, NACA, PABPC4, RPS15A, RPL36, RPL38, VARS, EIF3C, EIF3D, RPS26, EIF3A, RPS28, EIF3B, MRPL12, EIF3G, EIF3H, EIF3E, RPL9, LARS, EIF3K, EIF3I, RPL4, RPS20, RPS21, RPS24, MARS, RPSA, EEF1A1, RRBP1, EPRS, DENR, ETF1, RPS5, RPS7, RPL23, TSFM	9.62E-27
GO:0008380~RNA splicing	51	9.45E-22	SNRPD3, LSM7, SNRPD1, SNRPD2, SYNCRIP, SART1, PNN, DDX23, RBM8A, PRMT5, SRRM2, PCBP1, U2AF1, LUC7L3, SNRPA1, PPP2R1A, EFTUD2, PTBP1, MBNL1, HNRNPR, EIF4A3, SNRNP200, SNRPB, RBM39, SNRPE, NHP2L1, STRAP, TRA2B, SF3B4, SF3B3, SF3B2, PRPF19, HNRNPL, HNRNPA3, HNRNPM, SF3B1, DDX46, PPP2CA, PRPF8, DHX15, HNRNPD, PABPC1, DHX9, RNPS1, DDX5, SF3A2, SF3A1, HNRNPH3, HNRNPUL1, RBM14, PUF60	1.05E-18
GO:0016071~mRNA metabolic process	58	9.97E-22	SNRPD3, LSM7, SNRPD1, SNRPD2, SYNCRIP, HNRPLL, SART1, PNN, DCPS, APP, DNAJB11, DDX23, RBM8A, PRMT5, SRRM2, PCBP1, U2AF1, LUC7L3, SNRPA1, EFTUD2, PTBP1, MBNL1, HNRNPR, EIF4A3, SNRNP200, SNRPB, CPSF6, RBM39, SNRPE, NHP2L1, STRAP, TRA2B, RNH1, SF3B4, SF3B3, SF3B2, PRPF19, HNRNPL, HNRNPA3, HNRNPM, SF3B1, DDX46, PRPF8, EIF3E, DHX15, HNRNPD, PABPC1, DHX9, UPF1, ELAVL1, RNPS1, DDX5, SF3A2, SF3A1, HNRNPH3, HNRNPUL1, RBM14, PUF60	7.38E-19
GO:0006397~mRNA processing	52	3.98E-20	SNRPD3, LSM7, SNRPD1, SNRPD2, SYNCRIP, HNRPLL, SART1, PNN, APP, DDX23, RBM8A, PRMT5, SRRM2, PCBP1, U2AF1, LUC7L3, SNRPA1, EFTUD2, PTBP1, MBNL1, HNRNPR, EIF4A3, SNRNP200, SNRPB, CPSF6, RBM39, SNRPE, NHP2L1, STRAP, TRA2B, SF3B4, SF3B3, SF3B2, PRPF19, HNRNPL, HNRNPA3, HNRNPM, SF3B1, DDX46, PRPF8, DHX15, HNRNPD, PABPC1, DHX9, RNPS1, DDX5, SF3A2, SF3A1, HNRNPH3, HNRNPUL1, RBM14, PUF60	2.21E-17
GO:0006396~RNA processing	67	3.51E-19	SNRPD3, LSM7, SNRPD1, SNRPD2, SYNCRIP, HNRPLL, SART1, PNN, APP, DDX17, DDX23, RBM8A, PCBP1, PRMT5, SRRM2, U2AF1, RPL11, LUC7L3, SNRPA1, PPP2R1A, EFTUD2, PTBP1, MBNL1, HNRNPR, EIF4A3, PA2G4, RPS19, RPS17, RPS14, SNRNP200, SNRPB, CPSF6, RBM39, SNRPE, HSD17B10, NHP2L1, STRAP, TRA2B, PABPC4, SF3B4, SF3B3, SF3B2, HNRNPA3, PRPF19, HNRNPL, SRRT, HNRNPM, SF3B1, RPS28, DDX46, PPP2CA, PRPF8, HNRNPD, DHX15, PABPC1, RPS24, DHX9, RNPS1, DDX5, SF3A2, SF3A1, FBL, RPS7, HNRNPH3, HNRNPUL1, RBM14, PUF60	1.56E-16
GO:0000398~nuclear mRNA splicing, via spliceosome	34	1.83E-17	NHP2L1, TRA2B, SNRPD3, LSM7, SNRPD1, SNRPD2, SF3B4, SF3B3, SF3B2, HNRNPL, HNRNPA3, HNRNPM, SF3B1, DDX23, RBM8A, PRMT5, PRPF8, PCBP1, HNRNPD, U2AF1, DHX9, SNRPA1, EFTUD2, PTBP1, RNPS1, MBNL1, SF3A2, SF3A1, HNRNPR, HNRNPH3, HNRNPUL1, SNRNP200, SNRPB, SNRPE	6.79E-15
GO:0000375~RNA splicing, via transesterification reactions	34	1.83E-17	NHP2L1, TRA2B, SNRPD3, LSM7, SNRPD1, SNRPD2, SF3B4, SF3B3, SF3B2, HNRNPL, HNRNPA3, HNRNPM, SF3B1, DDX23, RBM8A, PRMT5, PRPF8, PCBP1, HNRNPD, U2AF1, DHX9, SNRPA1, EFTUD2,	6.79E-15

			PTBP1, RNPS1, MBNL1, SF3A2, SF3A1, HNRNPR, HNRNPH3, HNRNPUL1, SNRNP200, SNRPB, SNRPE	
GO:0000377~RNA splicing, via transesterification reactions with bulged adenosine as nucleophile	34	1.83E-17	NHP2L1, TRA2B, SNRPD3, LSM7, SNRPD1, SNRPD2, SF3B4, SF3B3, SF3B2, HNRNPL, HNRNPA3, HNRNPM, SF3B1, DDX23, RBM8A, PRMT5, PRPF8, PCBP1, HNRNPD, U2AF1, DHX9, SNRPA1, EFTUD2, PTBP1, RNPS1, MBNL1, SF3A2, SF3A1, HNRNPR, HNRNPH3, HNRNPUL1, SNRNP200, SNRPB, SNRPE	6.79E-15
GO:0006414~translational elongation	28	4.97E-17	RPS15A, RPL36, RPL38, VARS, RPS3, RPS26, RPS28, RPS3A, RPLP0, RPL9, RPL10, RPL11, RPL12, RPL4, RPS20, RPS21, RPS27A, RPS24, RPSA, EEF1A1, RPS5, RPS7, RPS19, RPL23, RPS17, RPS14, TSFM, RPS12	1.58E-14
GO:0051443~positive regulation of ubiquitin-protein ligase activity	24	6.85E-17	SKP1, PSMA7, UBE2N, PSMF1, PSMC6, PSMD13, PSMC5, PSMB1, PSMD12, PSMC4, PSMD11, PSMB3, PSMC2, PSMA4, PSMD1, PSMC1, PSMD2, PSMD4, PSME3, PSMD5, PSMD6, PSMD7, RPS27A, PSMD8	3.09E-14
GO:0051438~regulation of ubiquitin-protein ligase activity	25	7.97E-17	PSMA7, PSMF1, PSMB1, PSMB3, PSMD1, PSMD2, PSMD4, PSMD5, PSMD6, PSMD7, BUB3, RPS27A, PSMD8, SKP1, UBE2N, PSMC6, PSMC5, PSMD13, PSMD12, PSMC4, PSMD11, PSMA4, PSMC2, PSMC1, PSME3	2.74E-14
GO:0051439~regulation of ubiquitin-protein ligase activity during mitotic cell cycle	24	9.8E-17	SKP1, PSMA7, PSMF1, PSMC6, PSMD13, PSMC5, PSMB1, PSMD12, PSMC4, PSMD11, PSMB3, PSMC2, PSMA4, PSMD1, PSMC1, PSMD2, PSMD4, PSME3, PSMD5, PSMD6, PSMD7, RPS27A, PSMD8, BUB3	2.46E-14
GO:0031145~anaphase-promoting complex-dependent proteasomal ubiquitin-dependent protein catabolic process	23	1.59E-16	PSMA7, PSMF1, PSMC6, PSMD13, PSMC5, PSMB1, PSMD12, PSMC4, PSMD11, PSMB3, PSMC2, PSMA4, PSMD1, PSMC1, PSMD2, PSMD4, PSME3, PSMD5, PSMD6, PSMD7, RPS27A, PSMD8, BUB3	2.24E-14
GO:0051436~negative regulation of ubiquitin-protein ligase activity during mitotic cell cycle	23	1.59E-16	PSMA7, PSMF1, PSMC6, PSMD13, PSMC5, PSMB1, PSMD12, PSMC4, PSMD11, PSMB3, PSMC2, PSMA4, PSMD1, PSMC1, PSMD2, PSMD4, PSME3, PSMD5, PSMD6, PSMD7, RPS27A, PSMD8, BUB3	2.24E-14
GO:0051351~positive regulation of ligase activity	24	1.96E-16	SKP1, PSMA7, UBE2N, PSMF1, PSMC6, PSMD13, PSMC5, PSMB1, PSMD12, PSMC4, PSMD11, PSMB3, PSMC2, PSMA4, PSMD1, PSMC1, PSMD2, PSMD4, PSME3, PSMD5, PSMD6, PSMD7, RPS27A, PSMD8	4.11E-14
GO:0051340~regulation of ligase activity	25	2.1E-16	PSMA7, PSMF1, PSMB1, PSMB3, PSMD1, PSMD2, PSMD4, PSMD5, PSMD6, PSMD7, BUB3, RPS27A, PSMD8, SKP1, UBE2N, PSMC6, PSMC5, PSMD13, PSMD12, PSMC4, PSMD11, PSMA4, PSMC2, PSMC1, PSME3	3.8E-14
GO:0051444~negative regulation of ubiquitin-protein ligase activity	23	3.31E-16	PSMA7, PSMF1, PSMC6, PSMD13, PSMC5, PSMB1, PSMD12, PSMC4, PSMD11, PSMB3, PSMC2, PSMA4, PSMD1, PSMC1, PSMD2, PSMD4, PSME3, PSMD5, PSMD6, PSMD7, RPS27A, PSMD8, BUB3	5.28E-14
GO:0051352~negative regulation of ligase activity	23	3.31E-16	PSMA7, PSMF1, PSMC6, PSMD13, PSMC5, PSMB1, PSMD12, PSMC4, PSMD11, PSMB3, PSMC2, PSMA4, PSMD1, PSMC1, PSMD2, PSMD4, PSME3, PSMD5, PSMD6, PSMD7, RPS27A, PSMD8, BUB3	5.28E-14
GO:0051437~positive regulation of ubiquitin-protein ligase activity during mitotic cell cycle	23	4.73E-16	SKP1, PSMA7, PSMF1, PSMC6, PSMD13, PSMC5, PSMB1, PSMD12, PSMC4, PSMD11, PSMB3, PSMC2, PSMA4, PSMD1, PSMC1, PSMD2, PSMD4, PSME3, PSMD5, PSMD6, PSMD7, RPS27A, PSMD8	6.58E-14
GO:0031398~positive regulation of protein ubiquitination	25	5.28E-16	FKBP1A, PSMA7, PSMF1, PSMB1, PSMB3, PSMD1, PSMD2, PSMD4, PSMD5, PSMD6, PSMD7, RPS27A, PSMD8, SKP1, UBE2N, PSMC6, PSMC5, PSMD13, PSMD12, PSMC4, PSMD11, PSMA4, PSMC2, PSMC1, PSME3	7.7E-14
GO:0031397~negative regulation of protein ubiquitination	23	3.84E-15	PSMA7, PSMF1, PSMC6, PSMD13, PSMC5, PSMB1, PSMD12, PSMC4, PSMD11, PSMB3, PSMC2, PSMA4, PSMD1, PSMC1, PSMD2, PSMD4, PSME3, PSMD5, PSMD6, PSMD7, RPS27A, PSMD8, BUB3	5.08E-13
GO:0031396~regulation of protein ubiquitination	26	4.45E-15	FKBP1A, PSMA7, PSMF1, PSMB1, PSMB3, PSMD1, PSMD2, PSMD4, PSMD5, PSMD6, PSMD7, BUB3, RPS27A, PSMD8, SKP1, UBE2N, PSMC6, PSMC5, PSMD13, PSMD12, PSMC4, PSMD11, PSMA4, PSMC2, PSMC1, PSME3	5.48E-13
GO:0031400~negative regulation of protein modification process	28	4.81E-15	FKBP1A, PSMA7, PSMF1, PSMB1, PSMB3, PPP2CA, PSMD1, PSMD2, PSMD4, PSMD5, PSMD6, PSMD7, BUB3, RPS27A, PSMD8, PPP2R1A, YWHAB, PSMC6, PSMD13, PSMC5, PSMD12, PSMC4, PSMD11, BAX, PSMA4, PSMC2, PSMC1, PSME3	5.58E-13
GO:0032268~regulation of cellular protein metabolic process	54	4.58E-14	HSP90AB1, METAP1, EIF5, EIF5B, APP, PRKAR2A, RBM8A, PSMD1, PSMD2, PSMD4, PSMD5, PSMD6, PSMD7, PSMD8, RPS27A, DBNL, PPP2R1A, SKP1, UBE2N, EIF4G1, SARNP, MAPK1, EIF4A3, EIF4G2, PA2G4, PSMA4, EIF2S1, EIF4A2, F2, PSME3, FKBP1A, PSMA7, PSMF1, EIF3B, PSMB1, EIF3H, PSMB3, PPP2CA, EIF3E, EIF3K,	5.09E-12

			BUB3, UPF1, YWHAB, ETF1, RPS5, PSMC6, PSMD13, PSMC5, PSMD12, PSMC4, PSMD11, BAX, PSMC2, PSMC1	
GO:0043161~proteasomal ubiquitin-dependent protein catabolic process	24	6.03E-13	ERLIN2, PSMA7, PSMF1, PSMC6, PSMD13, PSMC5, PSMB1, PSMD12, PSMC4, PSMD11, PSMB3, PSMC2, PSMA4, PSMD1, PSMC1, PSMD2, PSMD4, PSME3, PSMD5, PSMD6, PSMD7, RPS27A, PSMD8, BUB3	6.38E-11
GO:0010498~proteasomal protein catabolic process	24	6.03E-13	ERLIN2, PSMA7, PSMF1, PSMC6, PSMD13, PSMC5, PSMB1, PSMD12, PSMC4, PSMD11, PSMB3, PSMC2, PSMA4, PSMD1, PSMC1, PSMD2, PSMD4, PSME3, PSMD5, PSMD6, PSMD7, RPS27A, PSMD8, BUB3	6.38E-11

Table S2. GO classification of the proteins influenced by the unbalanced process $\alpha = 1$

Increased protein expression in GBMwt+ and GBM EGFRVIII tumors due to $\alpha = 1$

GO Term	Count	EASE score	Proteins	Benjamini correction
GO:0007010~cytoskeleton organization	21	1.4E-11	ALDOA, ARHGEF2, CNN3, TLN2, CRYAB, BCAR1, ABI2, ACTN1, ITGB1, WAS, LLGL1, ACTG1, EPB41L2, TUBB, ERBB2IP, FGFR1OP, CFL1, MAP2, FGD5, ABL2, DBN1	1.4E-08
GO:0030036~actin cytoskeleton organization	15	4.7E-10	ALDOA, ARHGEF2, CNN3, BCAR1, ABI2, ACTN1, WAS, ITGB1, LLGL1, ACTG1, EPB41L2, CFL1, FGD5, DBN1, ABL2	2.4E-07
GO:0030029~actin filament-based process	15	1.1E-09	ALDOA, ARHGEF2, CNN3, BCAR1, ABI2, ACTN1, WAS, ITGB1, LLGL1, ACTG1, EPB41L2, CFL1, FGD5, DBN1, ABL2	3.7E-07
GO:0007015~actin filament organization	9	3.3E-08	ALDOA, ARHGEF2, BCAR1, CFL1, ABI2, ACTN1, ABL2, WAS, DBN1	8.5E-06
GO:0007173~epidermal growth factor receptor signaling pathway	6	1.3E-06	EGFR, EPS15, ERBB2IP, BCAR1, CBL, GAB1	2.6E-04
GO:0007169~transmembrane receptor protein tyrosine kinase signaling pathway	11	3.4E-06	EGFR, EPS15, DDR1, EPHA4, MPZL1, ERBB2IP, BCAR1, CBL, GAB1, PTPRA, STAT3	5.7E-04
GO:0006793~phosphorus metabolic process	21	9.2E-06	EGFR, FYB, DBNL, LYN, INPPL1, PTPRZ1, HCK, PTPRA, ABI2, MAPK11, FER, ACP1, DDR1, MAPK1, EPHA4, MAPK12, GAB1, MAP2, NDUFS8, CFL1, ABL2	1.3E-03
GO:0006796~phosphate metabolic process	21	9.2E-06	EGFR, FYB, DBNL, LYN, INPPL1, PTPRZ1, HCK, PTPRA, ABI2, MAPK11, FER, ACP1, DDR1, MAPK1, EPHA4, MAPK12, GAB1, MAP2, NDUFS8, CFL1, ABL2	1.3E-03
GO:0006468~protein amino acid phosphorylation	17	1.3E-05	EGFR, FYB, DBNL, LYN, HCK, PTPRA, ABI2, MAPK11, FER, DDR1, EPHA4, MAPK1, MAPK12, MAP2, CFL1, GAB1, ABL2	1.6E-03
GO:0006928~cell motion	14	2.4E-05	CCDC88A, BCAR1, ANXA1, ABI2, YWHAE, ITGB1, STAT3, VCL, ACTG1, EPHA4, TUBB, ROBO1, CFL1, HSPB1	2.6E-03
GO:0007167~enzyme linked receptor protein signaling pathway	12	2.4E-05	EGFR, EPS15, DDR1, EPHA4, MPZL1, ERBB2IP, BCAR1, ZFYVE16, CBL, GAB1, PTPRA, STAT3	2.5E-03
GO:0016310~phosphorylation	18	3.2E-05	EGFR, FYB, DBNL, LYN, HCK, PTPRA, ABI2, MAPK11, FER, DDR1, EPHA4, MAPK1, MAPK12, MAP2, NDUFS8, CFL1, GAB1, ABL2	2.9E-03
GO:0018108~peptidyl-tyrosine phosphorylation	5	2.9E-04	DDR1, LYN, ABI2, FER, ABL2	2.4E-02
GO:0006096~glycolysis	5	3.1E-04	ALDOA, GPI, LDHB, ALDOC, ENO1	2.4E-02
GO:0007155~cell adhesion	15	3.2E-04	EGFR, RPSA, INPPL1, TLN2, BCAR1, CTNND2, ACTN1, CTNND1, FER, ITGB1, VCL, DDR1, ERBB2IP, ROBO1, ABL2	2.3E-02
GO:0022610~biological adhesion	15	3.3E-04	EGFR, RPSA, INPPL1, TLN2, BCAR1, CTNND2, ACTN1, CTNND1, FER, ITGB1, VCL, DDR1, ERBB2IP, ROBO1, ABL2	2.2E-02
GO:0018212~peptidyl-tyrosine modification	5	3.4E-04	DDR1, LYN, ABI2, FER, ABL2	2.1E-02
GO:0032989~cellular component morphogenesis	11	4.3E-04	EGFR, ACTG1, EPHA4, ARHGEF2, ERBB2IP, PTPRZ1, ROBO1, CFL1, ITGB1, SLITRK5, LLGL1	2.5E-02
GO:0009719~response to endogenous stimulus	11	5.0E-04	MAPK1, A2M, LYN, CRYAB, ALDOC, BCAR1, GAB1, CFL1, PTPRA, IDH1, STAT3	2.8E-02
GO:0006006~glucose metabolic process	7	6.8E-04	ALDOA, GPI, LDHB, CRYAB, ALDOC, PHKA1, ENO1	3.6E-02

GO:0006007~glucose catabolic process	5	7.0E-04	ALDOA, GPI, LDHB, ALDOC, ENO1	3.5E-02
GO:0030030~cell projection organization	10	1.0E-03	EGFR, EPHA4, CCDC88A, PTPRZ1, ROBO1, MAP2, ABI2, FGD5, SLITRK5, VCL	4.8E-02

Decreased protein expression in GBMwt+ and GBM EGFRVIII tumors

There are no statistically significant biological categories.

Table S3. GO classification of the proteins influenced by the unbalanced process $\alpha = 2$

Increased protein expression in GBM39 and 59 due to $\alpha = 2$

GO Term	Count	EASE score	Proteins	Benjamini correction
GO:0030029~actin filament-based process	16	2.4E-09	MYL6, ALDOA, ARHGEF2, TLN1, ACTA1, MYL1, ACTN1, MYH4, MYH9, TPM1, ACTG1, EZR, PTK2B, FGD5, DBN1, ABL2	3.1E-06
GO:0030036~actin cytoskeleton organization	13	5.8E-07	ALDOA, TLN1, ARHGEF2, ACTA1, ACTN1, MYH9, TPM1, ACTG1, EZR, PTK2B, FGD5, DBN1, ABL2	3.9E-04
GO:0007015~actin filament organization	8	2.8E-06	ALDOA, ARHGEF2, EZR, ACTA1, PTK2B, ACTN1, ABL2, DBN1	1.2E-03
GO:0006928~cell motion	17	3.2E-06	TLN1, PODXL, ANXA1, MYH9, VAV2, TPM1, STAT3, TPM4, VCL, TPM3, ACTG1, CD44, PTK2B, HSPB1, MSN, THBS1, GAP43	1.1E-03
GO:0007173~epidermal growth factor receptor signaling pathway	6	3.7E-06	EGFR, EPS15, PTK2B, CBL, GAB1, SHC1	9.9E-04
GO:0007155~cell adhesion	20	8.3E-06	DCBLD2, EGFR, INPPL1, TNC, ACTN1, CD99, MYH9, CD151, PXN, VCL, LGALS3BP, EZR, COL14A1, CD44, PTK2B, COL6A3, COL6A2, MSN, THBS1, ABL2	1.9E-03
GO:0022610~biological adhesion	20	8.5E-06	DCBLD2, EGFR, INPPL1, TNC, ACTN1, CD99, MYH9, CD151, PXN, VCL, LGALS3BP, EZR, COL14A1, CD44, PTK2B, COL6A3, COL6A2, MSN, THBS1, ABL2	1.6E-03
GO:0030030~cell projection organization	14	1.7E-05	EGFR, UCHL1, CLU, GJA1, MYH9, VAV2, HPRT1, TPM1, VCL, CD44, PTK2B, FGD5, SLITRK5, GAP43	2.9E-03
GO:0007010~cytoskeleton organization	15	2.4E-05	ALDOA, ARHGEF2, TLN1, CAV1, ACTA1, ACTN1, MYH9, TPM1, ACTG1, EZR, PTK2B, FGFR1OP, FGD5, DBN1, ABL2	3.5E-03
GO:0030048~actin filament-based movement	5	4.1E-05	MYL6, MYL1, MYH4, MYH9, TPM1	5.5E-03
GO:0070252~actin-mediated cell contraction	4	5.1E-05	MYL6, MYL1, MYH4, TPM1	6.2E-03
GO:0030049~muscle filament sliding	4	5.1E-05	MYL6, MYL1, MYH4, TPM1	6.2E-03
GO:0033275~actin-myosin filament sliding	4	5.1E-05	MYL6, MYL1, MYH4, TPM1	6.2E-03
GO:0030705~cytoskeleton-dependent intracellular transport	6	8.3E-05	MYL6, MYL1, UCHL1, MYH4, MYH9, TPM1	9.2E-03
GO:0042692~muscle cell differentiation	8	8.5E-05	ACTG1, CAST, ACTA1, TNC, LGALS1, MYH9, CAPN2, TPM1	8.7E-03
GO:0051146~striated muscle cell differentiation	7	1.1E-04	ACTG1, CAST, ACTA1, TNC, MYH9, CAPN2, TPM1	1.1E-02
GO:0000768~syncytium formation by plasma membrane fusion	4	1.3E-04	CAST, CD44, MYH9, CAPN2	1.2E-02
GO:0007169~transmembrane receptor protein tyrosine kinase signaling pathway	10	1.4E-04	EGFR, EPS15, PTK2B, CBL, GAB1, ABI1, SHC1, STAT3, EPHA2, PXN	1.2E-02
GO:0032989~cellular component morphogenesis	13	1.6E-04	EGFR, ARHGEF2, ACTA1, UCHL1, CLU, GJA1, HPRT1, MYH9, TPM1, ACTG1, EZR, SLITRK5, GAP43	1.3E-02
GO:0007167~enzyme linked receptor protein signaling pathway	12	1.8E-04	EGFR, EPS15, PTK2B, ZFYVE16, CBL, GAB1, COL1A2, ABI1, SHC1, STAT3, EPHA2, PXN	1.3E-02
GO:0006949~syncytium formation	4	2.1E-04	CAST, CD44, MYH9, CAPN2	1.5E-02

GO:0043405~regulation of MAP kinase activity	8	2.2E-04	EGFR, SPRY1, CAV1, PTK2B, GAB1, SHC1, THBS1, SPRY4	1.5E-02
GO:0006936~muscle contraction	8	3.6E-04	MYL6, ALDOA, ACTA1, MYH1, MYL1, MYH4, GJA1, TPM1	2.3E-02
GO:0030182~neuron differentiation	13	4.0E-04	EGFR, UCHL1, CLU, GJA1, HPRT1, RTN1, EPHA2, STAT3, CD44, PTK2B, SLITRK5, TUBB3, GAP43	2.4E-02
GO:0034329~cell junction assembly	5	4.2E-04	TLN1, PTK2B, GJA1, ACTN1, VCL	2.4E-02
GO:0032507~maintenance of protein location in cell	5	4.2E-04	TLN1, CAV1, EZR, PDIA3, FGFR1OP	2.4E-02
GO:0007517~muscle organ development	9	4.9E-04	MYL6, CAV1, ACTA1, TNC, COL6A3, MYL1, LMNA, TAGLN2, TPM1	2.7E-02
GO:0006979~response to oxidative stress	8	5.5E-04	EGFR, PTK2B, CLU, GAB1, CA3, PDLIM1, TPM1, PXN	2.9E-02
GO:0003012~muscle system process	8	6.3E-04	MYL6, ALDOA, ACTA1, MYH1, MYL1, MYH4, GJA1, TPM1	3.2E-02
GO:0006096~glycolysis	5	7.1E-04	ALDOA, PKM2, ENO3, PGK1, ENO1	3.5E-02
GO:0051017~actin filament bundle formation	4	7.5E-04	EZR, PTK2B, ACTN1, ABL2	3.5E-02
GO:0051651~maintenance of location in cell	5	7.7E-04	TLN1, CAV1, EZR, PDIA3, FGFR1OP	3.5E-02
GO:0045185~maintenance of protein location	5	7.7E-04	TLN1, CAV1, EZR, PDIA3, FGFR1OP	3.5E-02
GO:0044275~cellular carbohydrate catabolic process	6	8.4E-04	ALDOA, PKM2, ENO3, PGK1, PYGB, ENO1	3.7E-02
GO:0043549~regulation of kinase activity	11	1.1E-03	EGFR, SPRY1, CAV1, YWHAG, PTK2B, GAB1, SHC1, VAV2, THBS1, SPRY4, GAP43	4.4E-02
GO:0051592~response to calcium ion	5	1.3E-03	EGFR, ACTG1, CAV1, PTK2B, THBS1	5.2E-02
GO:0051270~regulation of cell motion	8	1.4E-03	EGFR, LYN, PTK2B, GAB1, ACTN1, THBS1, TPM1, VCL	5.6E-02

Decreased protein expression in GBM39 and 59 due to $\alpha = 2$

GO Term	**Count**	**EASE score**	**Proteins**	**Benjamini correction**
GO:0006323~DNA packaging	8	2.1E-06	HIST1H2BB, SET, HIST1H4A, HIST1H2BL, HIST1H1B, SMARCA5, H2AFX, SMC4	0.002
GO:0006334~nucleosome assembly	7	4.2E-06	HIST1H2BB, SET, HIST1H4A, HIST1H2BL, HIST1H1B, SMARCA5, H2AFX	0.002
GO:0033554~cellular response to stress	14	4.7E-06	CDK1, HMGB1, MSH6, CRYAB, MAP1B, RPA3, TYMS, MAPK1, MAPK12, ALB, GSK3B, PCNA, H2AFX, APEX1	0.002
GO:0031497~chromatin assembly	7	5.1E-06	HIST1H2BB, SET, HIST1H4A, HIST1H2BL, HIST1H1B, SMARCA5, H2AFX	0.001
GO:0065004~protein-DNA complex assembly	7	6.7E-06	HIST1H2BB, SET, HIST1H4A, HIST1H2BL, HIST1H1B, SMARCA5, H2AFX	0.001
GO:0034728~nucleosome organization	7	7.6E-06	HIST1H2BB, SET, HIST1H4A, HIST1H2BL, HIST1H1B, SMARCA5, H2AFX	0.001
GO:0006333~chromatin assembly or disassembly	7	4.5E-05	HIST1H2BB, SET, HIST1H4A, HIST1H2BL, HIST1H1B, SMARCA5, H2AFX	0.007
GO:0006974~response to DNA damage stimulus	10	1.1E-04	CDK1, HMGB1, TYMS, MAPK1, MSH6, MAPK12, PCNA, H2AFX, APEX1, RPA3	0.015
GO:0007242~intracellular signaling cascade	18	1.4E-04	PRKCA, C9ORF86, CDK1, MSH6, CRYAB, PARK7, TYMS, MAPK1, MAPK12, HIST1H4A, GSK3B, ANP32A, PCNA, RHEB, GNAS, H2AFX, STMN1, PAG1	0.017
GO:0051276~chromosome organization	11	1.6E-04	HMGB1, HIST1H2BB, KDM1A, MSH6, SET, HIST1H4A, HIST1H2BL, HIST1H1B, SMARCA5, H2AFX, SMC4	0.017
GO:0034621~cellular macromolecular complex subunit organization	9	4.5E-04	NUP133, HIST1H2BB, SET, HIST1H4A, HIST1H2BL, HIST1H1B, SMARCA5, H2AFX, STMN1	0.042
GO:0006325~chromatin organization	9	6.5E-04	HMGB1, HIST1H2BB, KDM1A, SET, HIST1H4A, HIST1H2BL, HIST1H1B, SMARCA5, H2AFX	0.056

Table S4. GO classification of the proteins influenced by the unbalanced process $\alpha = 3$

Increased protein expression in GBM15 due to $\alpha = 3$

GO Term	Count	EASE score	Proteins	Benjamini correction
GO:0030036~actin cytoskeleton organization	10	3.2E-05	ACTG1, TLN1, CNN3, GSN, PTK2B, BCAR1, CFL1, FSCN1, FGD5, DBN1	0.032
GO:0007173~epidermal growth factor receptor signaling pathway	5	4.3E-05	EGFR, ERBB2IP, PTK2B, BCAR1, SRC	0.022
GO:0030029~actin filament-based process	10	5.2E-05	ACTG1, TLN1, CNN3, GSN, PTK2B, BCAR1, CFL1, FSCN1, FGD5, DBN1	0.018
GO:0007010~cytoskeleton organization	13	5.8E-05	TLN1, CNN3, BCAR1, FSCN1, ACTG1, ERBB2IP, PTK2B, GSN, FGFR1OP, CFL1, SYNM, FGD5, DBN1	0.015
GO:0007265~Ras protein signal transduction	7	1.0E-04	MAPK1, DBNL, NTRK1, MAPK3, CFL1, COL1A2, SRC	0.020
GO:0010035~response to inorganic substance	9	1.0E-04	EGFR, ACTG1, GSN, PTK2B, FGB, EEF1A2, PRDX5, COL1A1, PXN	0.018
GO:0006928~cell motion	13	1.3E-04	TLN1, CCDC88A, BCAR1, PODXL, VIM, VAV2, SRC, ACTG1, PTK2B, ROBO1, CFL1, HSPB1, GAP43	0.019
GO:0007015~actin filament organization	6	1.6E-04	GSN, PTK2B, BCAR1, CFL1, FSCN1, DBN1	0.020
GO:0030030~cell projection organization	11	2.8E-04	EGFR, PARD3, SEPT2, CCDC88A, S100B, ROBO1, PTK2B, UCHL1, FGD5, VAV2, GAP43	0.031

Decreased protein expression in GBM15 to $\alpha = 3$

There are no statistically significant biological categories.

Table S5. GO classification of the proteins influenced by the unbalanced process $\alpha = 4$

Increased protein expression in GBM59 due to $\alpha = 4$

GO Term	Count	EASE score	Proteins	Benjamini correction
GO:0006468~protein amino acid phosphorylation	16	9.7E-06	EGFR, CDK1, TAOK1, PMVK, EPHA2, EPHA4, MAPK1, MAPK12, MAPK14, NTRK1, DYRK1A, HIPK2, MAPK3, CFL1, YES1, ABL2	0.010
GO:0007265~Ras protein signal transduction	7	4.1E-05	MAPK1, MAPK12, MAPK14, NTRK1, MAPK3, CFL1, PARK7	0.020
GO:0016310~phosphorylation	16	8.0E-05	EGFR, CDK1, TAOK1, PMVK, EPHA2, EPHA4, MAPK1, MAPK12, MAPK14, NTRK1, DYRK1A, HIPK2, MAPK3, CFL1, YES1, ABL2	0.026
GO:0030029~actin filament-based process	9	1.0E-04	EPB41L2, ACTG1, EZR, MYL1, CFL1, MYH4, ACTN1, ABL2, DBN1	0.025
GO:0006796~phosphate metabolic process	17	2.1E-04	EGFR, CDK1, TAOK1, PMVK, ACP1, EPHA2, EPHA4, MAPK1, MAPK12, MAPK14, NTRK1, DYRK1A, HIPK2, MAPK3, CFL1, YES1, ABL2	0.040
GO:0006793~phosphorus metabolic process	17	2.1E-04	EGFR, CDK1, TAOK1, PMVK, ACP1, EPHA2, EPHA4, MAPK1, MAPK12, MAPK14, NTRK1, DYRK1A, HIPK2, MAPK3, CFL1, YES1, ABL2	0.040
GO:0030182~neuron differentiation	11	3.0E-04	EGFR, EPHA4, TUBB, S100B, CD44, MTPN, NTRK1, UCHL1, HPRT1, GAP43, EPHA2	0.049
GO:0006006~glucose metabolic process	7	3.3E-04	LDHB, LDHA, CRYAB, MAPK14, PKM2, ENO1, PGM2L1	0.045

Increased protein expression in GBM39 due to $\alpha = 4$

GO Term	Count	EASE score	Proteins	Benjamini correction

GO:0010033~response to organic substance	15	8.62E-05	A2M, LYN, HSPA1A, STAT1, B2M, DDR1, PTK2B, APOE, MAPK14, GAB1, COL6A2, PDGFRA, HSPB1, GNAS, THBS1	0.095433
GO:0018108~peptidyl-tyrosine phosphorylation	5	0.000161	DDR1, LYN, PTK2B, PDGFRA, STAT1	0.089328
GO:0006916~anti-apoptosis	8	0.00023	CDK1, TMX1, APOE, ANXA1, HSPB1, HSPA1A, HSPA5, THBS1	0.052103
GO:0042981~regulation of apoptosis	15	0.00027	TMX1, CDK1, ARHGEF6, TUBB2C, ANXA1, HSPA1A, VAV2, STAT1, YWHAE, ALB, APOE, HSPB1, HSPA5, MX1, THBS1	0.050988
GO:0043067~regulation of programmed cell death	15	0.000299	TMX1, CDK1, ARHGEF6, TUBB2C, ANXA1, HSPA1A, VAV2, STAT1, YWHAE, ALB, APOE, HSPB1, HSPA5, MX1, THBS1	0.048432
GO:0010941~regulation of cell death	15	0.00031	TMX1, CDK1, ARHGEF6, TUBB2C, ANXA1, HSPA1A, VAV2, STAT1, YWHAE, ALB, APOE, HSPB1, HSPA5, MX1, THBS1	0.044103
GO:0006928~cell motion	11	0.000521	PTK2B, MAPK14, TUBB2C, TXN, ANXA1, HSPB1, VAV2, TOP2B, THBS1, YWHAE, FN1	0.06519
GO:0006091~generation of precursor metabolites and energy	9	0.000558	TMX1, NDUFA5, SLC1A3, NDUFV1, NDUFS8, TXN, IDH2, GNAS, GAPDH	0.062865
GO:0022900~electron transport chain	6	0.000599	TMX1, NDUFA5, SLC1A3, NDUFV1, NDUFS8, TXN	0.06143

Table S6. GO classification of the proteins influenced by the unbalanced process $\alpha = 5$

Increased protein expression in GBM6 due to $\alpha = 5$

GO Term	**Count**	**EASE score**	**Proteins**	**Benjamini correction**
GO:0006091~generation of precursor metabolites and energy	17	8.6E-11	ATP5D, ALDOA, LDHB, NDUFA5, ATP5B, ALDOC, SLC1A3, GSK3B, IDH2, ATP5L, ATP5A1, GAPDH, ETFB, MDH2, ACAA1, ENO1, ETFA	0.000
GO:0007265~Ras protein signal transduction	8	4.2E-06	MAPK1, MAPK12, MAPK14, MAPK3, CFL1, COL1A2, SDCBP, PARK7	0.002
GO:0006006~glucose metabolic process	9	5.1E-06	ALDOA, LDHB, CRYAB, MAPK14, GSK3B, ALDOC, GAPDH, MDH2, ENO1	0.002
GO:0055114~oxidation reduction	16	9.1E-06	ALDH6A1, LDHB, NDUFA5, ACADM, PIPOX, CBR1, SLC1A3, HSDL2, PRDX6, AKR1B1, AKR7A2, IDH2, GAPDH, ETFB, MDH2, ETFA	0.003
GO:0006096~glycolysis	6	1.1E-05	ALDOA, LDHB, ALDOC, GAPDH, MDH2, ENO1	0.002
GO:0046164~alcohol catabolic process	7	1.1E-05	ALDOA, LDHB, ALDOC, COMT, GAPDH, MDH2, ENO1	0.002
GO:0006754~ATP biosynthetic process	7	2.0E-05	ATP5D, ALDOA, ATP5J2, ATP5B, ATP5L, ATP1A2, ATP5A1	0.003
GO:0019318~hexose metabolic process	9	2.7E-05	ALDOA, LDHB, CRYAB, MAPK14, GSK3B, ALDOC, GAPDH, MDH2, ENO1	0.004
GO:0006793~phosphorus metabolic process	19	2.7E-05	PRKCA, ATP5D, FYB, CDK1, PPP6C, NDUFA5, INPPL1, PTPRZ1, ATP5B, HCK, MAPK1, MAPK12, MAPK14, GSK3B, DYRK1A, MAPK3, CFL1, ATP5L, ATP5A1	0.003
GO:0006796~phosphate metabolic process	19	2.7E-05	PRKCA, ATP5D, FYB, CDK1, PPP6C, NDUFA5, INPPL1, PTPRZ1, ATP5B, HCK, MAPK1, MAPK12, MAPK14, GSK3B, DYRK1A, MAPK3, CFL1, ATP5L, ATP5A1	0.003
GO:0006007~glucose catabolic process	6	3.1E-05	ALDOA, LDHB, ALDOC, GAPDH, MDH2, ENO1	0.003
GO:0009206~purine ribonucleoside triphosphate biosynthetic process	7	3.4E-05	ATP5D, ALDOA, ATP5J2, ATP5B, ATP5L, ATP1A2, ATP5A1	0.003
GO:0009145~purine nucleoside triphosphate biosynthetic process	7	3.6E-05	ATP5D, ALDOA, ATP5J2, ATP5B, ATP5L, ATP1A2, ATP5A1	0.003
GO:0009201~ribonucleoside triphosphate biosynthetic process	7	3.6E-05	ATP5D, ALDOA, ATP5J2, ATP5B, ATP5L, ATP1A2, ATP5A1	0.003
GO:0015992~proton transport	6	3.9E-05	ATP5D, ATP5J2, ATP5B, ATP5L, ATP1A2, ATP5A1	0.003
GO:0009142~nucleoside triphosphate biosynthetic process	7	4.3E-05	ATP5D, ALDOA, ATP5J2, ATP5B, ATP5L, ATP1A2, ATP5A1	0.003
GO:0010035~response to inorganic substance	9	4.3E-05	PRKCA, ATP5D, SLC1A3, GATM, PRDX6, CRYAB, RELA, PARK7, MT3	0.003

GO:0006818~hydrogen transport	6	4.6E-05	ATP5D, ATP5J2, ATP5B, ATP5L, ATP1A2, ATP5A1	0.003
GO:0046034~ATP metabolic process	7	5.0E-05	ATP5D, ALDOA, ATP5J2, ATP5B, ATP5L, ATP1A2, ATP5A1	0.003
GO:0019320~hexose catabolic process	6	7.1E-05	ALDOA, LDHB, ALDOC, GAPDH, MDH2, ENO1	0.004
GO:0005996~monosaccharide metabolic process	9	7.5E-05	ALDOA, LDHB, CRYAB, MAPK14, GSK3B, ALDOC, GAPDH, MDH2, ENO1	0.004
GO:0046365~monosaccharide catabolic process	6	8.2E-05	ALDOA, LDHB, ALDOC, GAPDH, MDH2, ENO1	0.004
GO:0009152~purine ribonucleotide biosynthetic process	7	9.2E-05	ATP5D, ALDOA, ATP5J2, ATP5B, ATP5L, ATP1A2, ATP5A1	0.005
GO:0009205~purine ribonucleoside triphosphate metabolic process	7	9.2E-05	ATP5D, ALDOA, ATP5J2, ATP5B, ATP5L, ATP1A2, ATP5A1	0.005
GO:0009199~ribonucleoside triphosphate metabolic process	7	9.7E-05	ATP5D, ALDOA, ATP5J2, ATP5B, ATP5L, ATP1A2, ATP5A1	0.005
GO:0000302~response to reactive oxygen species	6	1.1E-04	PRKCA, PRDX6, CRYAB, RELA, PARK7, MT3	0.005
GO:0009144~purine nucleoside triphosphate metabolic process	7	1.2E-04	ATP5D, ALDOA, ATP5J2, ATP5B, ATP5L, ATP1A2, ATP5A1	0.005
GO:0016310~phosphorylation	16	1.2E-04	PRKCA, FYB, ATP5D, CDK1, NDUFA5, ATP5B, HCK, MAPK1, MAPK12, GSK3B, MAPK14, DYRK1A, MAPK3, CFL1, ATP5L, ATP5A1	0.005
GO:0007264~small GTPase mediated signal transduction	10	1.2E-04	GDI1, MAPK1, MAPK12, MAPK14, MAPK3, CFL1, COL1A2, SDCBP, VAV2, PARK7	0.005
GO:0009260~ribonucleotide biosynthetic process	7	1.3E-04	ATP5D, ALDOA, ATP5J2, ATP5B, ATP5L, ATP1A2, ATP5A1	0.005
GO:0009141~nucleoside triphosphate metabolic process	7	1.7E-04	ATP5D, ALDOA, ATP5J2, ATP5B, ATP5L, ATP1A2, ATP5A1	0.007
GO:0044275~cellular carbohydrate catabolic process	6	0.000192	ALDOA, LDHB, ALDOC, GAPDH, MDH2, ENO1	0.007
GO:0044271~nitrogen compound biosynthetic process	10	0.000198	ATP5D, ALDOA, GLUL, ATP5J2, SLC1A3, ATP5B, ATP5L, ATP1A2, ATP5A1, APRT	0.007
GO:0034404~nucleobase, nucleoside and nucleotide biosynthetic process	8	0.000208	ATP5D, ALDOA, ATP5J2, ATP5B, ATP5L, ATP1A2, ATP5A1, APRT	0.007
GO:0034654~nucleobase, nucleoside, nucleotide and nucleic acid biosynthetic process	8	0.000208	ATP5D, ALDOA, ATP5J2, ATP5B, ATP5L, ATP1A2, ATP5A1, APRT	0.007
GO:0009150~purine ribonucleotide metabolic process	7	0.000228	ATP5D, ALDOA, ATP5J2, ATP5B, ATP5L, ATP1A2, ATP5A1	0.008
GO:0034220~ion transmembrane transport	5	0.000248	ATP5D, ATP5B, ATP5L, ATP1A2, ATP5A1	0.008
GO:0006916~anti-apoptosis	8	0.00031	CDK1, PEA15, CRYAB, RELA, GSK3B, CFL1, ANXA1, HSPB1	0.010
GO:0009259~ribonucleotide metabolic process	7	0.000321	ATP5D, ALDOA, ATP5J2, ATP5B, ATP5L, ATP1A2, ATP5A1	0.010
GO:0006164~purine nucleotide biosynthetic process	7	0.000333	ATP5D, ALDOA, ATP5J2, ATP5B, ATP5L, ATP1A2, ATP5A1	0.010
GO:0009188~ribonucleoside diphosphate biosynthetic process	3	0.000385	ATP5D, ATP5B, ATP5A1	0.011
GO:0006172~ADP biosynthetic process	3	0.000385	ATP5D, ATP5B, ATP5A1	0.011
GO:0009136~purine nucleoside diphosphate biosynthetic process	3	0.000385	ATP5D, ATP5B, ATP5A1	0.011
GO:0009180~purine ribonucleoside diphosphate biosynthetic process	3	0.000385	ATP5D, ATP5B, ATP5A1	0.011
GO:0006979~response to oxidative stress	7	0.000575	PRKCA, GATM, PRDX6, CRYAB, RELA, PARK7, MT3	0.016
GO:0046031~ADP metabolic process	3	0.000576	ATP5D, ATP5B, ATP5A1	0.016
GO:0016052~carbohydrate catabolic process	6	0.000609	ALDOA, LDHB, ALDOC, GAPDH, MDH2, ENO1	0.017
GO:0006575~cellular amino acid derivative metabolic process	7	0.000613	SLC1A3, CKM, ACADM, GATM, GSTK1, DHPS, COMT	0.016
GO:0009133~nucleoside diphosphate biosynthetic process	3	0.000803	ATP5D, ATP5B, ATP5A1	0.021
GO:0009135~purine nucleoside diphosphate metabolic process	3	0.001066	ATP5D, ATP5B, ATP5A1	0.027

GO:0009179~purine ribonucleoside diphosphate metabolic process	3	0.001066	ATP5D, ATP5B, ATP5A1	0.027
GO:0009165~nucleotide biosynthetic process	7	0.001109	ATP5D, ALDOA, ATP5J2, ATP5B, ATP5L, ATP1A2, ATP5A1	0.027
GO:0006163~purine nucleotide metabolic process	7	0.001109	ATP5D, ALDOA, ATP5J2, ATP5B, ATP5L, ATP1A2, ATP5A1	0.027
GO:0042981~regulation of apoptosis	14	0.001451	PRKCA, BID, CDK1, CRYAB, RELA, ANXA1, VAV2, YWHAE, MIF, PEA15, MAPK1, GSK3B, CFL1, HSPB1	0.035
GO:0019226~transmission of nerve impulse	9	0.001577	PRKCA, MAPK1, SLC1A3, SDCBP, QKI, ATP1A2, COMT, NCAN, PARK7	0.037
GO:0043067~regulation of programmed cell death	14	0.001586	PRKCA, BID, CDK1, CRYAB, RELA, ANXA1, VAV2, YWHAE, MIF, PEA15, MAPK1, GSK3B, CFL1, HSPB1	0.036
GO:0010941~regulation of cell death	14	0.001639	PRKCA, BID, CDK1, CRYAB, RELA, ANXA1, VAV2, YWHAE, MIF, PEA15, MAPK1, GSK3B, CFL1, HSPB1	0.037
GO:0043066~negative regulation of apoptosis	9	0.001694	CDK1, PEA15, CRYAB, RELA, GSK3B, CFL1, ANXA1, HSPB1, MIF	0.037
GO:0001504~neurotransmitter uptake	3	0.001699	SLC1A3, ATP1A2, PARK7	0.037
GO:0009185~ribonucleoside diphosphate metabolic process	3	0.001699	ATP5D, ATP5B, ATP5A1	0.037
GO:0043069~negative regulation of programmed cell death	9	0.00185	CDK1, PEA15, CRYAB, RELA, GSK3B, CFL1, ANXA1, HSPB1, MIF	0.039
GO:0060548~negative regulation of cell death	9	0.001882	CDK1, PEA15, CRYAB, RELA, GSK3B, CFL1, ANXA1, HSPB1, MIF	0.039
GO:0015986~ATP synthesis coupled proton transport	4	0.002	ATP5D, ATP5B, ATP5L, ATP5A1	0.041
GO:0015985~energy coupled proton transport, down electrochemical gradient	4	0.002	ATP5D, ATP5B, ATP5L, ATP5A1	0.041

Decreased protein expression in GBM6 due to $\alpha = 5$

GO Term	**Count**	**EASE score**	**Proteins**	**Benjamini correction**
GO:0007169~transmembrane receptor protein tyrosine kinase signaling pathway	10	5.4E-06	EGFR, DDR1, EPHA4, MPZL1, ERBB2IP, NTRK1, BCAR1, PDGFRA, ABI1, EPHA2	0.005
GO:0007167~enzyme linked receptor protein signaling pathway	10	1.5E-04	EGFR, DDR1, EPHA4, MPZL1, ERBB2IP, NTRK1, BCAR1, PDGFRA, ABI1, EPHA2	0.045
GO:0018212~peptidyl-tyrosine modification	5	1.6E-04	TYK2, DDR1, PDGFRA, ABI1, FER	0.038
GO:0007010~cytoskeleton organization	11	1.9E-04	EPB41L2, ERBB2IP, CNN3, TLN2, BCAR1, MAP2, MAP1B, SDCBP, ACTN1, ITGB1, DBN1	0.035
GO:0030030~cell projection organization	10	2.6E-04	EGFR, ACTB, EPHA4, PARD3, MAP2K1, MAP2, CLU, CAPG, MAP1B, SDCBP	0.039
GO:0032989~cellular component morphogenesis	10	4.5E-04	EGFR, S100A4, ACTB, EPHA4, PARD3, MAP2K1, ERBB2IP, CLU, MAP1B, ITGB1	0.058

Table S7. GO classification of the proteins influenced by the unbalanced process $\alpha = 6$

Increased protein expression in GBM26 due to $\alpha = 6$

GO Term	Count	EASE score	Proteins	Benjamini correction
GO:0030036~actin cytoskeleton organization	12	6.94E-07	ACTG1, ALDOA, TLN1, PTK2B, BCAR1, CFL1, SDCBP, TMSB4X, FGD5, WAS, ITGB1, LLGL1	0.000774
GO:0006468~protein amino acid phosphorylation	19	1.19E-06	EGFR, FYB, DBNL, CDK1, LYN, TAOK1, PTPRA, TFG, FER, EPHA2, SPAG9, PTK2B, DYRK1A, CFL1, MAPK3, PDGFRA, SHC1, MERTK, YES1	0.000665

GO:0030029~actin filament-based process	12	1.31E-06	ACTG1, ALDOA, TLN1, PTK2B, BCAR1, CFL1, SDCBP, TMSB4X, FGD5, WAS, ITGB1, LLGL1	0.000486
GO:0007010~cytoskeleton organization	15	2.92E-06	ALDOA, TLN1, TLN2, BCAR1, MAP1B, DOCK7, WAS, ITGB1, LLGL1, ACTG1, PTK2B, CFL1, SDCBP, TMSB4X, FGD5	0.000813
GO:0016310~phosphorylation	20	3.84E-06	EGFR, FYB, DBNL, CDK1, LYN, TAOK1, PTPRA, TFG, FER, EPHA2, SPAG9, PTK2B, DYRK1A, CFL1, MAPK3, PDGFRA, SHC1, MERTK, YES1, ATP5I	0.000856
GO:0006796~phosphate metabolic process	22	4.91E-06	EGFR, FYB, DBNL, CDK1, LYN, TAOK1, PTPRA, TFG, FER, EPHA2, GPD1L, SPAG9, PTK2B, DYRK1A, CFL1, MAPK3, PDGFRA, SHC1, INPP5D, MERTK, YES1, ATP5I	0.000913
GO:0006793~phosphorus metabolic process	22	4.91E-06	EGFR, FYB, DBNL, CDK1, LYN, TAOK1, PTPRA, TFG, FER, EPHA2, GPD1L, SPAG9, PTK2B, DYRK1A, CFL1, MAPK3, PDGFRA, SHC1, INPP5D, MERTK, YES1, ATP5I	0.000913
GO:0032989~cellular component morphogenesis	13	2.88E-05	S100A4, EGFR, S100A6, MAP1B, GJA1, DOCK7, ITGB1, LLGL1, ACTG1, SLC1A3, ROBO1, CFL1, SLITRK5	0.004574
GO:0034329~cell junction assembly	5	0.000214	TLN1, TLN2, PTK2B, GJA1, VCL	0.029322
GO:0000902~cell morphogenesis	11	0.000252	EGFR, S100A4, S100A6, SLC1A3, ROBO1, CFL1, MAP1B, GJA1, DOCK7, SLITRK5, LLGL1	0.0307
GO:0007043~cell-cell junction assembly	4	0.000278	TLN1, TLN2, GJA1, VCL	0.030524
GO:0030030~cell projection organization	11	0.000328	EGFR, S100A6, ROBO1, PTK2B, MAP1B, SDCBP, GJA1, DOCK7, FGD5, SLITRK5, VCL	0.032685
GO:0018108~peptidyl-tyrosine phosphorylation	5	0.000335	LYN, PTK2B, DYRK1A, PDGFRA, FER	0.030621
GO:0018212~peptidyl-tyrosine modification	5	0.000395	LYN, PTK2B, DYRK1A, PDGFRA, FER	0.033288
GO:0051272~positive regulation of cell motion	6	0.000718	EGFR, SPAG9, LYN, PTK2B, BCAR1, PDGFRA	0.055613
GO:0034330~cell junction organization	5	0.000762	TLN1, TLN2, PTK2B, GJA1, VCL	0.055107

Decreased protein expression in GBM26 due to $\alpha = 6$

GO Term	**Count**	**EASE score**	**Proteins**	**Benjamini correction**
GO:0034728~nucleosome organization	8	4.19E-06	H1F0, HIST1H2BB, HIST2H2AA3, HIST1H4A, HIST1H1B, H2AFY, H2AFX, HMGA1	0.004635
GO:0006323~DNA packaging	8	1.91E-05	H1F0, HIST1H2BB, HIST2H2AA3, HIST1H4A, HIST1H1B, H2AFY, H2AFX, SMC4	0.010536
GO:0006334~nucleosome assembly	7	2.84E-05	H1F0, HIST1H2BB, HIST2H2AA3, HIST1H4A, HIST1H1B, H2AFY, H2AFX	0.01045
GO:0006333~chromatin assembly or disassembly	8	3.25E-05	H1F0, HIST1H2BB, HIST2H2AA3, HIST1H4A, HIST1H1B, H2AFY, H2AFX, HMGA1	0.008968
GO:0031497~chromatin assembly	7	3.47E-05	H1F0, HIST1H2BB, HIST2H2AA3, HIST1H4A, HIST1H1B, H2AFY, H2AFX	0.007668
GO:0065004~protein-DNA complex assembly	7	4.47E-05	H1F0, HIST1H2BB, HIST2H2AA3, HIST1H4A, HIST1H1B, H2AFY, H2AFX	0.008243

Table S8. GO classification of the proteins influenced by the unbalanced process $\alpha = 7$

Increased protein expression in GBM6 due to $\alpha = 7$

GO Term	**Count**	**EASE score**	**Proteins**	Benjamini correction
GO:0007173~epidermal growth factor receptor signaling pathway	7	2.45E-08	EGFR, EPS15, ERBB2IP, PTK2B, BCAR1, GAB1, SHC1	2.75E-05
GO:0007169~transmembrane receptor protein tyrosine kinase signaling pathway	12	2.65E-07	EGFR, EPS15, DDR1, EPHA4, MPZL1, ERBB2IP, PTK2B, BCAR1, GAB1, PDGFRA, ABI1, SHC1	0.000149
GO:0030029~actin filament-based process	12	5.5E-07	EPB41L2, ALDOA, ACTA1, CNN3, PTK2B, BCAR1, MYL1, MYH4, ACTN1, ARF6, FGD5, ITGB1	0.000206

GO:0007167~enzyme linked receptor protein signaling pathway	13	2.62E-06	EGFR, MPZL1, BCAR1, ABI1, EPS15, EPHA4, DDR1, ERBB2IP, PTK2B, ZFYVE16, GAB1, PDGFRA, SHC1	0.000735
GO:0030036~actin cytoskeleton organization	10	1.89E-05	EPB41L2, ALDOA, ACTA1, CNN3, PTK2B, BCAR1, ACTN1, ARF6, FGD5, ITGB1	0.004227
GO:0006796~phosphate metabolic process	19	6.09E-05	EGFR, NDUFA4, CDK1, INPPL1, ABI1, TIMM50, PPA1, GPD1L, TYK2, DDR1, EPHA4, PTK2B, UQCRH, GAB1, PDGFRA, STK39, SHC1, MERTK, YES1	0.01132
GO:0006793~phosphorus metabolic process	19	6.09E-05	EGFR, NDUFA4, CDK1, INPPL1, ABI1, TIMM50, PPA1, GPD1L, TYK2, DDR1, EPHA4, PTK2B, UQCRH, GAB1, PDGFRA, STK39, SHC1, MERTK, YES1	0.01132
GO:0018108~peptidyl-tyrosine phosphorylation	5	0.000241	TYK2, DDR1, PTK2B, PDGFRA, ABI1	0.037967
GO:0018212~peptidyl-tyrosine modification	5	0.000285	TYK2, DDR1, PTK2B, PDGFRA, ABI1	0.03919
GO:0010035~response to inorganic substance	8	0.000427	EGFR, BSG, SLC1A3, PTK2B, PDGFRA, PRDX3, PARK7, MT3	0.051902

Decreased protein expression in GBM6 due to $\alpha = 7$

GO Term	**Count**	**EASE score**	**Proteins**	Benjamini correction
GO:0065003~macromolecular complex assembly	21	1.85E-07	CUTA, H1F0, HIST2H2AA3, PARD3, HIST1H1B, HP1BP3, GJA1, WAS, LLGL1, TUBB, NDUFS4, HIST1H4A, APOE, NDUFS8, SMARCA5, TUBB6, H2AFY, H2AFX, SEPT7, TUBB3, SEPT9	0.000238
GO:0043933~macromolecular complex subunit organization	21	5.26E-07	CUTA, H1F0, HIST2H2AA3, PARD3, HIST1H1B, HP1BP3, GJA1, WAS, LLGL1, TUBB, NDUFS4, HIST1H4A, APOE, NDUFS8, SMARCA5, TUBB6, H2AFY, H2AFX, SEPT7, TUBB3, SEPT9	0.000339
GO:0034622~cellular macromolecular complex assembly	14	1.17E-06	H1F0, HIST2H2AA3, HIST1H1B, HP1BP3, WAS, TUBB, NDUFS4, HIST1H4A, NDUFS8, SMARCA5, TUBB6, H2AFY, H2AFX, TUBB3	0.000503
GO:0006323~DNA packaging	9	3.66E-06	H1F0, HIST2H2AA3, HIST1H4A, HP1BP3, HIST1H1B, SMARCA5, H2AFY, H2AFX, SMC4	0.00118
GO:0006334~nucleosome assembly	8	4.1E-06	H1F0, HIST2H2AA3, HIST1H4A, HP1BP3, HIST1H1B, SMARCA5, H2AFY, H2AFX	0.001056
GO:0034621~cellular macromolecular complex subunit organization	14	4.21E-06	H1F0, HIST2H2AA3, HIST1H1B, HP1BP3, WAS, TUBB, NDUFS4, HIST1H4A, NDUFS8, SMARCA5, TUBB6, H2AFY, H2AFX, TUBB3	0.000903
GO:0031497~chromatin assembly	8	5.19E-06	H1F0, HIST2H2AA3, HIST1H4A, HP1BP3, HIST1H1B, SMARCA5, H2AFY, H2AFX	0.000955
GO:0065004~protein-DNA complex assembly	8	7.01E-06	H1F0, HIST2H2AA3, HIST1H4A, HP1BP3, HIST1H1B, SMARCA5, H2AFY, H2AFX	0.001128
GO:0034728~nucleosome organization	8	8.09E-06	H1F0, HIST2H2AA3, HIST1H4A, HP1BP3, HIST1H1B, SMARCA5, H2AFY, H2AFX	0.001159
GO:0006333~chromatin assembly or disassembly	8	6.14E-05	H1F0, HIST2H2AA3, HIST1H4A, HP1BP3, HIST1H1B, SMARCA5, H2AFY, H2AFX	0.007887
GO:0030198~extracellular matrix organization	7	0.000164	LUM, HSD17B12, COL1A2, COL12A1, POSTN, NID1, ANXA2	0.018991
GO:0008104~protein localization	18	0.000476	EGFR, CUTA, FYB, RAB3GAP2, TLN1, PDIA3, LYN, TLN2, VTA1, AKAP12, ITGA2, CLTC, YWHAE, AP3M1, GSK3B, FGFR1OP, SDCBP, SRP9	0.049879

3. PCA analysis

Using as an input a matrix that included entire dataset (phosphorylated and unmodified proteins) we performed standard PCA analysis [10]. PCA analysis is a statistical approach that concentrates on variations relative to the mean. Rows of the input matrix correspond to 8 GBM tumors (observations), columns to the the mean-centered measured proteins (variables). At the end of the analysis we receive clusters of the proteins with similar behavior relatively to the mean. We show that only proteins with highest variance are resolved well.

The results of the PCA analysis yields a big 1766-by-1766 matrix, in which each column contains coefficients (or contributions of the examined proteins) for one principal component (PC). The analysis of the mean-centered data of 8 different GBM tumors can mathematically yield maximum of 7 non-zero principle components. Fig. S7a, b and c illustrates the representation of the measured protein data in the principal component space and shows sorted values of the protein coefficients for the PC1 (Fig.S7d). We used Matlab to calculate how many components account for 92% or 98% of the variance among the GBM tumors. Four first Principal components (PC) accounted for 92% of the data variance and 6 out of 7 PCs account for 98% of the variance. All the proteins with the coefficients more than 0.01 or less than -0.01 (Fig.S7d, proteins with the coefficients that exceed positively or negatively the zero red box in the plot) were examined further for fitting into the identified PC scores (Fig.S7) in order to eliminate noise. Only the proteins that change their expression levels according to the identified PC scores were included further in the classification according to the GO biological categories using DAVID database [5]. Proteins with noisy behaviors were excluded from the lists. For example proteins contributing significantly to the PC1 should show the same behavior in the GBM 10 and 12 (eg. increase in those tumors relatively to the average protein expression) but have an opposite behavior in the GBM39 (as shown in the PC1 score in Fig.S7a).

Biological categories were considered as statistically significant enriched groups if they had EASE score and Benjamini correction values ≤ 0.05. Tables including these categories are presented below (Tables S9–S13). Mainly phospho-proteins contribute to all PCs (Additional Table SI). Additional Table SI includes lists of all significant proteins contributing either to the constraints identified by Surprisal analysis or to the PCs identified by the PCA algorithm.

To decrease the effect of the variables with the highest variance that may dominate first principal components we used correlation matrix instead of covariance matrix to standardize the data. This method yielded plots without a flat region representing zero values, thereby not allowing identification of the significantly contributing proteins to the different PCs (Fig.S8).

Classification of the proteins contributing to the PCs according to the GO biological categories.

A more complete list of proteins that contribute significantly to the different constraints is provided in the **Additional Table SI**. Tables S9-S13 include both proteins with altered expression and altered phosphorylation. To distinguish between proteins with altered expression and altered phosphorylation in every constraint see **Additional Table SI**. Almost all the proteins contributing significantly to the principle components are phosphoproteins.

Principal component 1(PC1,GBM10 vs GBM39)

No significant biological categories were identified besides one GO category named"phosphorylation".

Table S9. GO protein classification of the proteins contributing to the PC2 (GBM15 vs GBM6)

Increased protein expression in GBM15

GO Term	Count	pValue	proteins	Benjamini correction
GO:0006468~protein amino acid phosphorylation	10	4.84E-06	EGFR, EPHA4, MAPK1, PRPF4B, GSK3B, HIPK2, MAPK3, MAP2, PTPRA, YES1	0.00273
GO:0006796~phosphate metabolic process	11	1.4E-05	EGFR, EPHA4, MAPK1, PRPF4B, PTPRZ1, GSK3B, HIPK2, MAPK3, MAP2, PTPRA, YES1	0.003957
GO:0006793~phosphorus metabolic process	11	1.4E-05	EGFR, EPHA4, MAPK1, PRPF4B, PTPRZ1, GSK3B, HIPK2, MAPK3, MAP2, PTPRA, YES1	0.003957
GO:0016310~phosphorylation	10	2.11E-05	EGFR, EPHA4, MAPK1, PRPF4B, GSK3B, HIPK2, MAPK3, MAP2, PTPRA, YES1	0.003957
GO:0007010~cytoskeleton organization	7	0.000223	EPB41L2, ACTG1, TUBB, CNN3, MAP2, ITGB1, DBN1	0.031026

Table S10. GO protein classification of the proteins contributing to the PC3 (GBM6 vs GBM39,59).

Increased protein expression in 6

GO Term	Count	pValue	proteins	Benjamini correction
GO:0006793~phosphorus metabolic process	9	2.66E-07	MAPK1, PRPF4B, MAPK12, PTPRZ1, MAPK14, GSK3B, HIPK2, DYRK1A, MAPK3	9.32E-05
GO:0006796~phosphate metabolic process	9	2.66E-07	MAPK1, PRPF4B, MAPK12, PTPRZ1, MAPK14, GSK3B, HIPK2, DYRK1A, MAPK3	9.32E-05
GO:0006468~protein amino acid phosphorylation	8	4.38E-07	MAPK1, PRPF4B, MAPK12, MAPK14, GSK3B, HIPK2, DYRK1A, MAPK3	7.68E-05
GO:0016310~phosphorylation	8	1.5E-06	MAPK1, PRPF4B, MAPK12, MAPK14, GSK3B, HIPK2, DYRK1A, MAPK3	0.000176
GO:0033554~cellular response to stress	6	7.81E-05	MAPK1, MAPK12, MAPK14, GSK3B, HIPK2, MT3	0.00683
GO:0007265~Ras protein signal transduction	4	9.5E-05	MAPK1, MAPK12, MAPK14, MAPK3	0.006647

Table S11. GO protein classification of the proteins contributing to the PC4 (GBM8 vs GBM15)

Increased protein expression in 15

GO Term	Count	pValue	proteins	Benjamini correction
GO:0018108~peptidyl-tyrosine phosphorylation	10	1.26E-13	TYK2, DDR1, LYN, PTK2B, PDGFRA, ABI2, ABI1, FER, ABL2, SRC	1.13E-10
GO:0018212~peptidyl-tyrosine modification	10	1.9E-13	TYK2, DDR1, LYN, PTK2B, PDGFRA, ABI2, ABI1, FER, ABL2, SRC	8.55E-11
GO:0006468~protein amino acid phosphorylation	20	4.11E-12	EGFR, DBNL, LYN, PTPRA, ABI2, ABI1, FER, SRC, TYK2, DDR1, EPHA4, PTK2B, MAPK14, GSK3B, HIPK2, MAPK3, GAB1, PDGFRA, YES1, ABL2	1.23E-09
GO:0016310~phosphorylation	20	9.63E-11	EGFR, DBNL, LYN, PTPRA, ABI2, ABI1, FER, SRC, TYK2, DDR1, EPHA4, PTK2B, MAPK14, GSK3B, HIPK2, MAPK3, GAB1, PDGFRA, YES1, ABL2	2.17E-08
GO:0007167~enzyme linked receptor protein signaling pathway	14	5.98E-10	EGFR, MPZL1, BCAR1, PTPRA, ABI1, SRC, DDR1, EPHA4, ERBB2IP, PTK2B, ZFYVE16, GAB1, HIPK2, PDGFRA	1.07E-07
GO:0007169~transmembrane receptor protein tyrosine kinase signaling pathway	12	1.03E-09	EGFR, DDR1, EPHA4, MPZL1, ERBB2IP, PTK2B, BCAR1, GAB1, PTPRA, PDGFRA, ABI1, SRC	1.54E-07
GO:0030036~actin cytoskeleton organization	12	1.13E-09	EPB41L2, ACTG1, TLN1, CNN3, PTK2B, BCAR1, ABI2, FGD5, ABL2, WAS, ITGB1, DBN1	1.45E-07
GO:0030029~actin filament-based process	12	2.23E-09	EPB41L2, ACTG1, TLN1, CNN3, PTK2B, BCAR1, ABI2, FGD5, ABL2, WAS, ITGB1, DBN1	2.5E-07
GO:0006793~phosphorus metabolic process	20	2.63E-09	EGFR, DBNL, LYN, PTPRA, ABI2, ABI1, FER, SRC, TYK2, DDR1, EPHA4, PTK2B, MAPK14, GSK3B, HIPK2, MAPK3, GAB1, PDGFRA, YES1, ABL2	2.63E-07
GO:0006796~phosphate metabolic process	20	2.63E-09	EGFR, DBNL, LYN, PTPRA, ABI2, ABI1, FER, SRC, TYK2, DDR1, EPHA4, PTK2B, MAPK14, GSK3B, HIPK2, MAPK3, GAB1, PDGFRA, YES1, ABL2	2.63E-07
GO:0007010~cytoskeleton organization	14	1.13E-08	TLN1, CAV1, CNN3, BCAR1, ABI2, WAS, ITGB1, ACTG1, EPB41L2, ERBB2IP, PTK2B, FGD5, DBN1, ABL2	1.01E-06
GO:0007173~epidermal growth factor receptor signaling pathway	6	7.68E-08	EGFR, ERBB2IP, PTK2B, BCAR1, GAB1, SRC	6.28E-06
GO:0006928~cell motion	12	2.17E-06	ACTG1, EPHA4, TLN1, ROBO1, PTK2B, MAPK14, BCAR1, VIM, ABI2, ITGB1, SRC, VCL	0.000163
GO:0007015~actin filament organization	6	9.58E-06	PTK2B, BCAR1, ABI2, ABL2, WAS, DBN1	0.000662
GO:0007155~cell adhesion	13	1.55E-05	EGFR, RPSA, BCAR1, CTNND2, FER, ITGB1, SRC, VCL, DDR1, ERBB2IP, PTK2B, ROBO1, ABL2	0.000993
GO:0022610~biological adhesion	13	1.57E-05	EGFR, RPSA, BCAR1, CTNND2, FER, ITGB1, SRC, VCL, DDR1, ERBB2IP, PTK2B, ROBO1, ABL2	0.00094

GO:0051270~regulation of cell motion	7	0.000114	EGFR, LYN, PTK2B, BCAR1, GAB1, PDGFRA, VCL	0.006387
GO:0070302~regulation of stress-activated protein kinase signaling pathway	5	0.000162	DBNL, LYN, PTK2B, HIPK2, GAB1	0.008517
GO:0010033~response to organic substance	11	0.000492	EGFR, DDR1, CAV1, LYN, PTK2B, MAPK14, BCAR1, GAB1, PTPRA, PDGFRA, SRC	0.024288
GO:0030334~regulation of cell migration	6	0.000553	EGFR, PTK2B, BCAR1, GAB1, PDGFRA, VCL	0.025836
GO:0009725~response to hormone stimulus	8	0.000603	CAV1, LYN, PTK2B, BCAR1, GAB1, PTPRA, PDGFRA, SRC	0.026764
GO:0030030~cell projection organization	8	0.000613	EGFR, EPHA4, SEPT2, ROBO1, PTK2B, ABI2, FGD5, VCL	0.025915
GO:0001932~regulation of protein amino acid phosphorylation	6	0.000615	EGFR, DBNL, CAV1, LYN, PTK2B, GAB1	0.02483
GO:0007166~cell surface receptor linked signal transduction	18	0.000617	EGFR, MPZL1, LYN, BCAR1, PTPRA, ABI1, ITGB1, SRC, DDR1, EPHA4, ERBB2IP, PTK2B, MAPK14, ZFYVE16, GSK3B, HIPK2, GAB1, PDGFRA	0.023825
GO:0051272~positive regulation of cell motion	5	0.00062	EGFR, LYN, PTK2B, BCAR1, PDGFRA	0.022981
GO:0007243~protein kinase cascade	8	0.000633	EGFR, TYK2, DBNL, CAV1, PTK2B, MAPK14, GAB1, SRC	0.022519
GO:0080135~regulation of cellular response to stress	5	0.000748	DBNL, LYN, PTK2B, HIPK2, GAB1	0.025553
GO:0043408~regulation of MAPKKK cascade	5	0.000925	DBNL, CAV1, PTK2B, HIPK2, GAB1	0.030349
GO:0040012~regulation of locomotion	6	0.000984	EGFR, PTK2B, BCAR1, GAB1, PDGFRA, VCL	0.03111
GO:0007242~intracellular signaling cascade	14	0.001066	EGFR, DBNL, CAV1, LYN, FER, SRC, TYK2, PTK2B, GSK3B, MAPK14, HIPK2, MAPK3, GAB1, PAG1	0.032509
GO:0009719~response to endogenous stimulus	8	0.001076	CAV1, LYN, PTK2B, BCAR1, GAB1, PTPRA, PDGFRA, SRC	0.031759
GO:0031399~regulation of protein modification process	7	0.001096	EGFR, DBNL, CAV1, LYN, PTK2B, PSMC2, GAB1	0.031287
GO:0051592~response to calcium ion	4	0.001362	EGFR, ACTG1, CAV1, PTK2B	0.037569

PC5 (GBM10 vs GBM59)

Increased protein expression in 10

No significant biological categories were identified , but in the list there are some proteins involved in the EGFR signaling and motion (Additional Table SI), such as pMAPK3, pPxn and pYes.

Table S12. GO protein classification of the proteins contributing to the PC6 (GBM8 vs GBM26).

Increased protein expression in 26

GO Term	Count	pValue	proteins	Benjamini correction
GO:0007010~cytoskeleton organization	13	3.38E-08	ALDOA, TLN1, CRYAB, TLN2, BCAR1, MAP1B, ABI2, WAS, ITGB1, LLGL1, ACTG1, TUBB, CFL1	2.81E-05
GO:0006468~protein amino acid phosphorylation	15	5.94E-08	FYB, LYN, TAOK1, HCK, PTPRA, ABI2, FER, MAPK12, GSK3B, MAPK14, HIPK2, DYRK1A, MAPK3, CFL1, GAB1	2.47E-05
GO:0030029~actin filament-based process	9	2.17E-06	ACTG1, ALDOA, TLN1, BCAR1, CFL1, ABI2, WAS, ITGB1, LLGL1	0.000301
GO:0007043~cell-cell junction assembly	4	3.51E-05	TLN1, TLN2, GJA1, VCL	0.00416
GO:0006928~cell motion	10	4.42E-05	ACTG1, TLN1, TUBB, MAPK14, BCAR1, CFL1, ANXA1, ABI2, ITGB1, VCL	0.004587
GO:0045216~cell-cell junction organization	4	0.000269	TLN1, TLN2, GJA1, VCL	0.022168
GO:0034329~cell junction assembly	4	0.000432	TLN1, TLN2, GJA1, VCL	0.032164
GO:0018212~peptidyl-tyrosine modification	4	0.000689	LYN, DYRK1A, ABI2, FER	0.043139

Table S13. GO protein classification of the proteins contributing to the PC7 (GBM12 vs GBM59).

Decrease in GBM12/Increase in GBM59

GO Term	Count	pValue	proteins	Benjamini correction
GO:0006793~phosphorus metabolic process	16	5.41E-07	EGFR, FYB, LYN, INPPL1, HCK, ABI2, ABI1, ACP1, EPHA2, EPHA4, MAPK12, MAPK14, CFL1, GAB1, SHC1, ABL2	0.000232
GO:0007169~transmembrane receptor protein tyrosine kinase signaling pathway	9	8.99E-07	EGFR, EPS15, EPHA4, CBL, GAB1, ABI1, SHC1, STAT3, EPHA2	0.000258
GO:0016310~phosphorylation	14	2.11E-06	FYB, EGFR, LYN, HCK, ABI2, ABI1, EPHA2, EPHA4, MAPK12, MAPK14, CFL1, GAB1, SHC1, ABL2	0.000454
GO:0007173~epidermal growth factor receptor signaling pathway	5	2.46E-06	EGFR, EPS15, CBL, GAB1, SHC1	0.000423
GO:0030182~neuron differentiation	10	1.64E-05	EGFR, EPHA4, TUBB, SEPT2, CD44, UCHL1, ABI2, GJA1, STAT3, EPHA2	0.00235
GO:0006096~glycolysis	5	2.04E-05	ALDOA, LDHA, TPI1, PKM2, ENO1	0.002193
GO:0046164~alcohol catabolic process	5	0.000175	ALDOA, LDHA, TPI1, PKM2, ENO1	0.010676
GO:0019318~hexose metabolic process	6	0.000517	ALDOA, LDHA, TPI1, MAPK14, PKM2, ENO1	0.023108
GO:0018212~peptidyl-tyrosine modification	4	0.000609	LYN, ABI2, ABI1, ABL2	0.023514

GO:0007010~cytoskeleton organization	8	0.00071	ACTG1, ALDOA, TLN1, CAV1, TUBB, CFL1, ABI2, ABL2	0.02616
GO:0010033~response to organic substance	10	0.000725	EGFR, CAV1, LYN, CD44, MAPK14, GAB1, CFL1, HSPB1, SHC1, STAT3	0.025608
GO:0048666~neuron development	7	0.001069	EGFR, EPHA4, SEPT2, CD44, UCHL1, ABI2, GJA1	0.034732
GO:0030036~actin cytoskeleton organization	6	0.001079	ACTG1, ALDOA, TLN1, CFL1, ABI2, ABL2	0.033749
GO:0030030~cell projection organization	7	0.001628	EGFR, EPHA4, SEPT2, CD44, UCHL1, ABI2, GJA1	0.048766

Increase in GBM12

No significant biological categories were identified besides one GO category named ”cell motion”.

4. K-means clustering

K-means clustering was performed using the Matlab code. The entire dataset was initially used to perform the clustering. Each protein was divided by its average value prior to clustering, as in Johnson et al [9] to improve clustering results. The data was divided into different numbers of clusters and each division was evaluated using Silhouette method [11]. The silhouette value for each point (each protein) is a measure of how similar that point is to other points in its own cluster. Different cluster solutions were evaluated using the silhouette value that was calculated for every protein. The best clustering solution (number of clusters) was defined when the majority of the proteins (> 95%) had positive values. Only proteins with the silhouette values > 0.2 were analyzed further. As shown in the Figure S10a there is a large number of proteins (>30%) that do not belong (negative Silhouette values, see Fig.S10 for more details) to the defined clusters or poorly belong (proteins with small Silhouette values < 0.2, ~50%). Similar results were obtained when the data was divided into different number of clusters, such as 5, 8 or 12 clusters.

To achieve a more precise division into clusters, phosphorylated subgroup of proteins was subjected to *k*-means clustering analysis. Using phosphoproteins only we were able to obtain clusters with relatively small amount of proteins that did not belong to the defined clusters (Fig.S10b). Proteins with Silhouette values > 0.2 were included in further biological analysis. Note that silhouette value ranges from -1 to +1. A high silhouette value indicates that protein *i* is well-matched to its own cluster, and poorly-matched to neighboring clusters. In our best clustering solution (10 clusters) most of the phosphoproteins had positive values. However the majority of the proteins did not approach value +1, pointing to the inability of the method to achieve a good resolution of the GBM proteomic signatures. 10 centroids (centers of the clusters) are shown in the Fig. S11 and the proteins belonging to these clusters were classified according to the biological processes. Only clusters 6 and 10 could be classified to statistically significant biological groups according to DAVID database (phosphorylation category in cluster 6 and MAPK activity in the cluster 10 were identified as statistically enriched groups according to EASE score and Benjamini correction).

Interestingly k-means clustering yields very similar results to the affinity propagation algorithm that was utilized by Johnson at al. to cluster phosphorylation sites [9]. Only cluster number 6 from the k-means clustering looked somewhat different in comparison with the results obtained by Johnson et al.

Every cluster included a relatively small number of the proteins with significant Silhouette values (>0.2, Table S14).

Table S14. Clustering of the phospho proteins using k-means clustering algorithm.

Proteins with the Silhouette values > 0.2 were used to generate the table.

cluster 1		cluster 2		cluster 3		cluster4		cluster5	
PHKA1	y511	GDI2	y203	CCDC88A	y1799	PLCG1	y481	PRAGMIN	y413
MERTK	y929	EphA2	y594	WWP2	y373	GARS	y453	PDLIM4	y293
PDGFRa	y731	TKT	y275	SEPT7	y30	ACLY	y682	SLITRK5	y945
		EphA2	y575	CTTN	y334	SEPT9	y278	DLG3	y673
		CDK1	t14 and y15	Fer	y714	PARD3	y1080	Vav2	y159
				GJA1	y313	NTRK1	y681	ANXA1	y21
				PTK2	y397	PRUNE2	y1738		
				ZFYVE16	y1381	VIM	y117		
				SDCBP	y56				
				MAP1B	y1062				
				ACTG1	y198				
				VIM	y61				
				DPYSL2	y32				
				Tyk2	y292				
				HIPK2	y361				
				HIST1H4A	y52				
				SET	y146				
				SHP2	y584				
				MAPK3	y204				
				Yes1	y537				
cluster 6		**cluster7**		**cluster8**		**cluster9**		**cluster10**	
Gab1	y406	CTNND2	y503	ZFYVE16	y578	GRLF1	y1087+s1070	INPPL1	y1135
PAG	y163	FGFR1OP	y317	C9orf86	y726	ARHGAP42	y376	ACP1	y131
MAPK12	y185	CTNND1	y334	LANCL2	y295	SEPT7	y141	NAA10	y137
MAPK14	y182 + t180	ACTN1	y215	DDR1	y792 + y977	MAPK11	y182	MPZL1	y263 + s260
ANXA2	y188	CTNND1	y257			ARHGEF40	y242	HGS/Hrs	y216
ROBO1	Y1114	PSMC2	y4			LLGL1	y510	ENO1	y287
DCBLD2	y750	PJA2	y63			CLTC	y899	ACTG1	y240
RPSA	y139	CNN3	y10			FHL1	y207	ENO1	y44
CRIP2	y77	CNN3	y320			AP3M1	y31	CTPS	y473
CGNL1	y108	AFAP1L2	y359			CLTC	y1477	PIK3R2	y605
PDGFRa	y988	STIM2	y666			CAPRIN1	y78	TLN2	y1665
MAPK1	y187	SND1	y908			ANXA1	y207	SPRY1	y53
Abi1	y213	TRIM9	y60			FGD5	y579	PIK3AP1	y694
VCL	y822	DBN1	y597			eIF1	y30	ABL2	y439
SEPT2	y211	AFAP1L2	y413			CFL1	y140	CAV1	y14

PTPRZ1	y2179	TBCB	y98			GRLF1	y1087	SPRY4	y52
CDK1	y15	ERBB2IP	y1107			FYB	y571	Hck	y522
		ITGB1	y783			PITPNA	y140	Gab1	y659
		EGFR	y992			GSK3b	y216 + s219	SHC1	y427
		EphA4	y779			ALDOA	y3		
		PAG1	y417			FAM118B	y303		
		PPP1R14B	y29			Lyn	y397		
		MPP5	y243			PROSC	y69		
		PAG1	y387			PTPRA	y798		
		DBNL	y162			TLN1	y70		
		NES	y925						

5. Comparison between CGH datasets from GBM tumors and iTRAQ proteomic datasets

To examine to what extent genomic changes have a proteomic output in GBM tumors we used CGH data available in GEO database (GSE39242) for GBM 12, 8,15, 26 and 59 tumors. Values representing gene copy numbers in the CGH experiments were normalized by the Female Reference Genome as described in (GSE39242, GEO). Since proteomic data was not normalized, we created two comparable datasets by dividing genomic and proteomic input values by the intensity values from the GBM8 tumor. Fig.S12 shows that normalization by the GBM8 didn't affect the unbalanced processes as identified using non-normalized GBM tissues.

To compare the CGH and iTRAQ datasets we used a similar CGH gene list as in the proteomic dataset (~1424 out of 1770 corresponding genes were found in the CGH dataset). The CGH dataset includes several probes for every gene thereby creating a list of ~9000 probes for the 1424 genes. Fig.S13 represents comparison between CGH and iTRAQ datasets. Although λ_α values are very similar between the proteomic and genomic datasets (Fig.S13 a and b), G_α vectors differ in their composition. To compare between the CGH and proteomic first unbalanced processes we created a list of the proteins with the $G_{i1} < -0.03$ (101 proteins, as shown in the Fig.S13d) and compared it to the gene list with $G_{i1} < -0.015$ (288 genes as shown in the Fig.S13c). 29 proteins (~30%) out of 101 proteins were found also in the genomic (as identified from the CGH dataset) first constraint. Similar result was obtained for the genes/ proteins with the significant G_{i1} positive values ($G_{i1} > 0.03$ for the proteins, and $G_{i1} > 0.015$ for the genes, Fig.S13c,d) and for the second constraint.

Some of the genes in which genomic changes correspond to the proteomic changes are involved in significant cellular functions, such as glycolytic genes ENO1 and LDHA, or signal transduction regulators, as Cbl, Gab1 and Gab3 (Table S15). It was shown previously that genomic/transcriptomic changes may lead to a significant phenotypic change executed by proteins, such as a shift from apoptosis to necrosis [12]. Further understanding of regulation processes that in some cases result in correlations between gene copy numbers and protein levels and in other cases lead to the lack of correlations or even anti-correlations is required.

Robust core

To identify genes that did not change copy numbers (those show increase/decrease in gene copy by less than 40% in comparison to the reference tissue) in different GBM tumors, we looked at the genes that have not been amplified/deleted in comparison with the reference female tissues (Table S16). These genes belong to the homeostatic biological groups, similarly to the proteomic dataset, such as protein synthesis, and mRNA metabolism. The overlap between the CGH and proteomic list was ~50% - twice bigger than the overlap between

the unbalanced biological processes. This result suggests that homeostatic robust core has significantly less alterations on the both genomic and proteomic levels.

Table S15. GO protein classification of the genes influenced by the unbalanced processes $\alpha = 1$ (GBM15 vs GBM12 and 59).

increase in GBM12 and 59/Decrease in GBM15

GO Term	Count	EASE score	Genes	Benjamini correction
GO:0046907~intracellular transport	51	1.61E-10	CLTA, CLTB, PDIA3, AP1B1, APP, RAE1, SEC24C, NUP133, OPA1, HSP90AA1, IPO9, ERGIC1, WAS, TIMM44, FLNA, BCAP31, MAPK1, TXNDC5, IPO4, F2, KPNA6, SORT1, THOC4, GNAS, KPNA4, SRP72, VPS26B, COPE, BID, SNX2, EEA1, TIMM13, SET, MACF1, AP3D1, PPP3CA, TNPO2, EHD1, UPF1, TOMM40, ARFIP1, AP2A2, SCFD1, ARF1, VCP, AP2A1, RAB35, PCNA, SPTBN1, NUTF2, SSR4	3.6E-07
GO:0006091~generation of precursor metabolites and energy	30	2.16E-08	LDHA, GNPDA1, PHKA1, PGAM1, HK1, ATP6V1B2, NDUFS8, PDHA1, NDUFS3, ATP6V0D1, ENO1, NDUFA4, TXNL1, ACO2, PFKL, SLC25A4, SUCLG2, MSH2, ACO1, PFKP, DLAT, PPP1CB, PYGL, ATP6V1E1, PGM1, ATP5C1, GAA, TXNRD1, GNAS, PGK1	2.41E-05
GO:0016044~membrane organization	33	4.13E-08	BID, CLTA, GNAI3, AP1B1, SAMM50, SNX2, EEA1, EPS15L1, TIMM13, APP, SEC24C, THBS1, EHD1, HIP1, EHD4, EGFR, HSP90AA1, OPA1, MRC2, LMNA, ELMO2, CORO1C, AP2A2, LRP1, ARF1, AP2A1, TXNDC5, RAB5A, SORT1, MERTK, COPE, EPN2, SH3GL1	3.08E-05
GO:0044275~cellular carbohydrate catabolic process	15	1.06E-07	LDHA, TALDO1, GNPDA1, PFKL, PGAM1, PFKP, HK1, DLAT, GPD1L, PYGL, PGM1, GAA, PDHA1, PGK1, ENO1	5.94E-05
GO:0016192~vesicle-mediated transport	41	1.54E-07	CLTA, GNAI3, CLTB, AP1B1, SNX2, EEA1, EPS15L1, LLGL1, APP, ACTR1A, AP3D1, RAB6A, THBS1, EHD1, SEC24C, HIP1, EHD4, MRC2, SCRN1, WAS, ERGIC1, FLNA, ELMO2, BCAP31, LRPAP1, CORO1C, AP2A2, SCFD1, LRP1, VCP, ARF1, AP2A1, TXNDC5, RAB35, RAB5A, CPNE1, SORT1, MERTK, COPE, SH3GL1, EPN2	6.91E-05
GO:0034613~cellular protein localization	33	2.35E-07	BID, CLTA, CLTB, PDIA3, AP1B1, SNX2, TIMM13, MACF1, AP3D1, PPP3CA, SEC24C, TNPO2, EGFR, TOMM40, IPO9, ARFIP1, TIMM44, FLNA, BCAP31, MAPK1, AP2A2, VCP, AP2A1, IPO4, F2, PCNA, KPNA6, SORT1, SPTBN1, NUTF2, SRP72, KPNA4, SSR4	8.78E-05
GO:0070727~cellular macromolecule localization	33	2.77E-07	BID, CLTA, CLTB, PDIA3, AP1B1, SNX2, TIMM13, MACF1, AP3D1, PPP3CA, SEC24C, TNPO2, EGFR, TOMM40, IPO9, ARFIP1, TIMM44, FLNA, BCAP31, MAPK1, AP2A2, VCP, AP2A1, IPO4, F2, PCNA, KPNA6, SORT1, SPTBN1, NUTF2, SRP72, KPNA4, SSR4	8.86E-05
GO:0006886~intracellular protein transport	31	3.04E-07	BID, CLTA, CLTB, PDIA3, AP1B1, SNX2, TIMM13, MACF1, AP3D1, PPP3CA, SEC24C, TNPO2, TOMM40, IPO9, ARFIP1, TIMM44, BCAP31, MAPK1, AP2A2, VCP, AP2A1, IPO4, F2, PCNA, KPNA6, SORT1, SPTBN1, NUTF2, SRP72, KPNA4, SSR4	8.52E-05
GO:0046164~alcohol catabolic process	14	4.14E-07	LDHA, TALDO1, GNPDA1, PFKL, PGAM1, PFKP, HK1, COMT, DLAT, GPD1L, PGM1, PDHA1, PGK1, ENO1	0.000103
GO:0030036~actin cytoskeleton organization	22	1.9E-06	TLN1, CNN3, ACTA1, ROCK2, BCAR1, CAPZA2, CAPZA1, ACTN1, FLNB, CAPZB, WAS, LLGL1, FLNA, EPB41L2, DYNLL1, PAK2, PTK2B, ABL2, DBN1, PLS3, LCP1, PARVA	0.000425
GO:0008104~protein localization	51	2.01E-06	TLN1, CLTA, CLTB, PDIA3, AP1B1, RAB5C, RAB6A, SEC24C, EGFR, CUTA, NUP133, G3BP2, IPO9, FLNB, TIMM44, FLNA, BCAP31, MAPK1, IPO4, F2, RAB5A, KPNA6, SORT1, GNAS, KPNA4, SRP72, VPS26B, COPE, BID, SNX2, TIMM13, MACF1, AP3D1, PPP3CA, TNPO2, SNX27, RRBP1, HSPG2, TOMM40, ARFIP1, EPS15, AP2A2, SCFD1, ARF1, VCP, AP2A1, RAB35, PCNA, SPTBN1, NUTF2, SSR4	0.000409
GO:0016052~carbohydrate catabolic process	15	2.41E-06	LDHA, TALDO1, GNPDA1, PFKL, PGAM1, PFKP, HK1, DLAT, GPD1L, PYGL, PGM1, GAA, PDHA1, PGK1, ENO1	0.00045
GO:0033365~protein localization in organelle	17	3.91E-06	BID, PDIA3, TOMM40, IPO9, TIMM13, TIMM44, MAPK1, MACF1, IPO4, F2, KPNA6, SPTBN1, NUTF2, SRP72, KPNA4, PPP3CA, TNPO2	0.000673

GO:0046365~monosaccharide catabolic process	12	4.64E-06	LDHA, GNPDA1, TALDO1, PFKL, PGM1, PGAM1, PFKP, HK1, PDHA1, DLAT, PGK1, ENO1	0.000742
GO:0006007~glucose catabolic process	11	4.67E-06	LDHA, TALDO1, PFKL, PGM1, PGAM1, PFKP, HK1, PDHA1, DLAT, PGK1, ENO1	0.000698
GO:0030029~actin filament-based process	22	5.28E-06	TLN1, CNN3, ACTA1, ROCK2, BCAR1, CAPZA2, CAPZA1, ACTN1, FLNB, CAPZB, WAS, LLGL1, FLNA, EPB41L2, DYNLL1, PAK2, PTK2B, ABL2, DBN1, PLS3, LCP1, PARVA	0.000739
GO:0006096~glycolysis	10	5.71E-06	LDHA, PFKL, PGM1, PGAM1, PFKP, HK1, PDHA1, DLAT, PGK1, ENO1	0.000752
GO:0045184~establishment of protein localization	45	7.01E-06	BID, CLTA, CLTB, PDIA3, AP1B1, RAB5C, SNX2, TIMM13, MACF1, AP3D1, RAB6A, PPP3CA, SEC24C, TNPO2, NUP133, SNX27, RRBP1, TOMM40, IPO9, ARFIP1, TIMM44, FLNA, BCAP31, EPS15, MAPK1, AP2A2, SCFD1, VCP, ARF1, AP2A1, IPO4, RAB35, F2, PCNA, RAB5A, KPNA6, SORT1, SPTBN1, NUTF2, GNAS, KPNA4, SRP72, SSR4, VPS26B, COPE	0.000872
GO:0010608~posttranscriptional regulation of gene expression	20	9.3E-06	PRKCA, METAP1, UPF1, ACO1, RBM3, DDX1, PRKDC, ELAVL1, IGF2BP2, GCN1L1, RPS4X, FLNA, EIF4G1, MAPK1, APP, PTK2B, SND1, EIF4A2, HSPD1, THBS1	0.001096
GO:0015031~protein transport	44	1.27E-05	BID, CLTA, CLTB, PDIA3, AP1B1, RAB5C, SNX2, TIMM13, MACF1, AP3D1, RAB6A, PPP3CA, SEC24C, TNPO2, NUP133, SNX27, RRBP1, TOMM40, IPO9, ARFIP1, TIMM44, BCAP31, EPS15, MAPK1, AP2A2, SCFD1, VCP, ARF1, AP2A1, RAB35, IPO4, F2, PCNA, RAB5A, KPNA6, SORT1, SPTBN1, NUTF2, GNAS, KPNA4, SRP72, SSR4, VPS26B, COPE	0.001418
GO:0043085~positive regulation of catalytic activity	34	1.35E-05	PARD3, GNAI2, PTPLAD1, GNA11, PSMA7, PSMB5, PTK2B, ILK, PSMD2, SHC1, THBS1, HIP1, EGFR, MSH6, MSH2, VAV2, PPP1CB, PSMB8, THY1, PSMA2, PSMC6, PSMD13, LRP1, VCP, GNB1, PSME2, NTRK1, PSMC1, F2, PPP2R4, GNAS, HSPD1, ABL2, GAP43	0.001438
GO:0010324~membrane invagination	20	1.68E-05	AP1B1, MRC2, SNX2, EPS15L1, EEA1, ELMO2, CORO1C, APP, AP2A2, LRP1, AP2A1, RAB5A, SORT1, MERTK, EHD1, THBS1, HIP1, EHD4, SH3GL1, EPN2	0.001708
GO:0006897~endocytosis	20	1.68E-05	AP1B1, MRC2, SNX2, EPS15L1, EEA1, ELMO2, CORO1C, APP, AP2A2, LRP1, AP2A1, RAB5A, SORT1, MERTK, EHD1, THBS1, HIP1, EHD4, SH3GL1, EPN2	0.001708
GO:0017038~protein import	15	2.09E-05	BID, PDIA3, TOMM40, IPO9, TIMM13, TIMM44, MAPK1, IPO4, F2, SPTBN1, KPNA6, NUTF2, KPNA4, PPP3CA, TNPO2	0.002035
GO:0019320~hexose catabolic process	11	2.31E-05	LDHA, TALDO1, PFKL, PGM1, PGAM1, PFKP, HK1, PDHA1, DLAT, PGK1, ENO1	0.002151
GO:0006414~translational elongation	13	2.82E-05	RPL35, EEF2, VARS, RPS4X, RPS25, RPS19, RPS28, RPL22, RPL3, EEF1G, RPL10, RPS10, EEF1D	0.002523
GO:0006006~glucose metabolic process	16	3E-05	LDHA, TALDO1, PFKL, PHKA1, PGAM1, PFKP, HK1, DLAT, PPP1CB, CPT1A, PYGL, PGM1, GAA, PDHA1, PGK1, ENO1	0.002578
GO:0007015~actin filament organization	11	3.37E-05	PAK2, ACTA1, PTK2B, BCAR1, ACTN1, ABL2, WAS, DBN1, PLS3, FLNA, LCP1	0.002795
GO:0006913~nucleocytoplasmic transport	16	3.76E-05	NUP133, UPF1, PDIA3, IPO9, MAPK1, SET, RAE1, IPO4, F2, KPNA6, SPTBN1, THOC4, NUTF2, KPNA4, PPP3CA, TNPO2	0.003007
GO:0051169~nuclear transport	16	4.37E-05	NUP133, UPF1, PDIA3, IPO9, MAPK1, SET, RAE1, IPO4, F2, KPNA6, SPTBN1, THOC4, NUTF2, KPNA4, PPP3CA, TNPO2	0.003368
GO:0044093~positive regulation of molecular function	35	6.21E-05	PARD3, GNAI2, PTPLAD1, GNA11, PRDX3, PSMA7, PSMB5, PTK2B, ILK, PSMD2, SHC1, THBS1, HIP1, EGFR, MSH6, MSH2, VAV2, PPP1CB, PSMB8, THY1, PSMA2, PSMC6, PSMD13, LRP1, VCP, GNB1, PSME2, NTRK1, PSMC1, F2, PPP2R4, GNAS, HSPD1, ABL2, GAP43	0.004626
GO:0005996~monosaccharide metabolic process	19	6.43E-05	LDHA, TALDO1, GNPDA1, PFKL, PHKA1, PGAM1, PFKP, HK1, DLAT, NAGK, PPP1CB, CPT1A, PYGL, PGM1, GAA, PDHA1, PGK1, ENO1, PRPS1	0.004633
GO:0006412~translation	24	7.34E-05	EGFR, YARS, CARS, RRBP1, RBM3, RPL35, EEF2, QARS, LRRC47, VARS, RPS4X, RPS25, EIF4G1, RPS19, RPS28, RPL22, EIF1AX, EIF4A2, RPL3, RPL10, EEF1G, RPS10, EIF2AK2, EEF1D	0.005127
GO:0006417~regulation of translation	14	0.000141	PRKCA, METAP1, UPF1, ACO1, DDX1, IGF2BP2, RPS4X, GCN1L1, EIF4G1, MAPK1, APP, PTK2B, EIF4A2, THBS1	0.009509
GO:0043161~proteasomal ubiquitin-dependent protein catabolic process	12	0.000147	PSMA2, PSMB5, CUL3, PSMC6, PSMD13, VCP, PSME2, PSMC1, PSMD2, PSMA7, STUB1, PSMB8	0.009644
GO:0010498~proteasomal protein catabolic process	12	0.000147	PSMA2, PSMB5, CUL3, PSMC6, PSMD13, VCP, PSME2, PSMC1, PSMD2, PSMA7, STUB1, PSMB8	0.009644
GO:0065003~macromolecular complex assembly	37	0.000153	PARD3, SAMM50, CAPZA2, CAPZA1, H1FX, CDH2, HPRT1, LLGL1, SET, PAK2, PTK2B, PRMT5, ILK, NDUFS8, TUBB6, H2AFX, TNPO2, HIP1, CUTA, HSP90AA1, PFKL, DDX1, PFKP,	0.009729

			IPO9, MCM2, MBNL1, SLC9A3R1, SF3A2, WAS, HMGA1, FLNA, PTRF, VCP, IPO4, CAPG, HSPD1, PARVA	
GO:0006606~protein import into nucleus	11	0.000157	MAPK1, PDIA3, IPO4, F2, KPNA6, SPTBN1, IPO9, NUTF2, PPP3CA, KPNA4, TNPO2	0.009699
GO:0016310~phosphorylation	42	0.000171	PRPF4B, GNAI2, PTPLAD1, PRDX4, PRKDC, CASK, ABI1, CAD, FER, ATP6V1B2, TOP1, APP, PAK2, PTK2B, ILK, NDUFS8, SHC1, NDUFS3, ATP6V0D1, THBS1, NDUFA4, EGFR, PRKCA, TAOK1, ROCK2, MSH2, MAP2K2, PTPRA, TRIM28, AK3, EPHA2, MAPK1, NTRK1, ATP6V1E1, DYRK1A, F2, ATP5C1, SPTBN1, MERTK, PGK1, EIF2AK2, ABL2	0.010278

decrease in GBM12 and 59/ Increase in GBM15

GO Term	Count	EASE score	Genes	Benjamini correction
GO:0006084~acetyl-CoA metabolic process	9	1.07E-07	SDHA, NNT, ACO2, DLD, CS, IDH2, SUCLA2, IDH3A, MDH2	0.000218
GO:0046356~acetyl-CoA catabolic process	8	1.97E-07	SDHA, NNT, ACO2, CS, IDH2, SUCLA2, IDH3A, MDH2	0.0002
GO:0006099~tricarboxylic acid cycle	8	1.97E-07	SDHA, NNT, ACO2, CS, IDH2, SUCLA2, IDH3A, MDH2	0.0002
GO:0009109~coenzyme catabolic process	8	5.02E-07	SDHA, NNT, ACO2, CS, IDH2, SUCLA2, IDH3A, MDH2	0.00034
GO:0008104~protein localization	40	1.53E-06	AP1M1, TLN1, TLN2, PML, NUP93, NAPA, TIMM50, LMAN2, CLTC, CDC37, CTNNB1, TMED2, NPM1, PPP3CA, TPR, TNPO1, KPNB1, AP3B1, EGFR, SEC23A, ARHGEF2, ACTN4, RRBP1, YWHAB, HSPG2, ITGA2, ATG3, FLNB, FLNA, RAB31, AP2A2, ERBB2IP, AP2A1, FGFR1OP, RAB35, SDCBP, NUTF2, PDCD6IP, YKT6, COPE	0.000778
GO:0051187~cofactor catabolic process	8	1.84E-06	SDHA, NNT, ACO2, CS, IDH2, SUCLA2, IDH3A, MDH2	0.00075
GO:0046907~intracellular transport	33	1.99E-06	NCBP1, AP1M1, PML, NAPA, CLTC, TPM1, CDC37, SLC1A3, NPM1, RANBP1, PPP3CA, TPR, TNPO1, KPNB1, AP3B1, SEC23A, ARHGEF2, HSP90AA1, MAP2K1, YWHAB, FLNA, AP2A2, SLC25A13, ERBB2IP, AP2A1, RAB35, TXNDC5, SDCBP, NUTF2, YKT6, COPE, DNM2, MYH10	0.000675
GO:0045333~cellular respiration	12	3.08E-06	SDHA, NNT, NDUFS4, SLC1A3, SLC25A13, ACO2, DLD, CS, IDH2, SUCLA2, IDH3A, MDH2	0.000895
GO:0006091~generation of precursor metabolites and energy	21	3.83E-06	ACOX1, PFKL, ACO2, CS, CYC1, UQCRFS1, IDH3A, SDHA, ACADVL, NNT, SLC1A3, SLC25A13, NDUFS4, PKM2, TXN, DLD, IDH2, ATP6V0A1, ATP5I, SUCLA2, MDH2	0.000972
GO:0009060~aerobic respiration	8	4.41E-06	SDHA, NNT, ACO2, CS, IDH2, SUCLA2, IDH3A, MDH2	0.000996
GO:0010033~response to organic substance	34	5.18E-06	PTGS1, PML, PRKDC, HSPA1A, ASNS, UQCRFS1, CTNNB1, GOT2, CASP3, PRKAR2A, GSTM3, NDUFS4, CD44, PTK2B, GSN, GAB1, HSPE1, PPP3CA, NUDC, EGFR, PRKCA, HSP90AA1, MAP2K1, PFKL, AARS, ITGA2, STAT3, DDR1, HDAC2, GNB2, TFRC, ABAT, PEBP1, HSPD1	0.001054
GO:0032268~regulation of cellular protein metabolic process	26	7.4E-06	NCBP1, PTPLAD1, PML, GCN1L1, PRKAR2A, NDUFS4, PTK2B, GAB1, QKI, PSMD3, PSMD5, PSMD7, BUB3, PSMD9, PRKCA, EGFR, DBNL, PAIP1, YWHAB, ITGA2, RPS5, PSMC6, HDAC2, PSMC3, PSMA4, PEBP1	0.001367
GO:0007010~cytoskeleton organization	24	1.72E-05	HRAS, ARHGEF2, TLN1, CAP2, ACTN4, TLN2, TPM1, FLNB, FLNA, LLGL1, CTNNB1, CORO2B, PFN2, PTK2, PAK2, ERBB2IP, PTK2B, GSN, FGFR1OP, NPM1, RHOA, SDCBP, RANBP1, MYH10	0.002908
GO:0065003~macromolecular complex assembly	31	1.9E-05	NCBP1, HRAS, PARD3, PML, LLGL1, CTNNB1, PTK2, NDUFS4, PAK2, PTK2B, GSN, NPM1, H2AFY, KPNB1, TNPO1, TUBB3, HIP1, HSP90AA1, PFKL, MAP2K1, YWHAB, EPRS, MCM2, SF3A1, FLNA, PRPF6, TBCA, CAPG, PEBP1, HSPD1, LAMC1	0.002965
GO:0016044~membrane organization	22	2.11E-05	EGFR, SEC23A, DBNL, HRAS, AP1M1, HSP90AA1, LMNA, NAPA, TIMM50, EPS15L1, CLTC, ELMO2, LETM1, AP2A2, TFRC, AP2A1, TXNDC5, COPE, MYH10, DNM2, AP3B1, HIP1	0.003066
GO:0070271~protein complex biogenesis	26	2.15E-05	HRAS, PARD3, PML, LLGL1, CTNNB1, PTK2, NDUFS4, PAK2, PTK2B, GSN, NPM1, KPNB1, TNPO1, TUBB3, HIP1, HSP90AA1, PFKL, MAP2K1, YWHAB, EPRS, FLNA, TBCA, CAPG, PEBP1, HSPD1, LAMC1	0.002912

GO:0006461~protein complex assembly	26	2.15E-05	HRAS, PARD3, PML, LLGL1, CTNNB1, PTK2, NDUFS4, PAK2, PTK2B, GSN, NPM1, KPNB1, TNPO1, TUBB3, HIP1, HSP90AA1, PFKL, MAP2K1, YWHAB, EPRS, FLNA, TBCA, CAPG, PEBP1, HSPD1, LAMC1	0.002912
GO:0031399~regulation of protein modification process	19	2.2E-05	PRKCA, EGFR, DBNL, PTPLAD1, YWHAB, PML, PRKAR2A, PSMC6, NDUFS4, PTK2B, PSMC3, PSMA4, GAB1, PEBP1, PSMD3, PSMD5, PSMD7, BUB3, PSMD9	0.002797
GO:0015980~energy derivation by oxidation of organic compounds	13	2.7E-05	ACO2, CS, IDH3A, ACADVL, SDHA, SLC25A13, NDUFS4, SLC1A3, NNT, DLD, IDH2, SUCLA2, MDH2	0.00323
GO:0043085~positive regulation of catalytic activity	26	3.49E-05	PARD3, PTPLAD1, PML, TPM1, PRKAR2A, PTK2B, NPM1, GAB1, PSMD3, HSPE1, PSMD5, PSMD7, PSMD9, HIP1, EGFR, DBNL, CAP2, SSBP1, MAP2K1, YWHAB, ITGA2, VAV2, PSMC6, PSMC3, PSMA4, HSPD1	0.003933
GO:0030036~actin cytoskeleton organization	16	4.12E-05	HRAS, TLN1, ARHGEF2, ACTN4, TPM1, FLNB, FLNA, LLGL1, CORO2B, PFN2, PAK2, PTK2B, GSN, RHOA, SDCBP, MYH10	0.004396
GO:0043648~dicarboxylic acid metabolic process	7	4.63E-05	SDHA, GOT2, DLD, CS, IDH3A, MDH2, PC	0.004693
GO:0045184~establishment of protein localization	33	4.84E-05	AP1M1, PML, NUP93, NAPA, TIMM50, LMAN2, CLTC, CDC37, TMED2, NPM1, PPP3CA, TPR, TNPO1, KPNB1, AP3B1, SEC23A, ARHGEF2, ACTN4, RRBP1, YWHAB, ITGA2, ATG3, FLNA, RAB31, AP2A2, ERBB2IP, AP2A1, RAB35, SDCBP, NUTF2, PDCD6IP, YKT6, COPE	0.004679
GO:0006732~coenzyme metabolic process	13	4.93E-05	COASY, ACO2, CS, IDH3A, MTHFD1, SDHA, GSR, PGLS, NNT, DLD, IDH2, SUCLA2, MDH2	0.004544
GO:0007049~cell cycle	33	5.71E-05	PPP6C, PARD3, KIAA0174, PML, SART1, CTNNB1, NUMA1, NPM1, PSMD3, RANBP1, PPP3CA, PSMD5, PSMD7, STAG2, BUB3, TUBB3, NUDC, PSMD9, EGFR, ARHGEF2, MAP2K1, ANXA1, UBE2I, MCM2, ARL3, PPM1G, PSMC6, ERBB2IP, PSMC3, PSMA4, PDCD6IP, DNM2, MYH10	0.005034
GO:0043933~macromolecular complex subunit organization	31	6.38E-05	NCBP1, HRAS, PARD3, PML, LLGL1, CTNNB1, PTK2, NDUFS4, PAK2, PTK2B, GSN, NPM1, H2AFY, KPNB1, TNPO1, TUBB3, HIP1, HSP90AA1, PFKL, MAP2K1, YWHAB, EPRS, MCM2, SF3A1, FLNA, PRPF6, TBCA, CAPG, PEBP1, HSPD1, LAMC1	0.005392
GO:0034613~cellular protein localization	22	6.38E-05	EGFR, SEC23A, ARHGEF2, AP1M1, YWHAB, PML, NAPA, CLTC, FLNA, CDC37, CTNNB1, AP2A2, ERBB2IP, AP2A1, NPM1, SDCBP, NUTF2, PPP3CA, TPR, TNPO1, KPNB1, AP3B1	0.00518
GO:0070727~cellular macromolecule localization	22	6.94E-05	EGFR, SEC23A, ARHGEF2, AP1M1, YWHAB, PML, NAPA, CLTC, FLNA, CDC37, CTNNB1, AP2A2, ERBB2IP, AP2A1, NPM1, SDCBP, NUTF2, PPP3CA, TPR, TNPO1, KPNB1, AP3B1	0.005415
GO:0030029~actin filament-based process	16	8.56E-05	HRAS, TLN1, ARHGEF2, ACTN4, TPM1, FLNB, FLNA, LLGL1, CORO2B, PFN2, PAK2, PTK2B, GSN, RHOA, SDCBP, MYH10	0.006425
GO:0044093~positive regulation of molecular function	27	9.25E-05	PARD3, PTPLAD1, PML, TPM1, PRKAR2A, PTK2B, NPM1, GAB1, PSMD3, HSPE1, PSMD5, PSMD7, PSMD9, HIP1, EGFR, DBNL, CAP2, ACTN4, SSBP1, MAP2K1, YWHAB, ITGA2, VAV2, PSMC6, PSMC3, PSMA4, HSPD1	0.006695
GO:0031400~negative regulation of protein modification process	11	0.000118	PRKCA, PSMC6, PSMC3, PSMA4, YWHAB, PSMD3, PEBP1, PSMD5, PSMD7, BUB3, PSMD9	0.008256
GO:0022402~cell cycle process	26	0.000132	PPP6C, PML, SART1, CTNNB1, NUMA1, NPM1, PSMD3, RANBP1, PSMD5, PPP3CA, PSMD7, BUB3, TUBB3, NUDC, STAG2, PSMD9, EGFR, ARHGEF2, MAP2K1, UBE2I, PPM1G, PSMC6, PSMC3, PSMA4, MYH10, DNM2	0.008921
GO:0032507~maintenance of protein location in cell	7	0.000138	TLN1, TLN2, FGFR1OP, YWHAB, PML, FLNB, FLNA	0.009002
GO:0055114~oxidation reduction	28	0.000151	ACOX1, PTGS1, CYC1, COX5A, UQCRFS1, FDFT1, MTHFD1, GSR, SLC1A3, NDUFS4, PLOD1, DHCR7, PLOD3, IDH2, HSD17B4, IMPDH2, GPD2, IDH3A, SDHA, ACADVL, NNT, SLC25A13, HSDL2, BLVRB, TXN, DLD, MDH2, ALDH9A1	0.009523
GO:0043161~proteasomal ubiquitin-dependent protein catabolic process	10	0.000178	RAD23B, PSMC6, PSMC3, PSMA4, RAD23A, PSMD3, PSMD5, PSMD7, BUB3, PSMD9	0.01094

Table S16. GO classification of the genes with no change in copy number (first 50 categories).

GO Term	Count	EASE score	Genes	Benjamini correction
GO:0046907~intracellular transport	86	1.82E-18	NCBP1, XPO1, ENAH, CLTB, AP1B1, AP1G1, CLTC, SSR1, AP2B1, APP, SLC1A3, RAE1, ZFYVE16, ANP32A, ATP5O, RANBP1, SAR1B, AP3B1, SEC23A, NUP133, ARHGEF2, HSP90AA1, ERP29, IPO9, MYH9, ERGIC1, MAPK1, IPO7, TXNDC5, ARCN1, F2, RAB14, KPNA6, SDCBP, GNAS, SRP72, KPNA4, VPS26B, LRPPRC, MYL6, YWHAZ, NUP98, STX7, NUP160, COPZ1, MYL1, PML, AKAP12, SNX2, SNX1, EEA1, CALR, TPM1, CDC37, STX12, MACF1, NPM1, AP3D1, TMED10, VPS35, PAFAH1B1, PPP3CA, EHD1, HSPA8, SEC61A1, FYB, MAP2K1, ARFIP1, NUP155, YWHAE, AP2A2, YWHAH, ATP2A2, VCP, ERBB2IP, AP2A1, TOMM70A, GSK3B, BAX, RAB35, YWHAQ, SPTBN1, XPO7, YKT6, MYH10, DNM2	5.27E-15
GO:0008104~protein localization	96	4.3E-15	XPO1, CLTB, AP1B1, RAB5B, AP1G1, TLN2, PDIA4, CLTC, CANX, RAB1A, SSR1, CTNNB1, AP2B1, ZFYVE16, RAB6A, SAR1B, RAB21, AP3B1, SEC23A, NUP133, ARHGEF2, LYN, ACTN4, ERP29, G3BP2, IPO9, MYH9, FLNB, MAPK1, RAB18, IPO7, FGFR1OP, ARCN1, F2, RAB5A, RAB14, KPNA6, SDCBP, GNAS, SRP72, PDCD6IP, COL1A1, KPNA4, RAB10, VPS26B, VPS29, YWHAZ, CAV1, NUP98, NACA, STX7, NUP160, COPZ1, PML, AKAP12, SNX2, SNX1, RDX, ARF5, SNX3, LMAN2, CALR, CDC37, STX12, TMED2, MACF1, DDX19A, NPM1, TMED10, AP3D1, VPS35, PPP3CA, SEC61A1, FYB, HSPG2, ITGA2, ARFIP1, NUP155, YWHAE, RAB31, HSP90B1, AP2A2, YWHAH, VCP, ERBB2IP, AP2A1, TOMM70A, GSK3B, BAX, RAB35, ARF4, YWHAQ, SPTBN1, FAF1, XPO7, YKT6	6.28E-12
GO:0045184~establishment of protein localization	86	3.37E-14	XPO1, CLTB, AP1B1, RAB5B, AP1G1, PDIA4, CLTC, CANX, RAB1A, SSR1, AP2B1, ZFYVE16, RAB6A, SAR1B, RAB21, AP3B1, SEC23A, NUP133, ARHGEF2, LYN, ACTN4, ERP29, IPO9, MYH9, MAPK1, RAB18, IPO7, ARCN1, F2, RAB5A, RAB14, KPNA6, SDCBP, GNAS, SRP72, PDCD6IP, COL1A1, KPNA4, VPS26B, RAB10, VPS29, YWHAZ, NUP98, NACA, STX7, NUP160, COPZ1, PML, AKAP12, SNX2, SNX1, ARF5, SNX3, LMAN2, CALR, CDC37, STX12, TMED2, MACF1, DDX19A, NPM1, AP3D1, TMED10, VPS35, PPP3CA, SEC61A1, FYB, ITGA2, ARFIP1, NUP155, YWHAE, RAB31, HSP90B1, AP2A2, YWHAH, VCP, ERBB2IP, AP2A1, TOMM70A, GSK3B, RAB35, ARF4, YWHAQ, SPTBN1, XPO7, YKT6	3.27E-11
GO:0015031~protein transport	85	5.64E-14	XPO1, CLTB, AP1B1, RAB5B, AP1G1, PDIA4, CLTC, CANX, RAB1A, SSR1, AP2B1, ZFYVE16, RAB6A, SAR1B, RAB21, AP3B1, SEC23A, NUP133, ARHGEF2, LYN, ACTN4, ERP29, IPO9, MYH9, MAPK1, RAB18, IPO7, ARCN1, F2, RAB5A, RAB14, KPNA6, SDCBP, GNAS, SRP72, PDCD6IP, COL1A1, KPNA4, VPS26B, RAB10, VPS29, YWHAZ, NUP98, NACA, STX7, NUP160, COPZ1, PML, AKAP12, SNX2, SNX1, ARF5, SNX3, LMAN2, CALR, CDC37, STX12, TMED2, MACF1, DDX19A, NPM1, AP3D1, TMED10, VPS35, PPP3CA, SEC61A1, FYB, ARFIP1, NUP155, YWHAE, RAB31, HSP90B1, AP2A2, YWHAH, VCP, ERBB2IP, AP2A1, TOMM70A, GSK3B, RAB35, ARF4, YWHAQ, SPTBN1, XPO7, YKT6	4.09E-11
GO:0006886~intracellular protein transport	51	1.13E-11	XPO1, CLTB, AP1B1, AP1G1, CLTC, SSR1, AP2B1, ZFYVE16, SAR1B, AP3B1, SEC23A, ARHGEF2, ERP29, IPO9, MAPK1, IPO7, F2, ARCN1, KPNA6, SDCBP, KPNA4, SRP72, NUP98, YWHAZ, STX7, COPZ1, SNX2, AKAP12, PML, SNX1, CALR, CDC37, STX12, MACF1, NPM1, AP3D1, PPP3CA, SEC61A1, FYB, ARFIP1, YWHAE, AP2A2, YWHAH, ERBB2IP, VCP, AP2A1, TOMM70A, GSK3B, YWHAQ, SPTBN1, XPO7	6.58E-09
GO:0070727~cellular macromolecule localization	54	1.44E-11	XPO1, CLTB, AP1B1, AP1G1, CLTC, CTNNB1, SSR1, AP2B1, ZFYVE16, SAR1B, AP3B1, SEC23A, ARHGEF2, ERP29, IPO9, MAPK1, IPO7, F2, ARCN1, KPNA6, SDCBP, KPNA4, SRP72, YWHAZ, NUP98, STX7, COPZ1, SNX2, AKAP12, PML, SNX1, CALR, CDC37, STAU1, STX12, MACF1, NPM1, AP3D1, PPP3CA, SEC61A1, FYB, ARFIP1, YWHAE, AP2A2, YWHAH, ERBB2IP, VCP, AP2A1, TOMM70A, GSK3B, BAX, YWHAQ, SPTBN1, XPO7	6.97E-09
GO:0034613~cellular protein localization	53	3.54E-11	XPO1, CLTB, AP1B1, AP1G1, CLTC, CTNNB1, SSR1, AP2B1, ZFYVE16, SAR1B, AP3B1, SEC23A, ARHGEF2, ERP29, IPO9, MAPK1, IPO7, F2, ARCN1, KPNA6, SDCBP, KPNA4, SRP72, NUP98, YWHAZ, STX7, COPZ1, SNX2, AKAP12, PML, SNX1, CALR, CDC37, STX12, MACF1, NPM1, AP3D1, PPP3CA, SEC61A1, FYB, ARFIP1, YWHAE, AP2A2, YWHAH, ERBB2IP, VCP, AP2A1, TOMM70A, GSK3B, BAX, YWHAQ, SPTBN1, XPO7	1.47E-08
GO:0006091~generation of precursor metabolites and energy	45	3.89E-11	UQCRC2, NDUFS4, GOT1, SLC1A3, SLC25A3, IDH2, IDH1, ATP5O, CAT, ERO1L, NDUFS3, ATP6V0D1, ETFB, NDUFS1, ETFA, DLST, ACO2, PFKL, MSH2, SUCLG2, NDUFA9, SUCLG1, CS, DLAT, PFKM, PPP1CB, SOD2, SDHA, ATP6V1A, NNT, GBE1, UQCRH, PYGL, GSK3B, PKM2, GFPT1,	1.41E-08

			ATP6V1E1, TXN, PGM1, ATP6V0A1, TXNRD1, GNAS, ATP5A1, UQCRB, MDH1	
GO:0015980~energy derivation by oxidation of organic compounds	27	2.1E-09	UQCRC2, SLC1A3, NDUFS4, GOT1, IDH2, IDH1, CAT, NDUFS3, NDUFS1, DLST, ACO2, SUCLG2, NDUFA9, SUCLG1, CS, PPP1CB, SOD2, SDHA, GBE1, NNT, PYGL, UQCRH, GFPT1, GSK3B, GNAS, UQCRB, MDH1	6.77E-07
GO:0009060~aerobic respiration	14	2.32E-09	UQCRC2, DLST, ACO2, SUCLG2, SUCLG1, CS, SDHA, NNT, UQCRH, IDH2, IDH1, CAT, MDH1, UQCRB	6.72E-07
GO:0051493~regulation of cytoskeleton organization	25	1.4E-08	XPO1, LIMA1, CAV1, RDX, CAPZB, TPM1, CTNNB1, ACTR3, MACF1, ARPC2, RAC1, NPM1, RHOA, RANBP1, ARHGEF2, ROCK2, MAP1B, ARPC1A, ARPC1B, ARPC5L, CAPG, MAP2, MAP4, SPTBN1, SPTAN1	3.69E-06
GO:0043933~macromolecular complex subunit organization	68	1.8E-08	NCBP1, XPO1, HP1BP3, SNRPD3, NAP1L1, SNRPD1, NAP1L4, CTNNB1, PICALM, NDUFS4, H2AFV, H2AFY, CAT, NUP133, PPP2R1A, HSP90AA1, DARS, PFKL, CRYAB, SF1, IPO9, MBNL1, DECR1, PFKM, SPAG9, IPO7, UQCRH, TBCA, RPS14, RRM1, SMARCA5, SNRPC, LAMC1, XRN2, PPP5C, PARVA, PARD3, NUP98, CAV1, FKBP4, PML, ABI2, CDH2, CALR, SF3B3, PXN, FGG, PTK2, PTK2B, FGB, USP39, NPM1, RAC1, HIP1, MAP2K1, DDX1, EPRS, SMAD2, ANXA5, ETF1, SF3A1, SF3A3, SOD2, VCP, BAX, THRAP3, CAPG, XPO7	4.36E-06
GO:0065003~macromolecular complex assembly	64	4.31E-08	NCBP1, XPO1, HP1BP3, SNRPD3, NAP1L1, SNRPD1, NAP1L4, CTNNB1, PICALM, NDUFS4, H2AFV, H2AFY, CAT, PPP2R1A, HSP90AA1, DARS, PFKL, CRYAB, SF1, IPO9, MBNL1, DECR1, PFKM, SPAG9, IPO7, UQCRH, TBCA, RPS14, RRM1, SMARCA5, SNRPC, LAMC1, PARVA, PPP5C, PARD3, NUP98, CAV1, FKBP4, PML, CDH2, CALR, SF3B3, PXN, PTK2, FGG, PTK2B, FGB, USP39, NPM1, RAC1, HIP1, MAP2K1, DDX1, EPRS, SMAD2, ANXA5, SF3A1, SF3A3, SOD2, VCP, BAX, THRAP3, CAPG, XPO7	9.62E-06
GO:0034621~cellular macromolecular complex subunit organization	42	7.31E-08	XPO1, NCBP1, NUP98, CAV1, HP1BP3, FKBP4, SNRPD3, SNRPD1, NAP1L1, ABI2, CALR, NAP1L4, PXN, PTK2, FGG, NDUFS4, PICALM, H2AFV, PTK2B, FGB, USP39, RAC1, NPM1, H2AFY, HIP1, NUP133, HSP90AA1, DDX1, SF1, IPO9, SMAD2, MBNL1, ETF1, SF3A1, SF3A3, TBCA, IPO7, RPS14, SMARCA5, SNRPC, XPO7, XRN2	1.52E-05
GO:0006412~translation	40	7.7E-08	RPL18, NACA, EEF1B2, RPL19, RPL14, NARS, PABPC4, EIF5B, IGF2BP3, VARS, KARS, IARS, WARS, RPS26, RPL31, RPS3A, RPL34, RPL8, LARS, RPL5, RPL10A, RPL4, YARS, DARS, AARS, EPRS, LRRC47, ETF1, EIF4B, EIF4G2, RPS18, RPL18A, RPS16, TSFM, RPS14, EIF2S1, RARS, RPS12, RPS13, EIF2AK2	1.49E-05
GO:0045333~cellular respiration	20	8.08E-08	UQCRC2, DLST, ACO2, SUCLG2, NDUFA9, SUCLG1, CS, SOD2, SDHA, NNT, NDUFS4, SLC1A3, UQCRH, IDH2, IDH1, CAT, NDUFS3, NDUFS1, UQCRB, MDH1	1.47E-05
GO:0006397~mRNA processing	39	1.01E-07	RALY, NCBP1, PRPF4B, STRAP, NHP2L1, SNRPD3, RBM4, LSM7, SNRPD1, SYNCRIP, HNRPLL, SF3B3, PNN, PRPF19, SF3B1, APP, DDX46, PRPF8, PCBP2, NUDT21, DNAJC8, USP39, DHX15, U2AF1, LSM3, PABPC1, KHDRBS3, EFTUD2, PTBP1, DDX1, SF1, MBNL1, SF3A1, PRPF4, SF3A3, CPSF6, SNRPC, XRN2, ADAR	1.72E-05
GO:0006414~translational elongation	20	1.59E-07	RPL18, RPL19, EEF1B2, RPL14, VARS, RPS26, RPS18, RPS16, RPL18A, RPS3A, RPL31, RPL34, RPS14, TSFM, RPL8, RPS12, RPS13, RPL5, RPL4, RPL10A	2.56E-05
GO:0010498~proteasomal protein catabolic process	20	1.87E-07	RAD23B, RAD23A, PSMA7, CUL3, PSMA1, HSP90B1, PSMB7, VCP, PSMD12, PSMD11, PSMB3, PSMA4, PSMD1, PSMC1, PSMA3, PSMD3, PSME3, FAF1, PSMD6, PSMD9	2.85E-05
GO:0043161~proteasomal ubiquitin-dependent protein catabolic process	20	1.87E-07	RAD23B, RAD23A, PSMA7, CUL3, PSMA1, HSP90B1, PSMB7, VCP, PSMD12, PSMD11, PSMB3, PSMA4, PSMD1, PSMC1, PSMA3, PSMD3, PSME3, FAF1, PSMD6, PSMD9	2.85E-05
GO:0034622~cellular macromolecular complex assembly	38	2.31E-07	XPO1, NCBP1, NUP98, CAV1, HP1BP3, SNRPD3, FKBP4, SNRPD1, NAP1L1, CALR, NAP1L4, PXN, PTK2, FGG, NDUFS4, PICALM, H2AFV, FGB, PTK2B, RAC1, NPM1, USP39, H2AFY, HIP1, HSP90AA1, DDX1, SF1, SMAD2, IPO9, MBNL1, SF3A1, SF3A3, TBCA, IPO7, RPS14, SMARCA5, SNRPC, XPO7	3.35E-05
GO:0016192~vesicle-mediated transport	56	2.53E-07	CLTB, AP1B1, AP1G1, EPS15L1, CLTC, RAB1A, CTNNB1, AP2B1, APP, PICALM, ZFYVE16, RAB6A, SAR1B, AP3B1, SEC23A, LYN, ERGIC1, RAB18, TXNDC5, ARCN1, RAB5A, RAB14, EPN2, SH3GL1, CAV1, YWHAZ, STX7, COPZ1, SNX2, SNX1, EEA1, SNX3, ARF5, STX12, TMED2, ITGAV, RAC1, AP3D1, TMED10, VPS35, EHD1, HSPA8, HIP1, HCK, SCRN1, CORO1C, AP2A2, LRP1, VCP, AP2A1, RAB35, ARF4, MERTK, YKT6, MYH10, DNM2	3.49E-05
GO:0033043~regulation of organelle organization	30	2.66E-07	XPO1, CAV1, LIMA1, PML, RDX, RCC1, CAPZB, TPM1, CTNNB1, PIN1, ACTR3, MACF1, ARPC2, RAC1, NPM1, RHOA, RANBP1, ARHGEF2, ROCK2, MAP1B, UBE2N, ARPC1A, ARPC1B, ARPC5L, GOLPH3, CAPG, MAP2, MAP4, SPTBN1, SPTAN1	3.51E-05

GO:0032268~regulation of cellular protein metabolic process	49	2.76E-07	NCBP1, METAP1, A2M, EIF5B, APP, PRKAR2A, NDUFS4, PSMD1, GAB1, PSMD3, PSMD6, PSMD9, PRKCA, PPP2R1A, LYN, UBE2N, EIF4G2, PSMA1, MAPK1, PSMA4, EIF2S1, F2, PSMA3, PSME3, CAV1, PTPLAD1, PML, IGF2BP2, IGF2BP3, PSMA7, GCN1L1, CALR, PIN1, PSMB7, PTK2B, ITGAV, PSMB3, DDX1, ITGA2, DOCK7, ETF1, YWHAE, EIF4B, HDAC2, PSMD12, PSMD11, BAX, PSMC1, PPP2R4	3.49E-05
GO:0006099~tricarboxylic acid cycle	10	4.25E-07	SDHA, DLST, NNT, ACO2, SUCLG2, SUCLG1, CS, IDH2, IDH1, MDH1	5.14E-05
GO:0046356~acetyl-CoA catabolic process	10	4.25E-07	SDHA, DLST, NNT, ACO2, SUCLG2, SUCLG1, CS, IDH2, IDH1, MDH1	5.14E-05
GO:0051443~positive regulation of ubiquitin-protein ligase activity	16	5.57E-07	PSMA7, PIN1, UBE2N, PSMA1, PSMB7, PSMD12, PSMD11, PSMB3, PSMA4, PSMC1, PSMA3, PSMD1, PSMD3, PSME3, PSMD6, PSMD9	6.47E-05
GO:0006457~protein folding	26	6.25E-07	FKBP4, PDIA6, CCT2, CCT3, CALR, CANX, PIN1, ERO1L, HSPA8, DNAJA2, HSP90AA1, CRYAB, AARS, ERP29, ST13, TRAP1, HSP90B1, CCT5, CCT4, TBCA, PFDN5, TBCD, PPID, RUVBL2, FKBP10, AHSA1	6.97E-05
GO:0006605~protein targeting	29	7.3E-07	XPO1, YWHAZ, NUP98, PML, AKAP12, CALR, CDC37, SSR1, MACF1, ZFYVE16, PPP3CA, SEC61A1, AP3B1, FYB, IPO9, YWHAE, MAPK1, ERBB2IP, TOMM70A, IPO7, GSK3B, F2, YWHAQ, KPNA6, SDCBP, SPTBN1, KPNA4, SRP72, XPO7	7.85E-05
GO:0006084~acetyl-CoA metabolic process	11	7.8E-07	SDHA, DLST, NNT, ACO2, SUCLG2, SUCLG1, CS, IDH2, IDH1, DLAT, MDH1	8.09E-05
GO:0032269~negative regulation of cellular protein metabolic process	26	8.6E-07	A2M, CAV1, PML, IGF2BP2, IGF2BP3, CALR, PSMA7, PSMB7, PSMB3, ITGAV, PSMD1, PSMD3, PSMD6, PSMD9, PRKCA, PPP2R1A, YWHAE, PSMA1, PSMD12, PSMD11, BAX, PSMA4, PSMC1, PSMA3, PSME3, PPP2R4	8.61E-05
GO:0007010~cytoskeleton organization	45	9.69E-07	LIMA1, CAV1, TLN2, CALD1, ABI2, RCC1, CALR, TPM1, CAPZB, CTNNB1, ACTG1, CORO2B, PTK2, MACF1, PTK2B, NPM1, RAC1, RHOA, PAFAH1B1, RANBP1, DYNC1H1, FGD5, ARHGEF2, CAP2, ACTN4, CKAP5, ROCK2, CRYAB, MAP1B, ACTN1, DOCK7, MYH9, PALLD, FLNB, VASP, ARPC1A, EPB41L2, ERBB2IP, FGFR1OP, MAP2, SDCBP, CRK, LCP1, PARVA, MYH10	9.37E-05
GO:0051351~positive regulation of ligase activity	16	9.87E-07	PSMA7, PIN1, UBE2N, PSMA1, PSMB7, PSMD12, PSMD11, PSMB3, PSMA4, PSMC1, PSMA3, PSMD1, PSMD3, PSME3, PSMD6, PSMD9	9.24E-05
GO:0008380~RNA splicing	34	1.08E-06	RALY, NCBP1, PRPF4B, STRAP, NHP2L1, SNRPD3, LSM7, RBM4, SNRPD1, SYNCRIP, SF3B3, PNN, PRPF19, SF3B1, DDX46, PRPF8, PCBP2, DNAJC8, NUDT21, USP39, DHX15, U2AF1, LSM3, PABPC1, PPP2R1A, EFTUD2, PTBP1, DDX1, SF1, MBNL1, SF3A1, PRPF4, SF3A3, SNRPC	9.76E-05
GO:0016044~membrane organization	41	1.12E-06	CAV1, STX7, AP1B1, AP1G1, COPZ1, SNX2, SNX1, EEA1, EPS15L1, SNX3, CLTC, CD9, APP, PICALM, ITGAV, RAC1, PAFAH1B1, EHD1, SAR1B, HSPA8, HIP1, AP3B1, SEC23A, DNM1L, HSP90AA1, HCK, LMNA, CORO1C, AP2A2, LRP1, RAB18, AP2A1, TXNDC5, BAX, ARCN1, RAB5A, MERTK, SH3GL1, MYH10, EPN2, DNM2	9.88E-05
GO:0016071~mRNA metabolic process	40	1.39E-06	RALY, NCBP1, PRPF4B, STRAP, NHP2L1, SNRPD3, RBM4, LSM7, SNRPD1, SYNCRIP, HNRPLL, SF3B3, PNN, PRPF19, SF3B1, APP, DDX46, PRPF8, PCBP2, NUDT21, DNAJC8, USP39, DHX15, U2AF1, LSM3, PABPC1, KHDRBS3, EFTUD2, PTBP1, DDX1, SF1, ELAVL1, MBNL1, SF3A1, PRPF4, SF3A3, CPSF6, SNRPC, XRN2, ADAR	0.000118
GO:0009109~coenzyme catabolic process	10	1.43E-06	SDHA, DLST, NNT, ACO2, SUCLG2, SUCLG1, CS, IDH2, IDH1, MDH1	0.000119
GO:0006396~RNA processing	52	1.46E-06	RALY, NCBP1, PRPF4B, RPL14, SNRPD3, LSM7, RBM4, SNRPD1, SYNCRIP, SART3, HNRPLL, PNN, APP, DDX17, PCBP2, DNAJC8, U2AF1, LSM3, PPP2R1A, KHDRBS3, EFTUD2, PTBP1, AARS, SF1, MBNL1, PRPF4, RPS16, RPS14, CPSF6, SNRPC, XRN2, NHP2L1, STRAP, PABPC4, SF3B3, PRPF19, SF3B1, DDX46, PRPF8, NUDT21, USP39, DHX15, RPL5, RPL10A, PABPC1, NSUN2, RTCD1, DDX1, SMAD2, SF3A1, SF3A3, ADAR	0.000118
GO:0051248~negative regulation of protein metabolic process	26	1.76E-06	A2M, CAV1, PML, IGF2BP2, IGF2BP3, CALR, PSMA7, PSMB7, PSMB3, ITGAV, PSMD1, PSMD3, PSMD6, PSMD9, PRKCA, PPP2R1A, YWHAE, PSMA1, PSMD12, PSMD11, BAX, PSMA4, PSMC1, PSMA3, PSME3, PPP2R4	0.000138
GO:0031400~negative regulation of protein modification process	20	2.19E-06	PRKCA, PPP2R1A, CAV1, PSMA7, YWHAE, PSMA1, PSMB7, PSMD12, PSMD11, PSMB3, BAX, PSMA4, PSMD1, PSMC1, PSMA3, PSMD3, PSME3, PPP2R4, PSMD6, PSMD9	0.000167
GO:0051438~regulation of ubiquitin-protein ligase activity	16	2.39E-06	PSMA7, PIN1, UBE2N, PSMA1, PSMB7, PSMD12, PSMD11, PSMB3, PSMA4, PSMC1, PSMA3, PSMD1, PSMD3, PSME3, PSMD6, PSMD9	0.000178
GO:0010033~response to organic substance	62	3.43E-06	A2M, RBM4, DEK, B2M, CTNNB1, GOT2, ACTR3, HSPH1, PRKAR2A, GOT1, NDUFS4, CD44, GAB1, PRKCA, PPP2R1A, HSP90AA1, LYN, GATM, PFKL, CRYAB, AARS, CLIC1, MMP14, MAPK1, DDR1, GLUL, GNB1,	0.000249

			PDGFRA, ABAT, GNAS, COL1A1, EIF2AK2, PPP2R2A, PPP5C, CAV1, ADH5, PML, PRKDC, COMT, VARS, PTK2B, IDH1, PPP3CA, ERO1L, NUDC, HSPA8, MAP2K1, MSH2, MAP1B, ITGA2, SMAD2, ANXA5, STAT1, STAT3, PTPN11, GART, HDAC2, VCP, MAPK14, ALDH2, FABP4, PARP1	
GO:0051340~regulation of ligase activity	16	3.92E-06	PSMA7, PIN1, UBE2N, PSMA1, PSMB7, PSMD12, PSMD11, PSMB3, PSMA4, PSMC1, PSMA3, PSMD1, PSMD3, PSME3, PSMD6, PSMD9	0.000277
GO:0070271~protein complex biogenesis	48	3.97E-06	XPO1, PARD3, NUP98, CAV1, FKBP4, PML, CDH2, CALR, SF3B3, PXN, CTNNB1, FGG, PTK2, NDUFS4, PICALM, PTK2B, FGB, NPM1, RAC1, CAT, HIP1, PPP2R1A, HSP90AA1, MAP2K1, DARS, PFKL, CRYAB, EPRS, IPO9, SMAD2, DECR1, PFKM, ANXA5, SOD2, SPAG9, VCP, TBCA, UQCRH, IPO7, BAX, THRAP3, CAPG, RRM1, SMARCA5, LAMC1, XPO7, PARVA, PPP5C	0.000275
GO:0006461~protein complex assembly	48	3.97E-06	XPO1, PARD3, NUP98, CAV1, FKBP4, PML, CDH2, CALR, SF3B3, PXN, CTNNB1, FGG, PTK2, NDUFS4, PICALM, PTK2B, FGB, NPM1, RAC1, CAT, HIP1, PPP2R1A, HSP90AA1, MAP2K1, DARS, PFKL, CRYAB, EPRS, IPO9, SMAD2, DECR1, PFKM, ANXA5, SOD2, SPAG9, VCP, TBCA, UQCRH, IPO7, BAX, THRAP3, CAPG, RRM1, SMARCA5, LAMC1, XPO7, PARVA, PPP5C	0.000275
GO:0006928~cell motion	46	4.01E-06	CALD1, PRKDC, ABI2, CDH2, TPM1, CAPZB, TPM4, VCL, ACTR3, ACTG1, GPX1, CD9, ACTR2, APP, PTK2, MACF1, CD44, ROBO1, ARPC2, PTK2B, RAC1, PAFAH1B1, TOP2B, FN1, PRKCA, MAP2K1, MSH2, PODXL, ANXA1, DPYSL5, ITGA2, MYH9, MMP14, VAV2, YWHAE, VASP, STAT3, ARPC1B, EPHA4, MAPK14, BAX, TXN, SDCBP, LAMC1, GAP43, MYH10	0.000271
GO:0031398~positive regulation of protein ubiquitination	16	6.26E-06	PSMA7, PIN1, UBE2N, PSMA1, PSMB7, PSMD12, PSMD11, PSMB3, PSMA4, PSMC1, PSMA3, PSMD1, PSMD3, PSME3, PSMD6, PSMD9	0.000413
GO:0030029~actin filament-based process	29	7.03E-06	MYL6, LIMA1, CALD1, MYL1, ABI2, CALR, CAPZB, TPM1, ACTG1, CORO2B, PTK2B, RAC1, RHOA, PAFAH1B1, FGD5, ARHGEF2, ACTN4, ROCK2, ACTN1, MYH9, FLNB, VASP, EPB41L2, ARPC1A, SDCBP, CRK, LCP1, PARVA, MYH10	0.000454
GO:0051436~negative regulation of ubiquitin-protein ligase activity during mitotic cell cycle	14	7.13E-06	PSMA7, PSMA1, PSMB7, PSMD12, PSMD11, PSMB3, PSMA4, PSMC1, PSMA3, PSMD1, PSMD3, PSME3, PSMD6, PSMD9	0.00045

6. Potential drug pathways, as identified by surprisal analysis

Utilizing String software [13] we examined protein-protein functional connectivity of the proteins influenced the most by the unbalanced processes (see for example Fig. S2, S4,S14 ,S15). To identify potential candidates for further research and/or targeted therapy we searched for the targets that had a relatively large number of protein-protein connections according to String score (for more details see Figure legend of the Figure S2).

The list below includes the main biological categories (as retrieved from GO and String) significantly involved in the unbalanced processes and suggested protein targets for further investigation.

Constraint $\alpha = 1$: hyperactive signaling in wt+ tumors due to $\alpha = 1$. Fig S2 and Table S2 indicate that pEGFR protein and its related downstream signaling play significant role in the $\alpha = 1$.

Constraint $\alpha = 2$: Elevated migration/cytoskeleton organization, MAPK signaling in EGFRvIII+ tumors due to $\alpha = 2$ (Table S3 and Fig.S4).

Protein candidates: pLyn (Src family), pPTK2B, pPxn, pCbl create a clear and very connected cluster (Fig. S4). This cluster is related to migration network according to Cell Migration Gateway database (by The Cell Migration Consortium (CMC), Nature Publishing Group (NPG)) as well as pSTAT3 and CD44.

Constraint $\alpha = 3$ **(GBM15 and GBM10 vs GBM12)**: Increased RAS/MAPK signaling and migration in GBM15 and GBM10 due to $\alpha = 3$.

GBM15 and GBM10 tumors possess unbalanced process comprised of a smaller cluster of migration proteins connected to the RAS/MAPK network and collagen proteins (TableS4). **Protein candidates**: pMAPK1, pMAPK3, pPxn and pBCAR1.

Constraint $\alpha = 4$ (**GBM39 vs GBM59**): Enhanced aerobic glycolysis/Ras signaling in GBM59 and migration in GBM39 due to $\alpha = 4$. Migration network connected to PDGFR[14],STAT1[15] and PLCγ [16] is induced in GBM39 but not in GBM59. Thus additional **potential proteins targets** for GBM39 are: STAT1, pPLCγ and PDGFR (Fig.S14). **Protein candidates** for GBM 59 tumor (but not GBM39) will include proteins involved in aerobic glycolysis, such as ENO1, LDHA, pPKM2 (y105), pPI3K and also induced targets from the EGFR/MAPK pathway, such as MAPK1 and MAPK3 (Fig.S15 and Table S5).

Constraint $\alpha = 5$ (**GBM6 vs GBM15**): Enhanced glycolysis through oxidative phosphorylation and Ras signaling in GBM6 due $\alpha = 5$. **Protein candidates** for GBM 6 : multiple ATP synthases, aldolase A, LDHB, pMAPK3/1, pp38, pMAPK12. (Table S6). In GBM15 there is a significant increase in EGFR/MAPK signaling due to $\alpha = 5$ in comparison with GBM6 (Table S6)

Constraint $\alpha = 6$ (**GBM26 vs GBM8**): Enhanced migration/cytoskeleton organization in GBM26 and DNA packaging in GBM8 due to $\alpha = 6$.

Protein targets/ pathways for further investigation are pWas, pYes, pLyn for GBM26 and multiple histones for GBM8 (Table S7).

Constraint $\alpha = 7$ (**GBM6 vs GBM8, GBM26**): induced EGFR signaling and glycolytic enzymes in GBM6 and DNA packaging in GBM8 due to $\alpha = 7$.

Protein processes and protein candidates for GBM6: pEGFR y1045/y1068 pathway and glycolysis and multiple histones in GBM8/GBM26 connected to the EGFR network (in this constraint EGFR protein expression levels, and not phosphorylation sites) are elevated in GBM8/GBM26 (Table S8).

7. Supplementary Figures

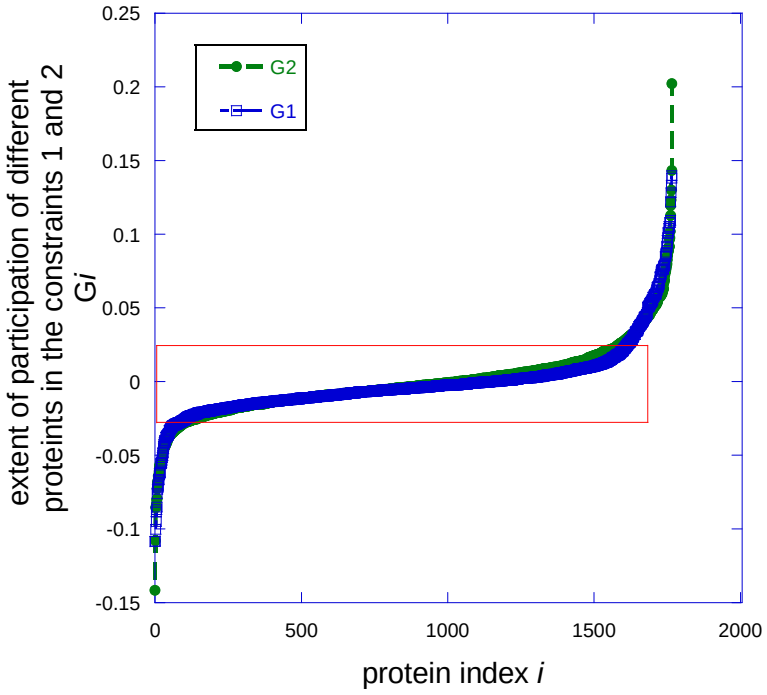

Figure S1. **Sorted values of $G_{i\alpha}$ from the unbalanced processes $\alpha = 1$ and $\alpha = 2$.** The proteins are not independent but are correlated due to the constraints since each given constraint influences a subset of proteins in a similar way by causing coordinated deviations of protein levels (up or down) from the basal level. All the proteins that had $G_{i\alpha} > 0.03$ or $G_{i\alpha} < -0.03$ (those that exceeded the 0 red box) were considered as influenced the most by the constraints $\alpha = 1,2$. Similarly for all other constraints $\alpha = 3,4..7$ only proteins with $G_{i\alpha} > 0.03$ or $G_{i\alpha} < -0.03$ were further analyzed. For every constraint we find that levels of about 100 proteins deviate significantly in either the upper ($G_{i\alpha} > 0.03$) or lower direction ($G_{i\alpha} < -0.03$) from the steady state .For many proteins the the extent of influence, $G_{i\alpha}$, is about zero for $\alpha = 1,2...7$, meaning that they are mostly players in the steady state (inside the 0 red box) . Only those proteins with the values $G_{i\alpha} > 0.03$ or $G_{i\alpha} < -0.03$ were included in the classification of biological categories using David database [5] as reported in Tables S1-S8. For example phospho- proteins were found to be influenced the most by $\alpha = 1$ and deviate in the same upper direction ($G_{i\alpha} > 0.03$).Proteins that had the values $-0.02 < G_{i\alpha} < 0.02$ in <u>all</u> constraints were considered as influenced by the steady state and not influenced by any of the ongoing unbalanced processes.

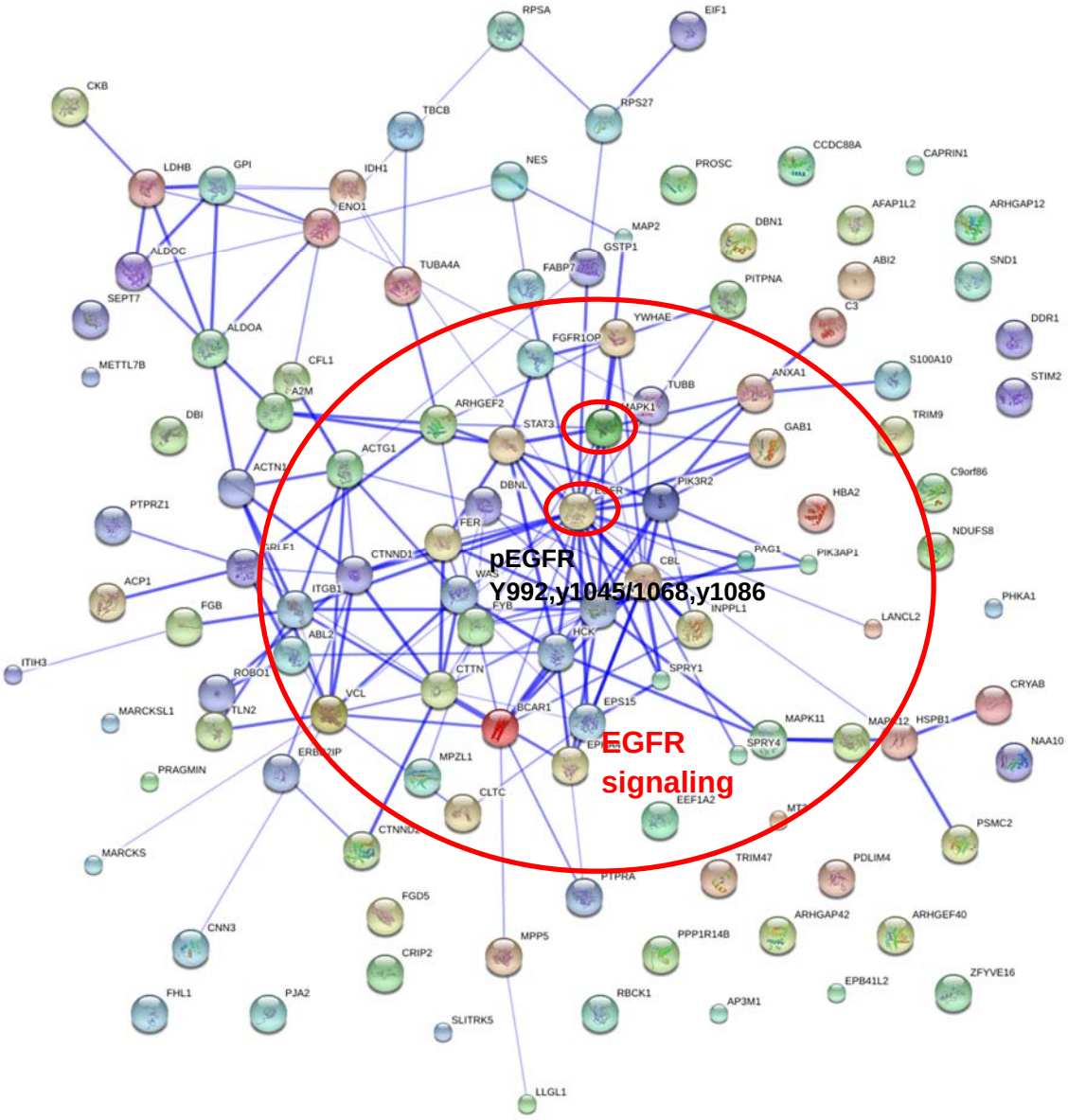

Figure S2.**Connectivity of the proteins influenced by the unbalanced process** $\alpha=1$. A String map, representing protein-protein functional connectivity, was generating using String software for those proteins influenced by the unbalanced process $\alpha=1$ ($G_{il} > 0.03$ values) and up-regulated in GBMwt+ and GBM EGFRvIII tumors due to $\alpha=1$. The vast majority of the proteins are tyrosine-phosphorylated. The thickness of the edges reflects the approximate probability of the protein-protein functional link for the related proteins as provided by the String score (confidence score in STRING correspond to the probability of finding the linked proteins within the same KEGG pathway [13]). Thick lines (as for EGFR and MAPK1 (red small circles), String score = 0.98) represent high probability for the functional connectivity based on biochemical verification.

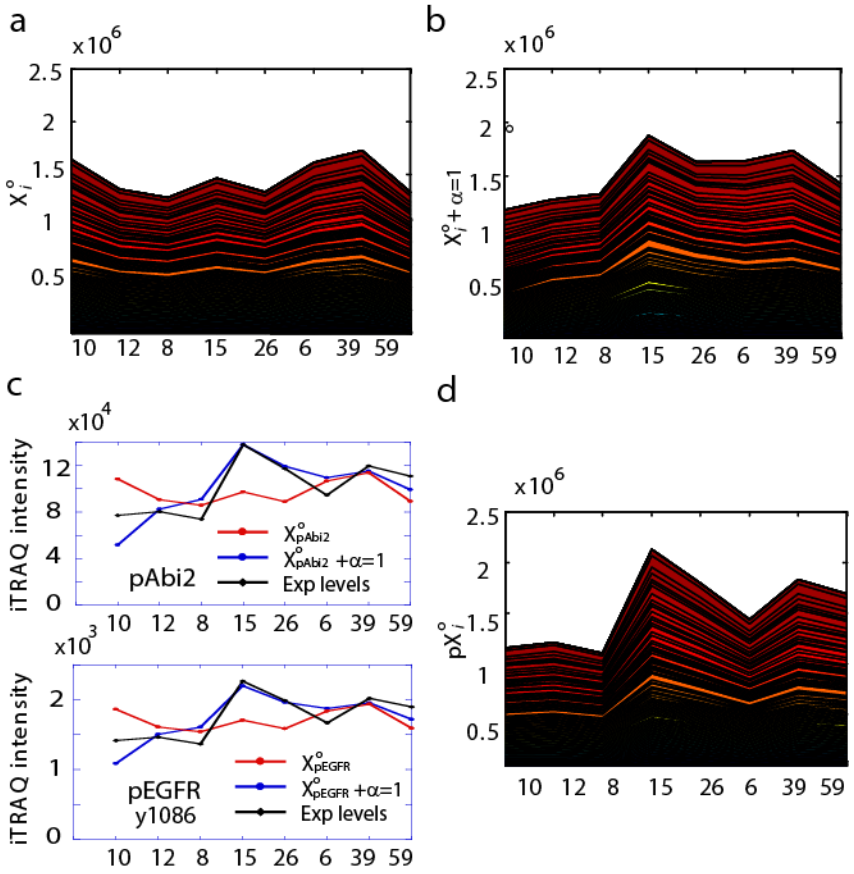

Figure S3. **Identification of regulatory constraint $\alpha = 1$. (a)** Steady state expression levels pX_i^o for 192 phosphoproteins were computed using $\lambda_0(k)$ and G_{i0} parameters obtained from the analysis of the entire dataset (unmodified and phosphorylated proteins). **(b)** Influence of the constraint $\alpha = 1$ on the phospho levels of the phosphoproteins, $X_i^o + (\alpha = 1)$, was calculated using $\lambda_\alpha(k)$ and $G_{i\alpha}$ parameters (for $\alpha = 0,1$) obtained from the analysis of the entire dataset. The sum $X_i^o + (\alpha = 1)$ was compared to the pX_i^o values from **(d)**. **(c)** For every measured phosphoprotein the importance of the unbalanced process $\alpha = 1$ is determined by comparison of the $X_i^o + (\alpha = 1)$(blue curve), sum of the stable state and the $\alpha = 1$ deviation term, to the experimental phosphoprotein expression levels (black curves). This constraint is highly important in a large subset of the phosphorylated proteins. **(d)** Steady state expression levels pX_i^o for 192 phosphoproteins were computed using $\lambda_0(k)$ and G_{i0} parameters obtained from the surprisal analysis of the subgroup of phosphorylated proteins (*pGBM*). When that subset is analyzed separately, the $\alpha = 1$ constraint of the full data is found to become an integral part of the phospho steady state pX_i^o. Addition of the first original constraint $\alpha = 1$ to the original steady state expression levels **(b)** reproduces closely the pX_i^o levels **(d).** Thus the first constraint $\alpha = 1$ of the full data set can therefore be regarded as a regulatory constraint of the GBM system.

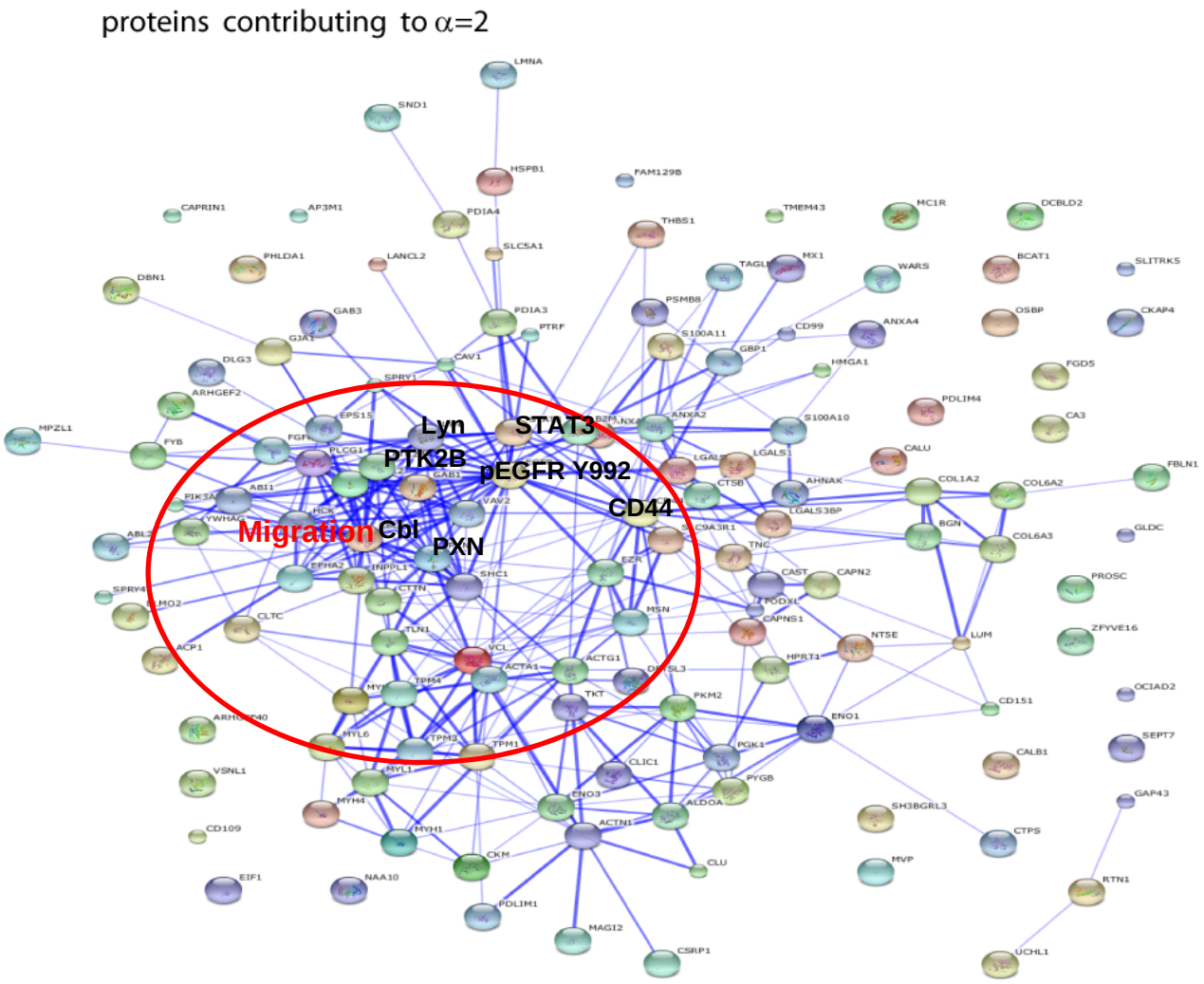

Figure S4.**Connectivity of the proteins influenced by the unbalanced process** $\alpha=2$ .A String map, representing protein-protein functional connectivity, was generating using String software for the proteins influenced by the unbalanced process $\alpha=2$ ($Gi2>0.03$ values) and up-regulated in GBM EGFRvIII tumors due to $\alpha=2$. Potential drug targets are the hub proteins involved in ell migrations that have a big number of partners : pLyn, pPTK2B, pPxn,pCbl, pSTAT3 and CD44.

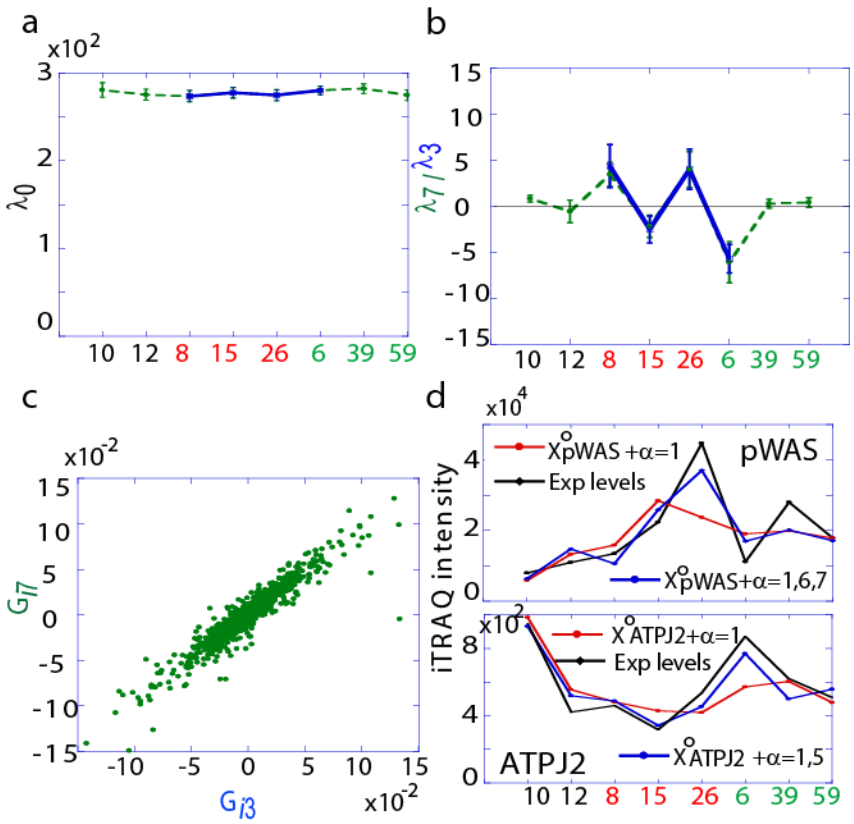

Figure. S5**. Minor unbalanced processes** $\alpha = 5,6,7$ (a) GBM dependent steady state term, $\alpha = 0$, was calculated using either the original dataset including 8 GBM tumors (green plot) or only a subset of 4 GBM tumors (*k* =8,15,26,6, blue plot). **(b)** Amplitude $\lambda_7(k)$ of the unbalanced process $\alpha = 7$ from the original matrix (green plot) was compared to the amplitude $\lambda_3(k)$, representing the unbalanced process $\alpha = 3$ as obtained from a small matrix containing only 4 GBM tumors (blue plot). Similarity between two curves, that were calculated using different data sets as indicated above, points to the significance of the $\alpha = 7$ constraint in the analysis and characterization of the GBM tumors. **(c)** Scatter plot represents extent of correlation between the G_{i3} values calculated for $\alpha = 3$ using the smaller matrix and G_{i7} values obtained from the entire dataset. (**d)** pWAS and ATPJ2 are examples for the proteins influenced by the unbalanced processes $\alpha = 5,6,7$. Experimental protein expression levels (black curve) could be closely reproduced when for pWAS the $\alpha = 6$ and $\alpha = 7$ deviation term was added to the sum $X_i^o + (\alpha = 1)$ and for ATPJ2 the term $\alpha = 5$ terms was added to the sum $X_i^o + (\alpha = 1)$ (blue curves), pointing to the significant influence of the constraints $\alpha = 5,6,7$ on the protein expression levels of these proteins.

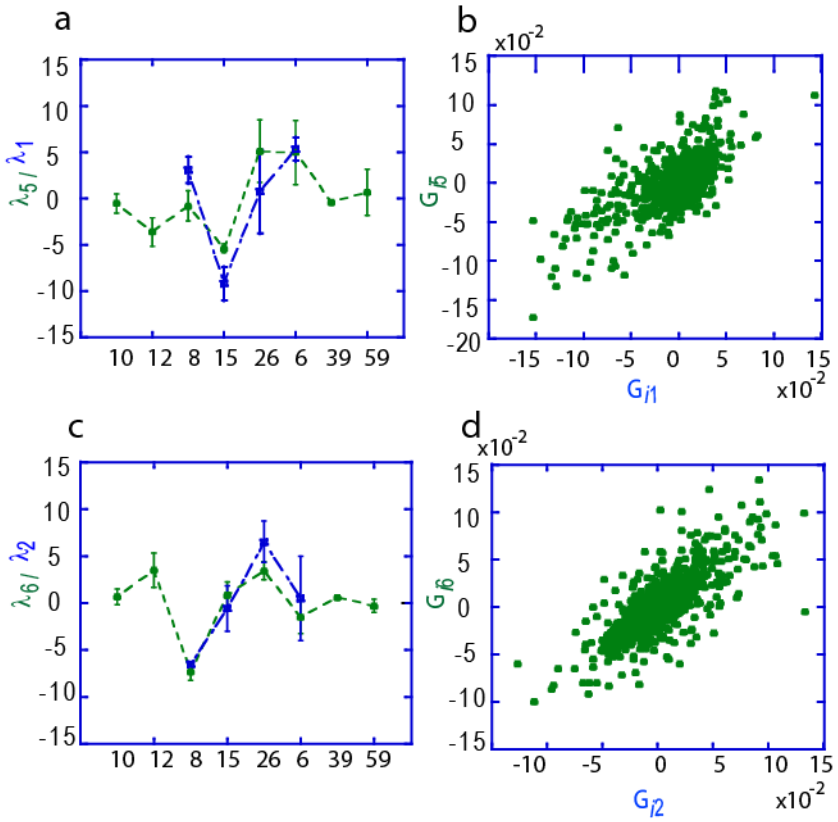

Figure S6. **Minor constraints as identified using Surprisal analysis. (a,c)** Amplitude $\lambda_5(k)$ of the unbalanced process $\alpha = 5$ **(a)** or amplitude $\lambda_6(k)$ of the unbalanced process $\alpha = 6$ **(c)** from the original matrix (green plots) were respectively compared to the amplitudes $\lambda_1(k)$ and $\lambda_2(k)$ that represent the unbalanced process $\alpha = 1$ **(a)** and $\alpha = 2$ **(c)** as obtained from a small matrix containing only 4 GBM tumors (blue plots). was calculated using either the original dataset including 8 GBM tumors (green plot) or only a subset of 4 GBM tumors (k =8,15,26,6, blue plot). Similarity between two curves, that were calculated using different matrices as indicated above, points to the significance of the $\alpha = 5$ and $\alpha = 6$ constraints in the characterization of the GBM tumors. **(b,d)** Scatter plot representing extent of correlation between the G_{i1} values calculated for $\alpha = 1$ using the smaller matrix and G_{i5} values obtained from the entire dataset **(b)** and between the G_{i2} values calculated for $\alpha = 2$ using the smaller matrix and G_{i6} values obtained from the entire dataset (**d**).

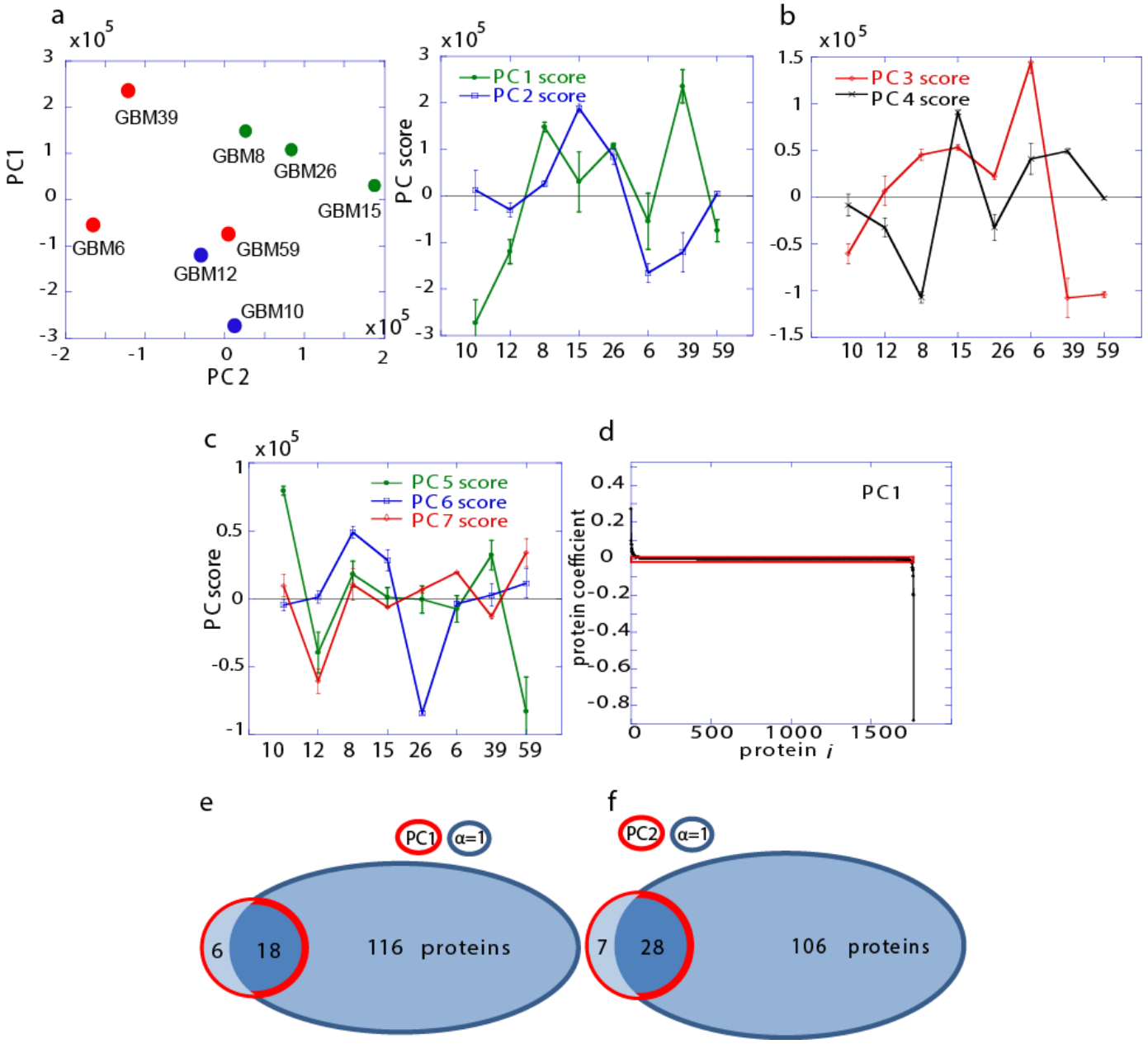

Figure S7. **PCA analysis**. **(a-c)** Representation of the measured protein data in the principal component space by Principal component scores. PC scores correspond to the eigenvectors of a smaller (8x8) matrix and represent coordination between GBM tumors. **(a)** Principal component scores 1 and 2 are presented via plotting PC1 vs PC2 (left panel) or PC1, PC2 vs tumor index (right panel). **(b)** Principal components scores 3 and 4. **(c)** Principal components scores 5,6 and 7. **(d)** Sorted values of the protein coefficients corresponding to the PC1 (protein coefficients corresponding to other principle components (PC2-PC7) are presented in the Additional Table SI (excel table) .Proteins inside the red box were considered as not contributing to the PC1. Same considerations were applied to other PCs . **(e)**. Using PCA analysis 24 proteins contributing significantly to the PC1 were identified. 18 of them appeared to contribute to the unbalanced process $\alpha = 1$ (constraint of phosphorylation, increased intensity in GBMwt+ and GBM EGFRVIII) as identified utilizing surprisal analysis. 6 other contributed to the $\alpha = 2$. (**f**). 28 out of the 35 proteins contributing significantly to the PC2 were found to contribute significantly to the $\alpha = 1$.

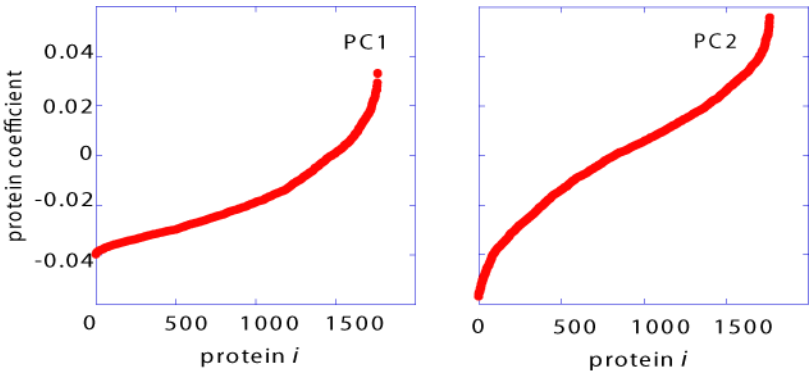

Figure S8. **Principle components from PCA analysis using correlation matrix**. Sorted values of the protein coefficients for the PC1 and PC2. Correlation matrix doesn't allow clear identification of the proteins contributing to the Principal components.

		PC1	PC2	PC3	PC4	PC5	PC6	PC7
wt	10	- -		-		+ +		
	12	-			-	-		-
wt+	8	+		+	- -		+	
	15		+ +	+	+ +		+	
	26	+	+		-		- -	
VIII+	6		- -	+ +	+			
	39	+ +	- -	- -	+	+		
	59	-		- -		- -		+
assosiated bio-categories:		no/no	P and C/no	RASs/ MAPKs and M/no	M/ C and P/no	no/no	M/ C and P/no	AG and P and C/no

Phosphorylation – P
Migration – M
Cytoskeleton organization – C
RAS /MAPK signaling - RASs/MAPKs
Aerobic glycolysis – AG
no significant GO categories - no

Figure S9. **Summary of the GO categories associated with different PC (PC1-PC7)**. Notation + or – indicates the direction of change from the mean value. For example constraint PC =2 includes enhanced phosphorylation (P) in GBM15 tumor (++). The size of the + / – and number of the signs reflect relative importance of a particular PC for that GBM tumor. This table is quite different from Figure 5 in particular because some proteins that deviate from the stable state in one direction are identified by PCA to deviate in an opposite direction from the mean or not to deviate. In part this is because

PCA is more sensitive to the higher variance of the phosphoproteins. Furthermore, some of the important biological categories, such as glycolysis through oxidative phosphorylation or DNA packaging were not identified in the PCA analysis.

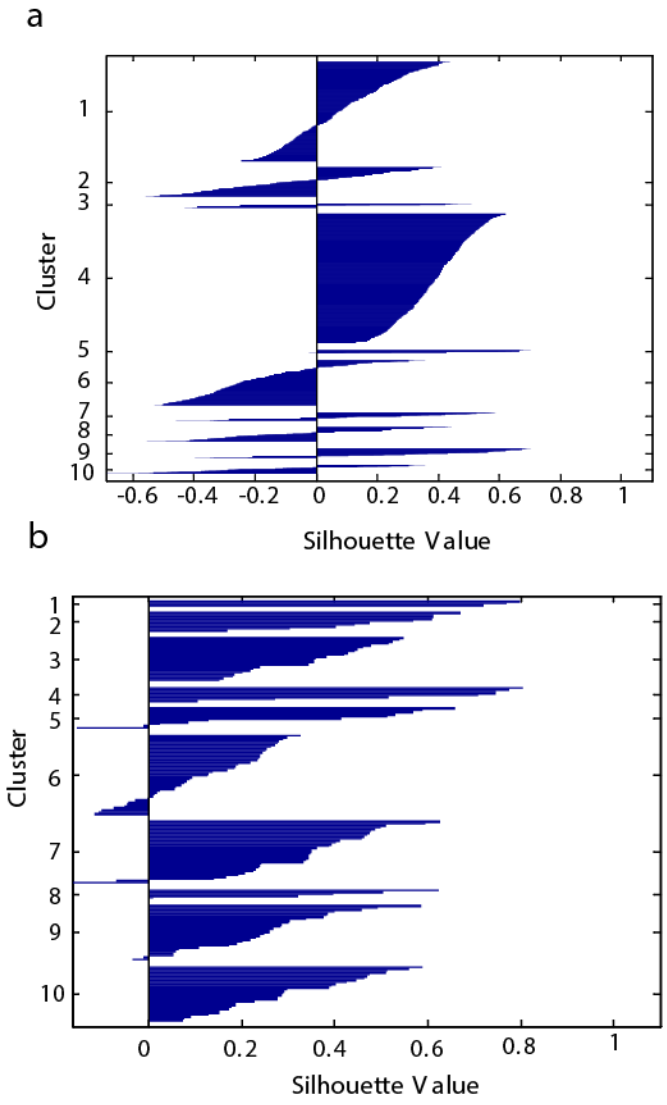

Figure S10. **Silhouette evaluation plot.**The silhouette value for each protein is a measure of how similar that protein is to proteins in its own cluster. A +1 value for the proteins in a given cluster would indicate that that cluster contains proteins with completely distinct biological behaviors relative other clusters. For example, if the proteins in a cluster all exhibit positive and large Silhouette values, this implies a level of uniqueness to that cluster. By contrast, if many proteins in a cluster exhibit a small or negative silhouette value, then those proteins are not uniquely identified as distinct from neighboring clusters. **(a)** k-means clustering using the entire dataset. The majority of the proteins exhibit Silhouette values < 0.2 . **(b)** k-means clustering using the subset of phosphoproteins. Here, almost >95% of the proteins exhibit a positive Silhouette value. Only those proteins with Silhouette values >0.2 were further analyzed.

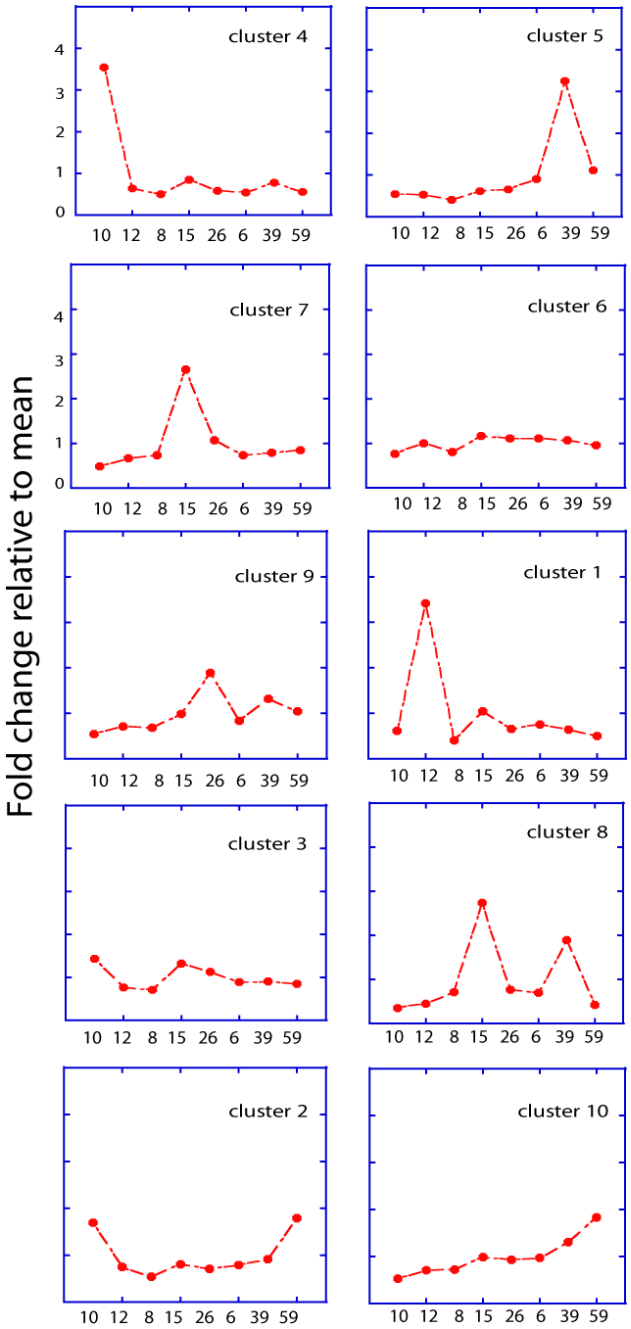

Figure S11.**K-means clustering algorithm.** Analysis using k-means clustering using the subset of phosphorylated proteins. This analysis identified an optimal number of clusters as being near 10, meaning that this was the minimal number of clusters accounted for the majority of the phospho-proteins (>95% of the proteins had Silhouette values > 0) . An example of how this analysis is interpreted is as follows. Cluster #7 contains about 33 phosphoproteins, and strongly influences GBM15. Those phosphoproteins were then analyzed using the Silhouette evaluation (Fig S6). Proteins with Silhouette values > 0.2 ,(26 proteins from Cluster #7), were included in further biological analysis. For these curves, only the centroids (centers of the clusters) are presented.

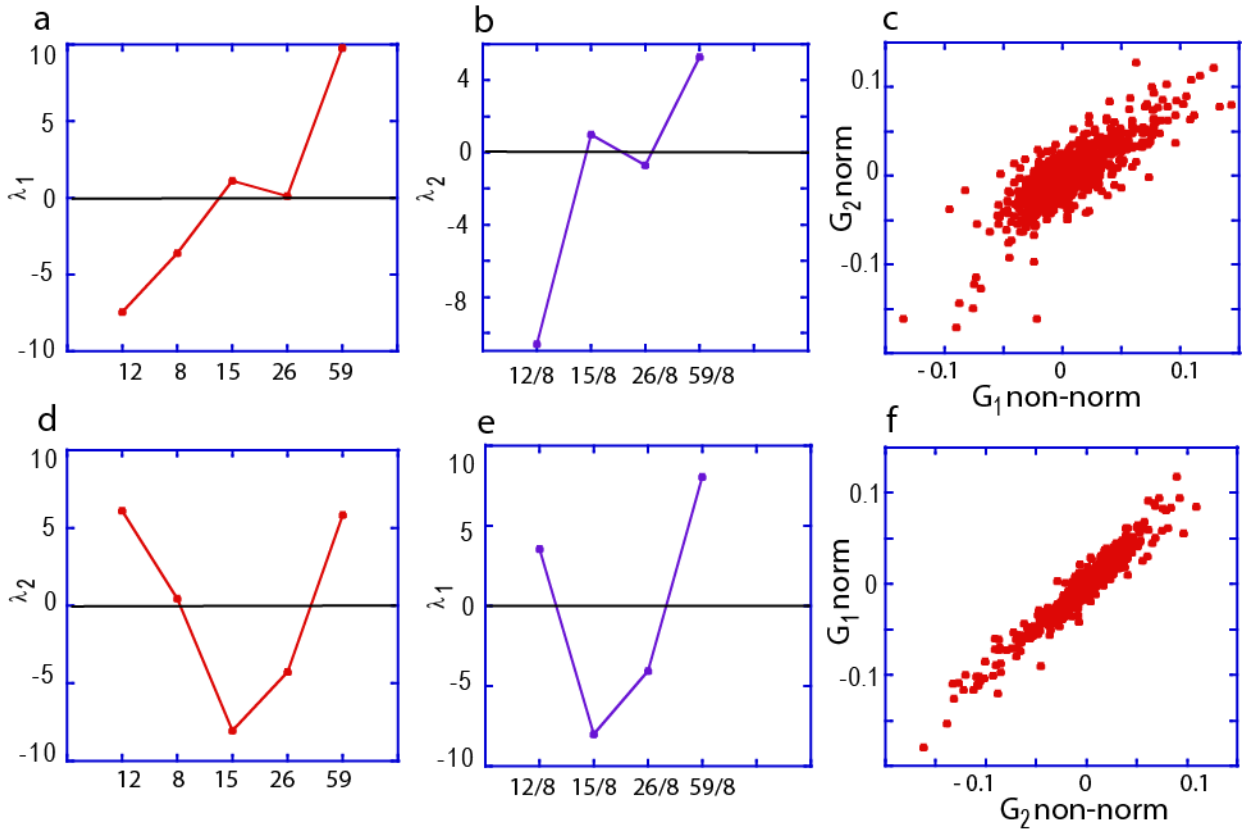

Figure S12. **Comparison between non-normalized and normalized iTRAQ proteomic datasets**. To show that normalization, in which protein intensity levels from GBM 12,15,26 and 59 were divided by the protein intensity levels from GBM8,don't influence the constraints, surprisal analysis was performed using either normalized or non-normalized datasets. Figure S9 shows comparison between the results obtained from normalized or non-normalized datasets. (**a, b**) Amplitude $\lambda_1(k)$ of the unbalanced process $\alpha = 1$ **(a)** was calculated using non-normalized protein values for GBM 12, 8, 15, 26 and 59. This constraint was compared to the $\alpha = 2$ constraint as identified using a normalized dataset. For that normalization, the protein intensity levels from GBM 12,15,26 and 59 were divided by the protein intensity levels from GBM8 (**b**) . **(c)** Scatter plot representing extent of correlation between the G_{i2} values calculated for $\alpha = 2$ using the normalized dataset and G_{i1} values obtained from the non-normalized dataset. (**d, e**) The amplitude $\lambda_2(k)$ of the unbalanced process $\alpha = 2$ **(d)** was calculated using non-normalized protein values for GBM 12, 8, 15, 26 and 59, and then again **(e)** following normalization with GBM8. Similar to figure parts **a** and **b**, this constraint was compared to the $\alpha = 1$ constraint as identified using the normalized dataset. **(f)** Scatter plot representing extent of correlation between the G_{i1} values calculated for $\alpha = 1$ using normalized dataset and G_{i2} values obtained from the non-normalized dataset. The unbalanced processes are the same in the normalized and non-normalized datasets as expected.

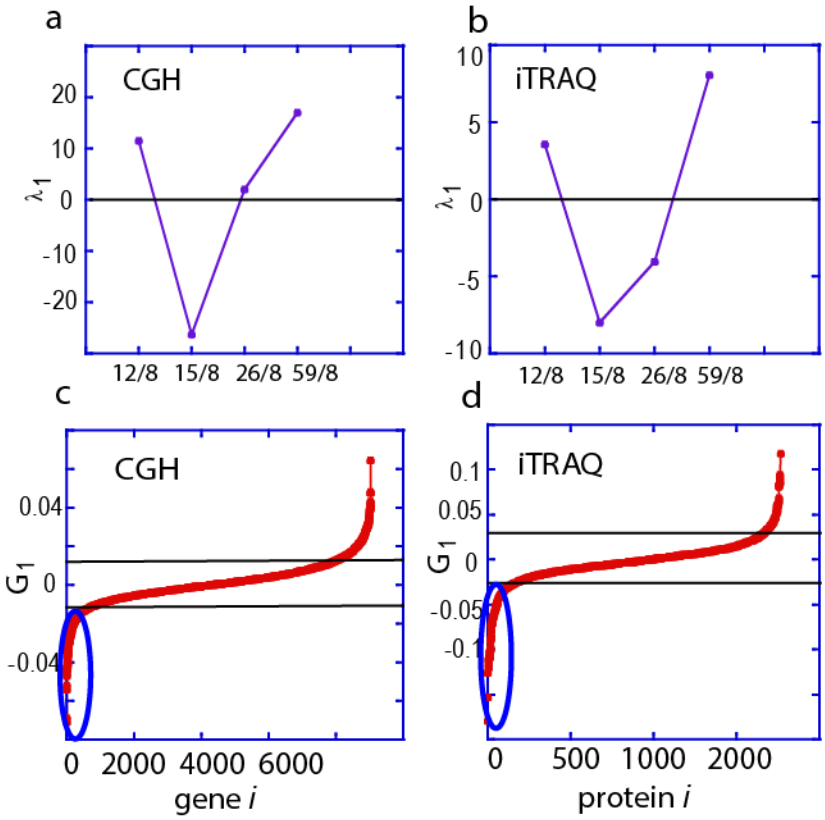

Figure S13. **Comparison between the unbalanced processes as identified using CGH and iTRAQ datasets**. (**a, b**) Amplitude $\lambda_1(k)$ of the unbalanced process $\alpha = 1$ as identified using CGH normalized dataset **(a)** was compared to the amplitude $\lambda_1(k)$ as identified using iTRAQ dataset .(**c,d**) Sorted values of G_{i1} from the CGH (**c**) and iTRAQ (**d**) datasets. All the genes that had $G_{i1} < -0.015$ (encircled in blue oval) or $G_{i1} > 0.015$ were considered as influenced significantly by the α=1 constraint and were compared to the list of the proteins with the values $G_{i1} < -0.03$ or $G_{i1} > 0.03$ correspondingly.

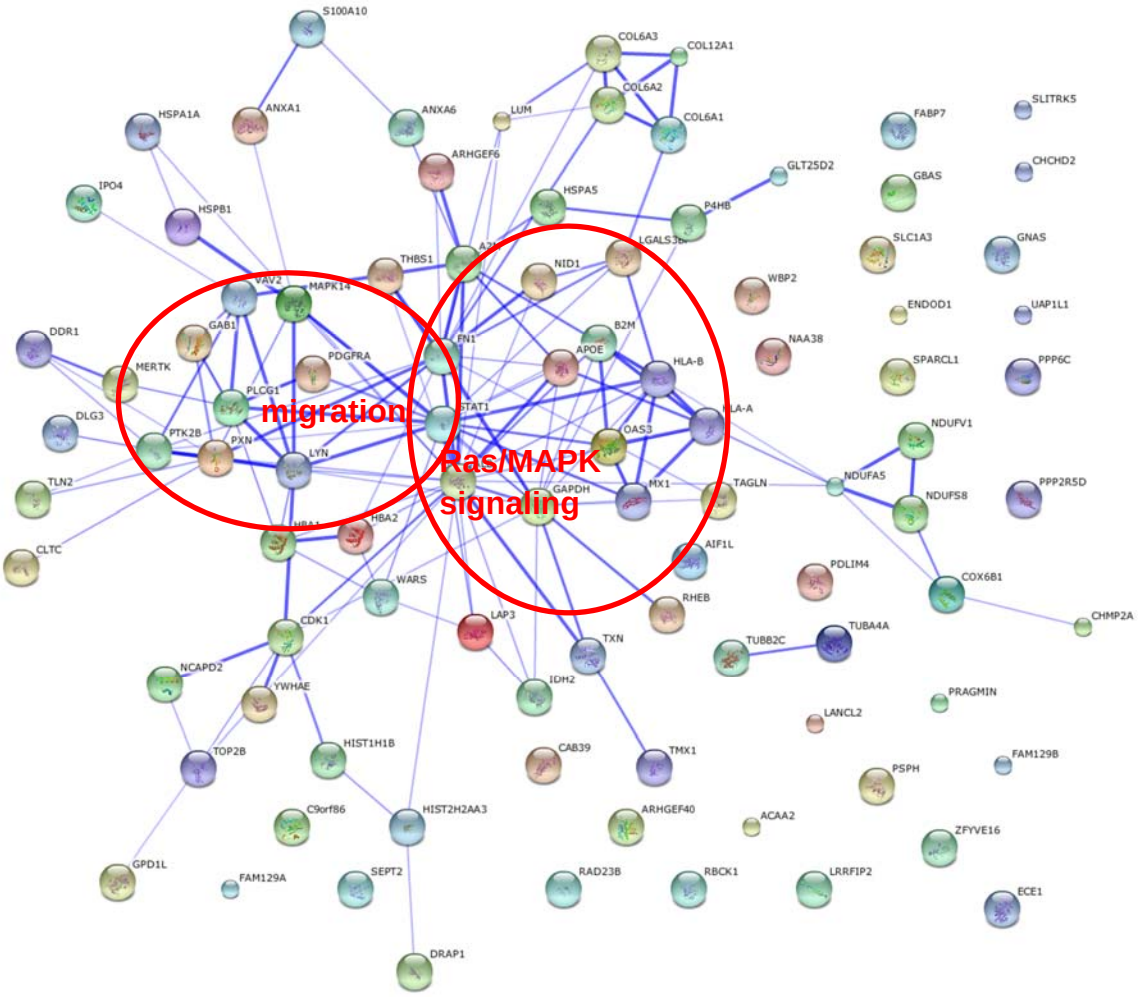

Figure S14.**Connectivity of the proteins influenced by the unbalanced process** α=4.A String map representing protein-protein functional connectivity for the proteins influenced by the unbalanced process α=4 ($G_i4 > 0.03$ values) and up-regulated in GBM39 due to α=4. Potential candidates identified from the 4th are located in the red circle.

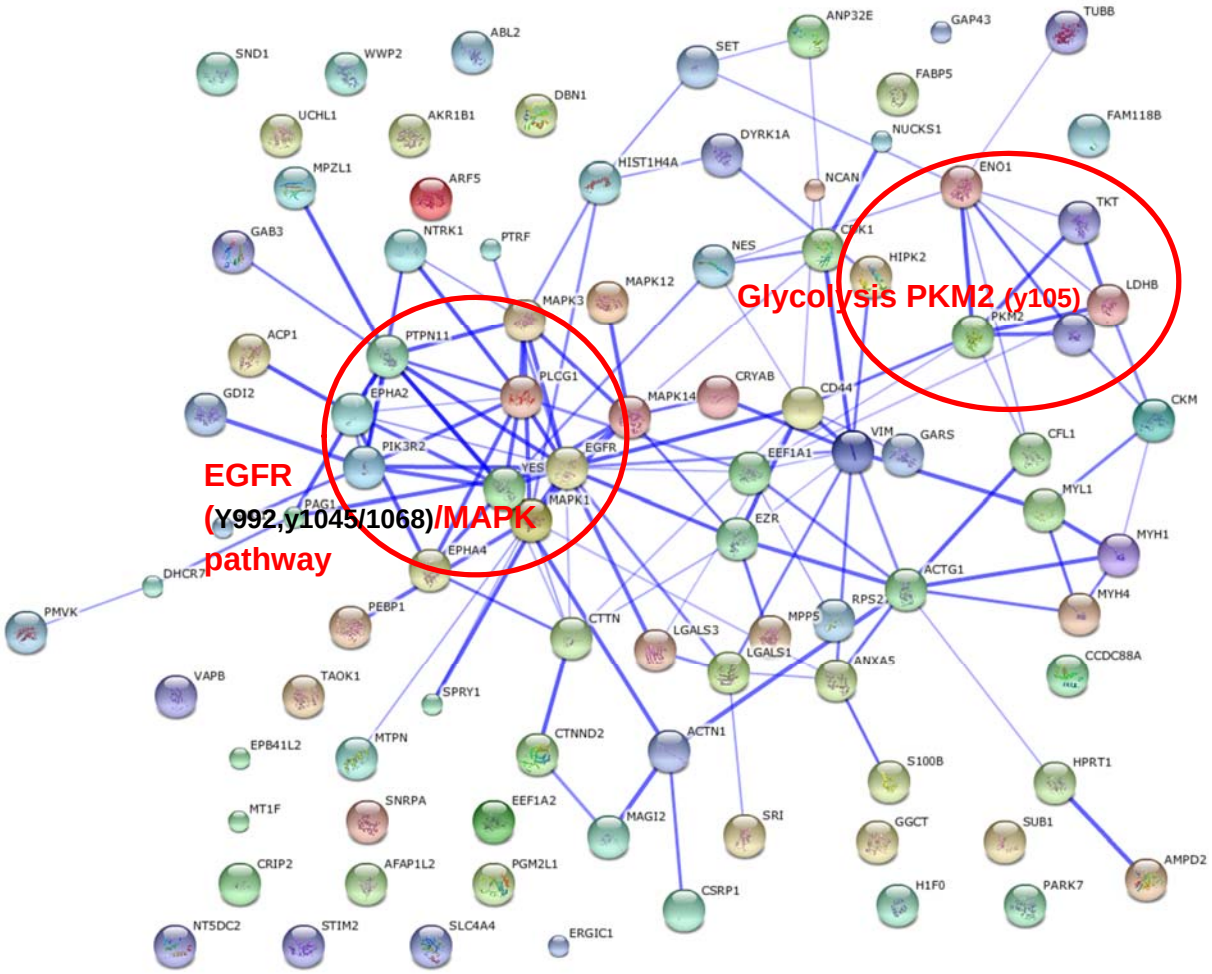

Figure S15.**Connectivity of the proteins influenced by the unbalanced process** α=4. A String map representing protein-protein functional connectivity for the proteins influenced by the unbalanced process α=4 ($G_i4 < -0.03$ values) and up-regulated in GBM59 due to α=4. Potential candidate processes in GBM59 are encircled in red.

8. Abbreviations

EGFR - epidermal growth factor receptor

EGFRvIII - EGFR variant(v)III oncoprotein

p-STAT3- phospho(p)-Signal Transducer and Activator of Transcription3

Abi2 - p-Abelson Interactor2

pLyn - phospho(p)-Lck-Yes-related novel tyrosine kinase

pPLCγ- p-Phospholipase Cγ

CD44 - Cell Surface Glycoprotein

pPxn - p-paxillin

pMAPK1,3 – p- Mitogen-Activated Protein Kinase 1,3

pSRC – p- V-Src Avian Sarcoma (Schmidt-Ruppin A-2) Viral Oncogene Homolog pBCAR1- Breast Cancer Anti-Estrogen Resistance 1

PTEN - Phosphatase And Tensin Homolog

pPI3K - p-Phosphatidylinositol-4,5-Bisphosphate 3-Kinase

LDHA – lactate dehydrogenase A

Ras - Rat Sarcoma Viral Oncogene Homolog

LDHB - lactate dehydrogenase B

IDH2 - Isocitrate Dehydrogenase 2

pP38 - p-Mitogen-Activated Protein Kinase 14

p - phosphorylation

pPKM2 - p-pyruvate kinase

PCA - Principal component analysis

GBM - glioblastoma multiforme

SVD- singular value decomposition

iTRAQ - Isobaric tags for relative and absolute quantitation

CGH - Comparative genomic hybridization

9. Supplementary References

1. Kravchenko-Balasha, N.; Wang, J.; Remacle, F.; Levine, R. D.; Heath, J. R., Glioblastoma cellular architectures are predicted through the characterization of two-cell interactions. *Proc Natl Acad Sci U S A* **2014,** *111* (17), 6521-6.
2. Remacle, F.; Kravchenko-Balasha, N.; Levitzki, A.; Levine, R. D., Information-theoretic analysis of phenotype changes in early stages of carcinogenesis. *Proc Natl Acad Sci U S A* **2010,** *107* (22), 10324-9.
3. Kravchenko-Balasha, N.; Levitzki, A.; Goldstein, A.; Rotter, V.; Gross, A.; Remacle, F.; Levine, R. D., On a fundamental structure of gene networks in living cells. *Proc Natl Acad Sci U S A* **2012,** *109* (12), 4702-7.
4. Levine, R. D.; Bernstein, R. B., Energy disposal and energy consumption in elementary chemical reactions. Information theoretic approach. *Accounts of Chemical Research* **1974,** *7* (12), 393-400.
5. Dennis, G., Jr.; Sherman, B. T.; Hosack, D. A.; Yang, J.; Gao, W.; Lane, H. C.; Lempicki, R. A., DAVID: Database for Annotation, Visualization, and Integrated Discovery. *Genome Biol* **2003,** *4* (5), P3.
6. Mayer, J. E.; Mayer, M. G., *Statistical mechanics*. 2nd ed ed.; Wiley: New York, 1977.
7. Hill, E. G.; Schwacke, J. H.; Comte-Walters, S.; Slate, E. H.; Oberg, A. L.; Eckel-Passow, J. E.; Therneau, T. M.; Schey, K. L., A statistical model for iTRAQ data analysis. *J Proteome Res* **2008,** *7* (8), 3091-101.
8. Gross, A.; Levine, R. D., Surprisal analysis of transcripts expression levels in the presence of noise: a reliable determination of the onset of a tumor phenotype. *PLoS One* **2013,** *8* (4), e61554.
9. Johnson, H.; Del Rosario, A. M.; Bryson, B. D.; Schroeder, M. A.; Sarkaria, J. N.; White, F. M., Molecular characterization of EGFR and EGFRvIII signaling networks in human glioblastoma tumor xenografts. *Mol Cell Proteomics* **2012,** *11* (12), 1724-40.56
10. Seber, G. A. F., *Multivariate observations*. Wiley: New York, 1984; p xx, 686 p.
11. Rousseeuw, P. J., Silhouettes: A graphical aid to the interpretation and validation of cluster analysis. *Journal of Computational and Applied Mathematics* **1987,** *20* (0), 53-65.
12. Kravchenko-Balasha, N.; Mizrachy-Schwartz, S.; Klein, S.; Levitzki, A., Shift from apoptotic to necrotic cell death during human papillomavirus-induced transformation of keratinocytes. *J Biol Chem* **2009,** *284* (17), 11717-27.
13. Szklarczyk, D.; Franceschini, A.; Kuhn, M.; Simonovic, M.; Roth, A.; Minguez, P.; Doerks, T.; Stark, M.; Muller, J.; Bork, P., et al., The STRING database in 2011: functional interaction networks of proteins, globally integrated and scored. *Nucleic acids research* **2011,** *39* (Database issue), D561-8.
14. Ding, Q.; Stewart, J., Jr.; Olman, M. A.; Klobe, M. R.; Gladson, C. L., The pattern of enhancement of Src kinase activity on platelet-derived growth factor stimulation of glioblastoma cells is affected by the integrin engaged. *J Biol Chem* **2003,** *278* (41), 39882-91.
15. Xie, B.; Zhao, J.; Kitagawa, M.; Durbin, J.; Madri, J. A.; Guan, J. L.; Fu, X. Y., Focal adhesion kinase activates Stat1 in integrin-mediated cell migration and adhesion. *J Biol Chem* **2001,** *276* (22), 19512-23.
16. Kassis, J.; Moellinger, J.; Lo, H.; Greenberg, N. M.; Kim, H. G.; Wells, A., A role for phospholipase C-gamma-mediated signaling in tumor cell invasion. *Clin Cancer Res* **1999,** *5* (8), 2251-60.